

THESE DE DOCTORAT DE

L'UNIVERSITE DE NANTES
COMUE UNIVERSITE BRETAGNE LOIRE
ECOLE DOCTORALE N° 605
Biologie Santé

UNIVERSIDAD SANTIAGO DE COMPOSTELA
ESPAGNE

Par

Petar VUKOJICIC

« Affitin-dendrimer conjugates for multivalency-enhanced targeting »

Thèse présentée et soutenue à Nantes, le 28 Janvier 2019

Unité de recherche : CRCINA U1232

CIQUS

Rapporteurs avant soutenance :

Jan Van HEST Professeur, Eindhoven University of Technology
Michael MALKOCH Professeur, Royal Institute of Technology (KTH)

Composition du Jury :

| | | |
|--------------------|-------------------------|--|
| Président : | Elena ISHOW | Professeur, Université de Nantes |
| Examineur : | Patrice SOUMILLION | Professeur, Université catholique de Louvain |
| Dir. de thèse : | Barbara MOURATOU | Maitre de conférences, Université de Nantes |
| Co-dir. de thèse : | Eduardo FERNANDEZ-MEGIA | Professeur, Universidad Santiago de Compostela |

Mom ocu i mojoj baki, u ime večnog zaveta koji sam im dao.

(To my father and my grandmother, in the name of the pledge I made.)

Table of contents

| | |
|---|-----|
| Acknowledgements..... | 3 |
| Synopsis..... | 6 |
| Abbreviations..... | 9 |
| Chapter I: Introduction..... | 13 |
| Chapter II: Objectives..... | 102 |
| Chapter III: Synthesis and characterization of Affitin-dendrimer conjugates for multivalent targeting of <i>Staphylococcus aureus</i> Protein A..... | 107 |
| Chapter IV: Interaction of Affitin-dendrimer conjugates with <i>Staphylococcus aureus</i> | 170 |
| Chapter V: Conclusions and perspectives..... | 202 |

Acknowledgements

The work presented in the following pages is an achievement of my family, friends, coworkers and mentors whose vast, selfless support kept my hand steady in the most difficult of times. No words can fully express the gratitude I feel towards this amazing group of people that I am proud to call my own.

Firstly, I need to express deep appreciation to my supervisors Dr Barbara Mouratou and Dr Eduardo Fernandez-Megia for the opportunity to work with them and benefit from their knowledge, experience and leadership. Their persistent confidence in me, along with the support in all professional and personal affairs, made all the difference.

I would like to thank the members of thesis committee Dr Jean-Francois Gestin and Dr Anxo Vidal for important insights and stimulating discussions during our meetings. I am also grateful to the members of the jury for my thesis defense Dr Jan Van Hest, Dr Michael Malkoch, Dr Elena Ishow and Dr Patrice Soumillion for agreeing to evaluate this work.

During the last years, I was fortunate to work in three different countries and three different laboratories. First, I want to thank my group in France: Fred and Axelle, who always had the most patience to discuss my work in detail in our meetings, inspiring and providing innovative perspectives and thus improving the quality of my research immensely; Ghislaine, whose invaluable experience in the laboratory is exceeded only

by her kindness, selflessness and willingness to help; my peers Stanimir, Valentina and Benjamin with whom I have shared everything and who will always stay in the circle of my closest friends. Furthermore, I thank other members of Team 13 and Unit 1232 who supported me – Michel, Stephanie, Bertrand, Stephan, Mike, Laurent, Francois, Cindy, Patricia, Steven and others. Special gratitude goes to people who made Nantes my second home with their friendship: Kubat, Abdulaye, David, Dušan, Zhenya, Roxana, Alex, Barbara and others.

For the time I spent in Spain, I had the opportunity to work with Marcos, Juan, Susana, Muna and many others. I thank them for making a mark in my life with their exceptional kindness and invaluable help. I owe a special gratitude to Maun, whose friendship and contribution to my work were truly incredible, as well as to Sorel and Ulung for all the cafeteria lunches, late nights in the lab (and elsewhere) and putting a smile on my face every day.

During the two months I spent at Stanford, California, I was privileged to work with Dr Carolyn Bertozzi and Dr Han Xiao and learn so much from them in such a short time. I owe them immense gratitude for this rewarding experience, as well as Asia Avelinho and all others for the amazingly warm welcome I received in their lab.

This PhD also blessed me with the opportunity to meet Maha, who quickly became an integral part of all my endeavors. Her kindness, incredible

selflessness and commitment are built into this thesis and in everything else I do as the strongest and most reliable foundation. Thank you for making it all worth it.

My family and friends back at home, with whom I have grown up and to whom I owe more than I can ever repay, have a claim to all my successes and share in all the happiness. I cannot thank them enough for their unconditional love. My love and gratitude to my mother and my grandfather cannot be properly expressed here – my biggest rewards are the moments when I am able to make them more proud than they already are. Hvala vam.

Synopsis

Achieving selectivity in order to balance therapeutic and adverse effects has always been a central challenge of medicine. Nanotechnology is a modern field that allows us to tackle the selectivity issue in medicine in a completely new way, using “smart”, targeted nanoparticles. Most of medical research today is about identifying factors characteristic for certain conditions and finding efficient ways to target them in a specific manner, thus avoiding healthy cells and tissues.

There are two main ways this targeting is achieved with nanoparticles. First is by modulating the pharmacokinetics of the agents by controlling their size and physicochemical properties, causing them to accumulate in the desired compartments of the organism – passive targeting. Second is by functionalizing their surface with targeting agents that will bind to a defined molecular target in a highly specific manner – active targeting.

Dendrimers are a very versatile class of nanoparticles. They are synthetic, tree-like, globular structures obtained through a step-wise synthesis that allows a small-molecule-like level of control. Their monodispersity and highly customizable size, structure and surface functionalization distinguishes them from other nanoparticles as an especially attractive platform. Beside these general advantages of dendrimers, Gallic Acid-Triethylene Glycol (GATG) dendrimers take

advantage of terminal azides present in the repeating unit allowing a simple, fast and reliable synthetic procedures and high structural versatility.

Among the agents used for molecular targeting, antibodies are traditionally considered to be unmatched in terms of narrow specificity and high affinity towards their targets. Lately, the development of targeting scaffolds alternative to antibodies has been pursued in the search of complementary properties. Affitins are such a scaffold, offering nanomolar affinities and narrow specificities for the targets, that either match or outperform those of antibodies, along with twenty-fold smaller size and high thermal and pH stability. Furthermore, Affitins are easily obtained in high quantities via production in *E. coli*.

The improved selectivity provided by targeted nanoparticles has been most extensively employed for cancer-related purposes. However, considering the increased occurrence of multiresistance to antibiotics in bacteria, highly specific targeting and delivery tools in the field of infectious diseases are quickly gaining in importance. Separating the targeting from the effector function of antimicrobial agents might not only render ineffective most of the resistance mechanisms of bacteria, but also allow for usage of more toxic antimicrobial agents due to the specific delivery that bypasses host cells.

The main aim of this thesis was to combine the enhanced targeting properties of Affitins with the advantages that GATG dendrimers offer as

carriers and to obtain powerful nanoscale devices with wide potential for diverse applications. Our first objective was to develop a versatile conjugation method that will allow customization of final products in terms of size, structure, surface functionalization and target specificity. Our second objective was to showcase Affitin-dendrimer conjugates by deliberately designing a set of conjugates highly specific for *Staphylococcus aureus* Protein A (SpA) and demonstrating their usefulness.

A click-chemistry conjugation method was developed and used to obtain four distinct populations of conjugates, allowing for fluorescent labelling and surface modification during the process. Products were thoroughly characterized in terms of size, structure and valency. Their enhanced multivalent binding to SpA was demonstrated by surface plasmon resonance, while their narrow specificity for SpA-expressing *S. aureus* strains was demonstrated in an agglutination assay. Strong, concentration-dependant agglutination triggered by the conjugates was also used to modulate their ability to form biofilms.

The high versatility and multivalency of GATG dendrimers as nanocarriers combined with the customizable target-specificity of Affitins provides powerful nanoscale devices for targeting, capable of carrying large amounts of diverse payloads and therefore performing diverse functions.

Abbreviations

| | |
|-------|--|
| AAC | Huisgen 1,3-dipolar Azide-Alkyne Cycloaddition |
| Aap | Accumulation-associated protein |
| Ab | Antibody |
| ABT | Azabisphosphonate |
| ADCs | Antibody-drug conjugates |
| Ag | Antigens |
| Agr | Accessory gene regulator |
| BCN | Bicyclononyne |
| BLI | Bio-Layer Interferometry |
| BNCT | Boron Neutron Capture Therapy |
| CD | Cyclodextrin |
| CDRs | Complementarity-determining regions |
| ClfA | Clumping factor A |
| CMDPs | Critical Molecular Design Parameters |
| CNPs | Carbon-based nanoparticles |
| CuAAC | Copper-catalyzed Azide-Alkyne Cycloaddition |
| CV | Crystal Violet |

| | |
|--------|---|
| DARPin | Designed Ankyrin Repeat Protein |
| DHB | Dihydroxybenzoic acid |
| EDC | 1-Ethyl-3-(3-Dimethylaminopropyl)Carbodiimide |
| ELISA | Enzyme-Linked ImmunoSorbent Assay |
| EPR | Enhanced Permeation and Retention |
| Fab | Antigen-binding fragments |
| Fc | Cystallisable fragment |
| FcR | Fc receptor |
| GATG | Gallic acid-triethylene glycol |
| GFP | Green fluorescent protein |
| HER2 | Human Epidermal growth factor Receptor 2 |
| HIV | Human immunodeficiency virus |
| HOBt | Hydroxybenzotriazol |
| HRP | HorseRadish Peroxidase |
| IBPs | IgG Binding Proteins |
| IG | Immunoglobulins |
| IgGs | Immunoglobulins G |
| IMAC | Immobilized metal ion affinity chromatography |

| | |
|----------|---|
| INPs | Inorganic nanoparticles |
| LNPs | Lipid nanoparticles |
| MAC | Minimum Agglutination Concentrations |
| MNPs | Magnetic nanoparticles |
| MRI | Magnetic Resonance Imaging |
| MRSA | Methicillin-resistant <i>Staphylococcus aureus</i> |
| MSCRAMMs | Microbial Surface Components Recognizing Adhesive Matrix Molecules |
| Nb | Nanobodies |
| NMR | Nuclear Magnetic Resonance |
| NNI | National Nanotechnology Initiative |
| NPs | Nanoparticles |
| PAMAM | Polyamidoamine |
| PCA | Protein complementation assay |
| PDT | Photodynamic therapy |
| PEG | Polyethylene glycol |
| PHA | Polyhydroxyalkanoates |
| PhoA | Phosphatase A |

| | |
|---------------|--|
| PIA | Polysaccharide Intercellular Adhesin |
| PIC | Polyion Complex |
| PLGA | Poly-(lactic-co-glycolic acid) |
| PNPs | Polymeric nanoparticles |
| PPI | Poly(propylene imine) |
| PSM | Phenol-soluble modulin |
| RA | Rheumatoid arthritis |
| RU | Resonance Units |
| SA | Sinapic acid |
| SEC | Size-exclusion chromatography |
| SIA | Sialic acid |
| SpA | <i>S. aureus</i> protein A |
| SPAAC | Strain Promoted Azide-Alkyne Cycloaddition |
| SPR | Surface Plasmon Resonance |
| SSLs | Staphylococcal superantigen-like proteins |
| SSTIs | Skin and soft tissue infections |
| TCEP | Tris(2-carboxyethyl)phosphine |
| β -PFTs | β -barrel pore forming toxins |

Chapter I:

Introduction

Table of Contents

| | |
|--|-----------|
| I. Selectivity and targeting in medicine..... | 15 |
| I.1 Nanoparticles | 18 |
| I.1.1 Nanoparticles in biomedicine | 18 |
| I.1.2 Classification of NPs | 25 |
| I.1.3 Dendrimers | 28 |
| I.1.4 Dendrimers on the market and in clinical trials..... | 37 |
| I.2 Molecular targeting | 38 |
| I.2.1 Antibodies | 39 |
| I.2.2 Alternative scaffolds for molecular targeting | 45 |
| II. <i>Staphylococcus aureus</i>..... | 53 |
| II.1 Clinical significance of <i>S. aureus</i> | 53 |
| II.1.1 SSTIs | 54 |
| II.1.2 Bloodstream infections | 55 |
| II.2 Molecular basis of pathogenicity and immune evasion | 55 |
| II.2.1 Neutrophil extravasation and chemotaxis..... | 57 |
| II.2.2 Complement activation and phagocytosis..... | 57 |
| II.2.3 Neutrophil-mediated killing | 58 |
| II.2.4 Staphylococcal killing of host cells | 58 |
| II.2.5 Other factors of pathogenicity and immune evasion | 59 |
| II.3 SpA | 60 |
| II.3.1 Structure of SpA | 60 |
| II.3.2 Roles of SpA in <i>S. aureus</i> | 60 |
| II.4 <i>S. aureus</i> biofilms | 63 |
| II.4.1 Biofilm formation | 63 |
| II.4.2 Biofilm formation assays..... | 67 |
| III. References | 70 |

I. Selectivity and targeting in medicine

The main struggle of modern medicine is not to achieve higher effectiveness of drugs, but to reduce or eliminate their adverse effects. The concept of a “magic bullet”, introduced by Paul Ehrlich more than a hundred years ago,¹⁻³ has evolved along with many advances achieved throughout the 20th century, only to become more relevant than it ever was. There is a vast amount of agents available today that achieve a wide range of effects on particular receptor molecules, but the challenge that remains is for these agents to differentiate between diseased and healthy cells/tissues, acting only on the former, thus avoiding adverse effects that typically occur when they act on the latter.

Traditional pharmaceuticals are typically single-small-molecule agents whose activity depends on acting upon a certain molecular receptor. This single interaction has to satisfy the requirements of selectivity and efficacy at the same time. Therefore, the number of available therapeutic targets has been limited to those that are not relevant to healthy tissues or cells. When this selectivity is not achieved, a trade-off between the efficacy and adverse effects of the drug must be controlled by carefully choosing the dosage and/or the administration route.

Having this in mind, it comes as no surprise that the greatest advances in the area have been achieved in the field of antibiotics. The antibiotic era, commonly considered to have started with the discovery of

penicillin by Alexander Flemming in 1928,⁴ was possible at such an early stage of medical science due to the fact that pathogenic microbes, being procaryotic organisms, possess a cellular machinery so different from human cells that targeting a wide variety of mechanisms crucial for viability and virulence was possible without seriously affecting human cells.

Evolution of the “magic bullet” paradigm has been driven by two main challenges.⁵ First was the fact that many other pathologies, such as cancer or autoimmune diseases, have much less distinct phenomena in their origin since they are not caused by foreign organisms, and are therefore much more difficult to target without harming the patient. Second, even though the antibiotics initially achieved revolutionary results, many microbes quickly adapted by evolving resistance mechanisms that render more and more antibiotics inefficient. As the limits of the traditional approach to increase selectivity of the effector were reached, a new approach started to emerge focusing on its selective delivery.⁶

Two major pillars of this new approach are: (i) control over the physicochemical properties of the agent, affecting its pharmacokinetics, which includes passive targeting; and (ii) incorporation of a targeting agent which recognizes and binds to a molecule present on the desired target, which is dubbed active targeting. These modern pharmaceuticals are therefore composed of a few moieties combined either as a single, multifunctional molecule or a supramolecular structure. Beside the effector,

that achieves the therapeutic, imaging and/or diagnostic goals, they often contain separate targeting ligands for active targeting, and an underlying platform that serves as a delivery vehicle and provides desirable physicochemical properties. This separation allows the requirements of selectivity and efficacy to be met using multiple different interactions in a dynamic way, thus overcoming the limitations of traditional pharmaceuticals.

Delivery vehicles have evolved from the original *macroscopic* devices such as implants, capsules and patches, through the stage of the *microscopic* polymer systems, to the *nanoscopic* era of targeted nanocarriers which offer some unprecedented possibilities that are currently being translated into new and exciting, clinically successful products.⁶

Targeting agents used to direct these vehicles to specific molecular targets can be different kinds of molecules, including sugars, peptides, small molecules, antibodies etc.⁷⁻¹⁴ Antibodies are considered our organisms “magic bullet” due to their narrow and adaptive specificity towards any identified threat.¹⁵⁻¹⁶ Many alternative targeting scaffolds with improved properties compared to antibodies are available today and widely used for molecular recognition and active targeting.¹⁷

I.1 Nanoparticles

Nanotechnology is a rapidly advancing field that has been made possible through the convergence of many scientific fields, including chemistry, biology, physics, mathematics and engineering.¹⁸ The National Nanotechnology Initiative (NNI) defines nanotechnology as science, engineering, and technology conducted at the nanoscale, which is about 1 to 100 nanometers.¹⁹ Therefore, nanoparticles (NPs), previously dubbed ultra-fine particles in order to differentiate them from larger, fine particles (100-2500 nm), are particles of any shape with dimensions between 1 and 100 nm.²⁰⁻²² The basis for 100 nm limit is the fact that novel properties that differentiate particles from bulk material typically develop at a critical length scale of under 100 nm.²³

I.1.1 NPs in biomedicine

Nanotechnology offers unprecedented possibilities in the biomedical field. Designing supramolecular structures in a deliberate way allows control over pharmacokinetics that is impossible to achieve with traditional small-molecule pharmaceuticals. Encapsulating molecules inside NPs protects them from biodegradation until they have reached their site of action. Control over physicochemical properties of NPs might bring completely new concepts and provide more effective strategies for addressing complex endeavors in biomedical research. Finally, the large capacity for surface functionalization typically found in NPs makes it possible to use multivalency

based phenomena and active targeting concept to achieve high precision in engineering desired effects of final products.²⁴

I.1.1.1 Challenges facing nanoparticle-based formulations

Pharmacokinetics/Pharmacodynamics (PK/PD) studies for small-molecule pharmaceuticals follow a well defined structure that is known to provide information relevant for their safety/effectiveness profile. Similar rules relating to clinical trials are available. Therefore, the selection of the most suitable small molecules to advance in pharmaceutical development follows a set of “Critical Molecular Design Parameters” (CMDPs) which are determined to affect their properties in a quantized and predictable way. The challenge that NPs face today is establishing a set of similar “Critical Nanoscale Design Parameters” (CNDPs) that would allow more precise engineering of properties through rational design. Furthermore, additional complexity in the patterns of PK/PD behaviors exhibited by NPs requires setting more elaborate standards for studies necessary in their approval. Some of the proposed critical parameters of design, as well as the critical outcomes for the safety/effectiveness studies and the approval process are listed in Figure 1.²⁵⁻²⁹

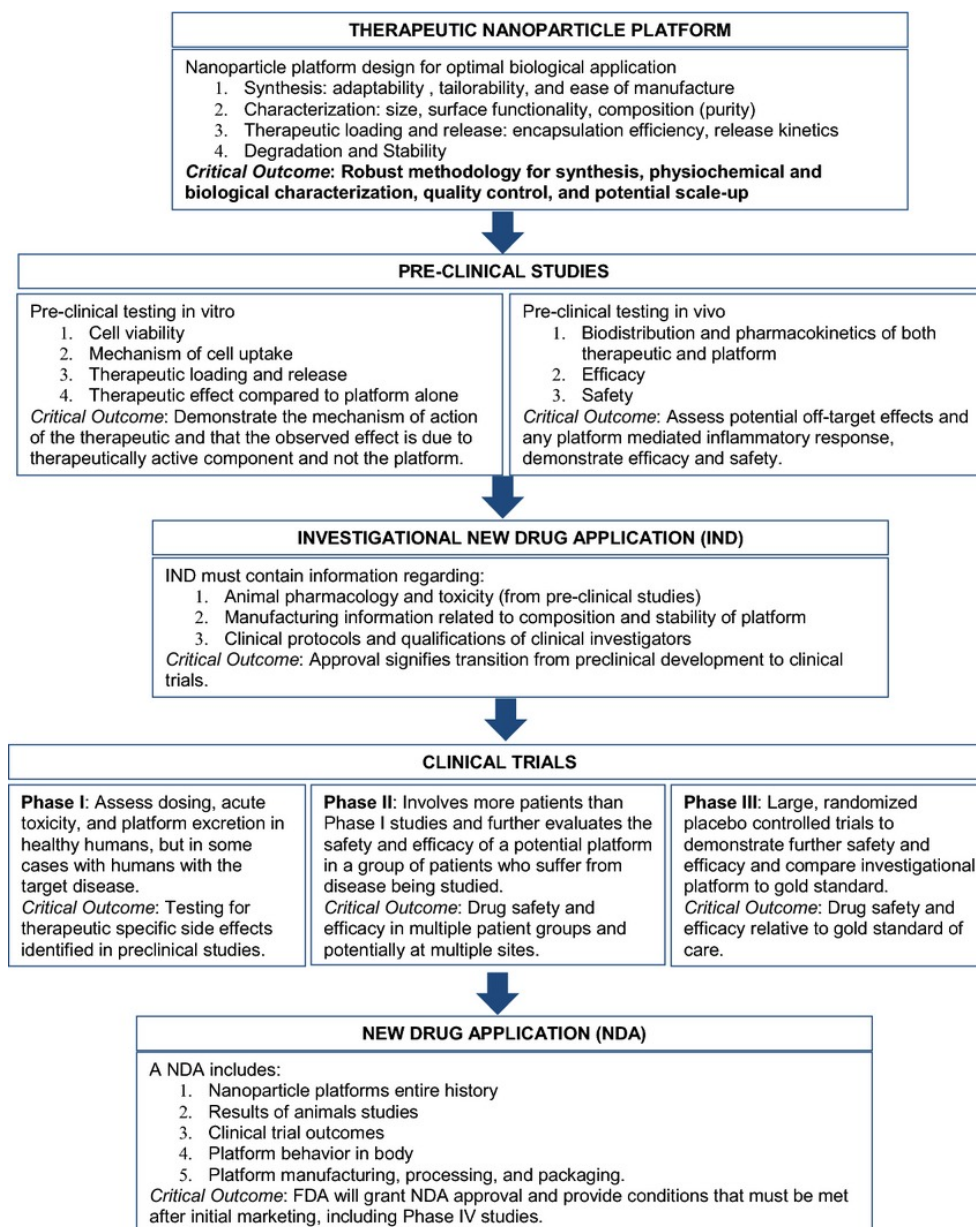


Figure 1. Some of the proposed critical design parameter and critical outcomes in the regulatory process for nanoparticle-based products (from 25)

Two parameters suggested to have the largest effect on properties such as cellular uptake, transport and accumulation *in vivo*, are size and shape.^{30,31} Beside those two major factors, other parameters found to be extremely relevant are surface chemistry, flexibility and architecture.³²

I.1.1.2 Examples of nanoparticle-based products on the market or in clinical trials

Since 1995, around 50 nanopharmaceuticals have received Food and Drug Administration (FDA) approval and are currently available for clinical use. Table 1 lists FDA approved nanopharmaceuticals, along with their indications and benefits related to their nanometric formulation.³³

Most of the nanoparticle-based pharmaceuticals that enter clinical trials are nanoformulations of previously approved drugs. As of October 2018, 66 clinical trials that include the term “nano” were listed as recruiting or active on ClinicalTrials.gov.³⁴ This is an increase of 10 compared to October 2017, when there were 56.³³

Table 1. Overview of the FDA approved nanoparticle-based products (adapted from 33)

| Trade Name (Manufacturer) | Indication(s) [*] | Benefit of NP ^{**} |
|------------------------------|---|--|
| Liposome NPs | | |
| Curosurf (Chiesi USA) | Respiratory distress syndrome | Increased delivery with smaller volume, decreased toxicity |
| Doxil (Janssen) | Karposi’s sarcoma, ovarian cancer, multiple myeloma | Increased delivery to disease site, decreased systemic toxicity of free drug |
| Abelcet (Sigma-Tau) | Fungal infections | Decreased toxicity |

| Trade Name (Manufacturer) | Indication(s)* | Benefit of NP** |
|------------------------------------|--|---|
| AmBIsome (Gilead Sciences) | Fungal/protozoal infections | Decreased nephrotoxicity |
| DepoDur (Pacira Pharmaceuticals) | Postoperative analgesia | Extended release |
| DepoCyt (Sigma-Tau) | Lymphomatous meningitis | Increased delivery to tumor site, decreased systemic toxicity |
| Marqibo (Spectrum Pharmaceuticals) | ALL | Increased delivery to tumor site, decreased systemic toxicity |
| Onivyde (Ipsen Biopharmaceuticals) | Pancreatic cancer | Increased delivery to tumor site, decreased systemic toxicity |
| Visudyne (Bausch and Lomb) | Wet AMD, ocular histoplasmosis, myopia | Increased delivery to site of diseased vessels, photosensitive release |
| Vyxeos (Jazz Pharmaceuticals) | AML, AML with myelodysplasiarelated changes | Increased efficacy through synergistic delivery of co-encapsulated agents |
| Polymer NPs | | |
| Adagen (Leadiant Biosciences) | SCID | Longer circulation time, decreased immunogenicity |
| Adynovate (Shire) | Hemophilia | Greater protein stability, longer half-life |
| Cimzia (UCB) | Crohn's disease, rheumatoid arthritis, psoriatic arthritis, ankylosing spondylitis | Longer circulation time, greater stability <i>in vivo</i> |
| Copaxone (Teva) | Multiple sclerosis | Controlled clearance |
| Eligard (Tolmar) | Prostate cancer | Longer circulation time, controlled payload delivery |

| Trade Name (Manufacturer) | Indication(s)* | Benefit of NP** |
|---|----------------------------------|---|
| Krystexxa (Horizon) | Chronic gout | Greater protein stability |
| Macugen (Bausch and Lomb) | Neovascular AMD | Greater aptamer stability |
| Mircera (Vifor) | Anemia associated with CKD | Greater aptamer stability |
| Neulasta (Amgen) | Chemotherapy-induced neutropenia | Greater protein stability |
| Oncaspar (Baxalta U.S.) | ALL | Greater protein stability |
| Pegasys (Genentech) | Hepatitis B, hepatitis C | Greater protein stability |
| PegIntron (Merck) | Hepatitis C | Greater protein stability |
| Plegridy (Biogen) | Multiple sclerosis | Greater protein stability |
| Rebinyn (Novo Nordisk) (available in 2018) | Hemophilia B | Longer half-life, greater drug levels between infusions |
| Renvela (Genzyme); and Renagel (Genzyme) | CKD | Longer circulation time and therapeutic delivery |
| Somavert (Pfizer) | Acromegaly | Greater protein stability |
| Zilretta (Flexion Therapeutics) | Osteoarthritis knee pain | Extended release |
| Micelle NPs | | |
| Estrasorb (Novavax) | Vasomotor symptoms in menopause | Controlled delivery |
| Nanocrystal NPs | | |
| Avinza (Pfizer) | Psychostimulant | Greater drug loading and bioavailability, ER |
| EquivaBone (Zimmer Biomet) | Bone substitute | Mimics bone structure |

| Trade Name (Manufacturer) | Indication(s)* | Benefit of NP** |
|--------------------------------------|---|---|
| Emend (Merck) | Antiemetic | Greater absorption and bioavailability |
| Focalin (Novartis) | Psychostimulant | Greater drug loading and bioavailability |
| Invega Sustenna (Janssen) | Schizophrenia, schizoaffective disorder | Slow release of injectable low-solubility drug |
| Megace ES (Par Pharmaceuticals) | Antianorexic | Lower dosing |
| NanOss (RTI Surgical) | Bone substitute | Mimics bone structure |
| Ostim (Heraeus Kulzer) | Bone substitute | Mimics bone structure |
| OsSatura (IsoTis Orthobiologics) | Bone substitute | Mimics bone structure |
| Rapamune (Wyeth Pharmaceuticals) | Immunosuppressant | Greater bioavailability |
| Ritalin LA (Novartis) | Psychostimulant | Greater drug loading and bioavailability |
| Ryanodex (Eagle Pharmaceuticals) | Malignant hypothermia | More rapid rate of administration at higher doses |
| Tricor (AbbVie) | Hyperlipidemia | Greater bioavailability simplifies administration |
| Vitoss (Stryker) | Bone substitute | Mimics bone structure |
| Zanaflex (Acorda) | Muscle relaxant | Greater drug loading and bioavailability |
| Inorganic NPs | | |
| Dexferrum (American Regent) | Iron deficiency in CKD | Increased dose |

| Trade Name (Manufacturer) | Indication(s) [*] | Benefit of NP ^{**} |
|---------------------------------|---|---|
| Feraheme (AMAG Pharmaceuticals) | Iron deficiency in CKD | Prolonged, steady release with less frequent dosing |
| Ferrlecit (Sanofi-Aventis) | Iron deficiency in CKD | Increased dose |
| Infed (Actavis Pharma) | Iron deficiency in CKD | Increased dose |
| Venofer (American Regent) | Iron deficiency in CKD | Increased dose |
| Protein NPs | | |
| Abraxane (Celgene) | Breast cancer, NSCLC, pancreatic cancer | Greater solubility, increased delivery to tumor |
| Ontak (Eisai) | Cutaneous T-cell lymphoma | Targeted T-cell specificity, lysosomal escape |

I.1.2 Classification of NPs

NPs are generally classified based on the nature of the building blocks they are made of: organic, inorganic (INPs) and carbon-based (CNPs).³⁵ CNPs have found many applications in material science, but their role in biomedicine is only starting to be explored and more insight into their safety profile is needed.³⁶ Organic NPs are further classified into two main groups, lipid (LNPs) and polymeric (PNPs) (Figure 2).

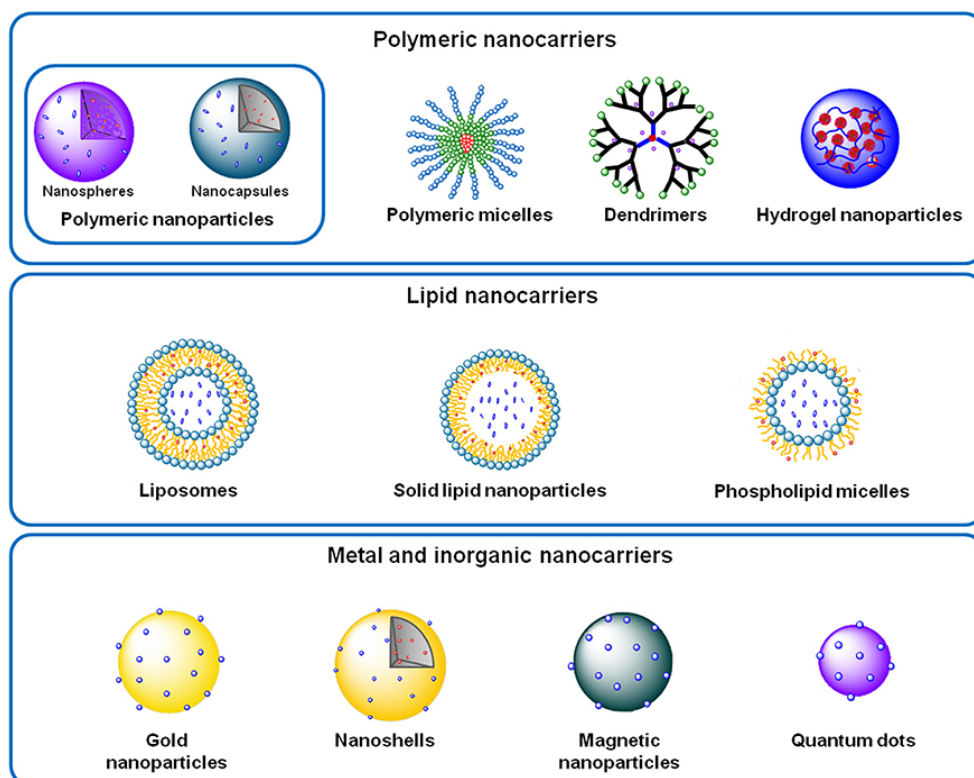


Figure 2. Examples of NPs classified based on the building blocks they are made of (from 37)

I.1.2.1 Polymeric NPs

Some of the most commonly used PNPs are based on polymers such as polyhydroxyalkanoates (PHA), poly-(lactic-co-glycolic acid)(PLGA) and cyclodextrin (CD).^{38,39} Since PNPs are most extensively explored nanocarriers, many targeted and non-targeted delivery systems based on them are currently available. 34% of all NP based approved drugs are PNPs as of 2017,³⁹ most of them used for treating cancer patients.⁴⁰

I.1.2.2 Lipid NPs

Properties that differentiate LNPs as an attractive choice for designing delivery vehicles are their biocompatibility, biodegradability and the ability to capture both hydrophilic and hydrophobic agents into their amphiphilic structure. First anti-cancer FDA approved drug based on a nanocarrier was a liposomal formulation of doxorubicin (Doxil™/Caelyx™).⁴¹ The majority of nanoparticle-based formulations currently undergoing clinical trials are based on LNPs.³⁹

I.1.2.3 Inorganic NPs

Metal-based core of most inorganic NPs provides them with unique characteristics that make them especially useful as imaging agents. Semiconductor quantum dots, that are commercially available, offer a viable alternative to fluorescently labelled particles for certain purposes, while iron oxide NPs have been approved for human use in MRI as contrasts.^{42,43} An ability to display a localized surface plasmon resonance bands in the UV-visible-near IR range, that certain gold and silver based INPs possess, offers exciting new possibilities that are lately being explored and utilized.^{42,44}

I.1.3 Dendrimers

Dendrimers are synthetic, highly branched macromolecules with a repetitive structure and well-defined spatial location of functional groups. Unlike traditional polymers, dendrimers are synthesized in a step-wise fashion, which allows single-molecule-chemistry level of control over their structure.⁴⁵⁻⁴⁷ Beginning with a core, their structure grows in concentric layers, with each branch from the previous layer further branching outwards. These layers are dubbed generations, since each generation of a dendrimer represents a single, well defined increment in size of the molecule and number of functional groups present on the outer layer (Figure 3). This outer layer, also referred to as the surface of a dendrimer, is an interface through which dendrimers interact with their surroundings, thus many of their characteristics can be correlated to its composition.²⁵

The unique molecular architecture of dendrimers provides distinct features such as monodispersity, globular shape and highly customizable size and surface functionalization, which differentiate them from other NPs. The versatility that they offer makes them applicable to various medical research and development areas, including delivery systems, diagnostics and biomedical engineering.⁴⁸

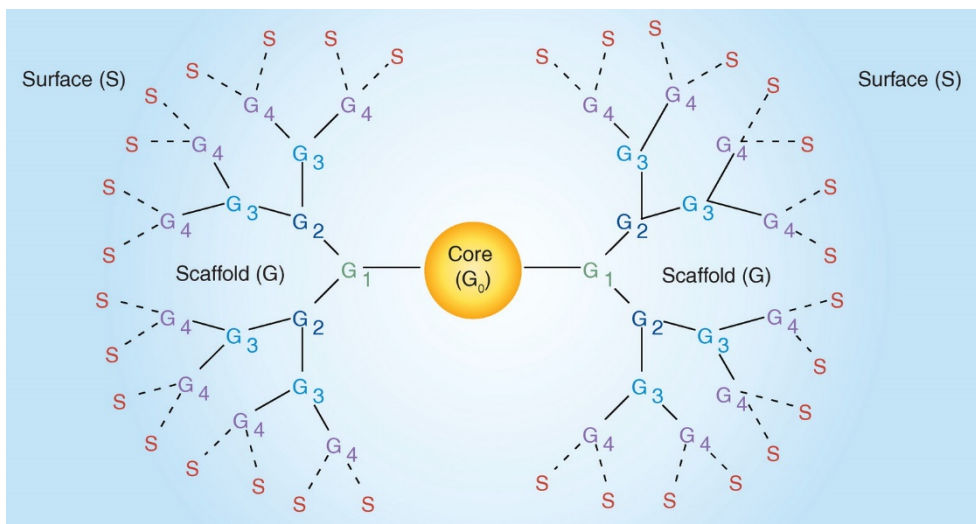


Figure 3. Unique molecular architecture of dendrimers (from 49)

I.1.3.1 Dendrimer synthesis

Much of the desirable characteristics of dendrimers are related to the way they are synthesized. Unlike classical polymers, that are generally synthesized in a one-step polymerization reaction, dendrimers are synthesized step-by-step in an iterative fashion, where each growth step is preceded by an activation step, ensuring well-defined, symmetrical structures to be formed.⁵⁰

Dendrimer synthesis is performed by two major approaches, either divergent or convergent. In the divergent approach, the dendrimer is synthesized starting from the core and built up generation by generation.^{46,51} The limitation of this approach is that very effective transformations are necessary to avoid defects in structure. For example, only 25% of the “structurally perfect” G₅-PPI dendrimer can be obtained

using divergent method.^{52,53} This can be addressed by developing and using more efficient, accelerated approaches based on different coupling reactions, such as fluoride-promoted esterification via imidazolide-activated compounds.⁵⁴

Another way to tackle limitations of the divergent approach is the alternative convergent approach, where the synthesis starts from the surface and ends up at the core, thus converging from multiple dendrons to a single dendrimer structure (Figure 4).^{46,55} Despite some advantages, the convergent approach suffers from more demanding couplings when dealing with high generations. To solve these inconveniences, alternative accelerated strategies based on hypercores, hypermonomers and repeating units with orthogonal functionalities have been devised.⁵⁶⁻⁵⁸

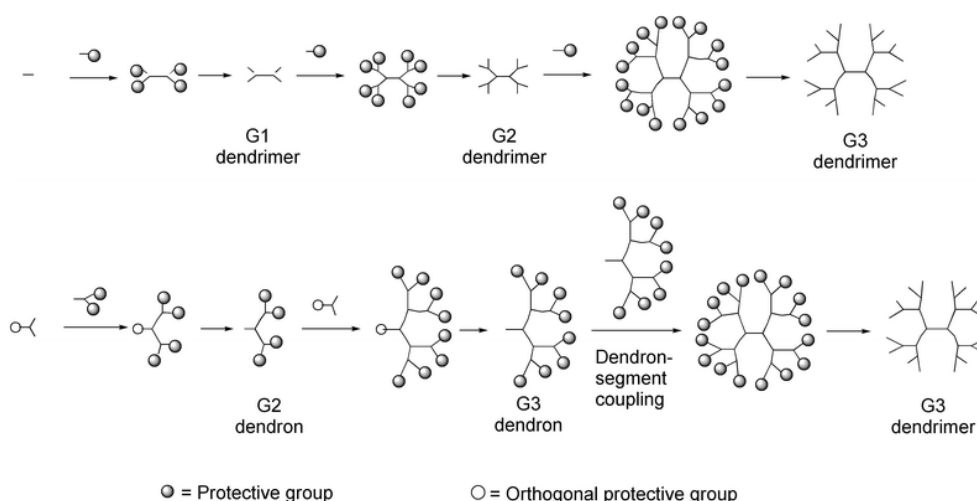


Figure 4. Divergent (top) and convergent (bottom of the figure) approach to dendrimer synthesis (from 51)

I.1.3.2 Toxicity and biodistribution profile of dendrimers

Early *in vitro* toxicity studies of dendrimers revealed a strong correlation between cationic surface and cytotoxicity. Both polyamidoamine (PAMAM) and poly(propylene imine) (PPI) dendrimers, two of the most studied families of dendrimers, showed significant cytotoxicity in their cationic form.⁵⁹⁻⁶¹ However, subsequent *in vivo* studies showed almost complete absence of this effect. Only high generations of cationic dendrimers were toxic *in vivo* and only at very high doses (> 10 mg/kg). Low and middle generation dendrimers, even the ones that showed cytotoxicity *in vitro* have been found non-toxic *in vivo*.⁶²

Accumulation of dendrimers in the liver, pancreas, heart and kidneys normally does not affect these organs in a negative way. Both accumulation and clearance of dendrimers depends strongly on their surface properties and the most efficient strategies to affect biodistribution were relying on surface modifications (Figure 5).⁶²

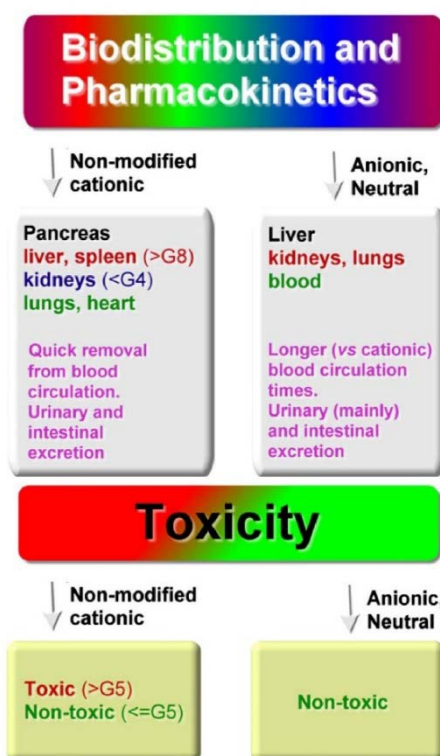


Figure 5. Dendrimer biodistribution and toxicity, generalized from observations based on different classes of dendrimers (modified from 62)

I.1.3.3 Surface modifications of dendrimers

Since surface properties are responsible for most of the dendrimer interaction with the external environment, chemical modification of terminal groups has been extensively used in order to affect properties such as toxicity,⁶³ solubility,^{64,65} cellular uptake,⁶⁶ circulation times,⁶⁷ etc. Some examples of common modifications used to achieve these effects are PEGylation and carbohydrate coating.

I.1.3.3.1 PEGylation of dendrimers

PEGylation is a longstanding procedure of linking one or more polyethylene glycol (PEG) molecules to a target molecule. PEGylated agents typically show prolonged circulation times, higher stability to metabolic degradation and reduction in immunogenicity.^{68,69}

PEGylation of dendrimers is most commonly performed as a way to reduce their toxicity, since first studies of this strategy showed reduced haemolytic and haematological toxicity, along with some improvement in drug loading capacity and reduced drug leakage.⁷⁰ PEGylation was further found to improve properties of dendrimers such as reticuloendothelial system uptake, immunogenicity and stability.⁶¹

I.1.3.3.2 Carbohydrate coating of dendrimers

Dendrimers that contain carbohydrate residues in their structure are called “glycodendrimers”. Carbohydrate coating is one of the most widely used surface modifications that helps achieve a variety of different goals.

Many important physiological and pathophysiological processes in nature involve multivalent carbohydrate-protein interactions, such as cell-to-cell signaling, bacterial adhesion, cancer cell proliferation, etc. Glycodendrimers are a useful tool in studying these complex phenomena.

They have been used as microbial anti-adhesins,⁷¹ inhibitors of bacterial toxins adhesion^{72,73} and biofilm formation inhibitors.⁷⁴ Potential application in Alzheimer's disease treatment⁷⁵ and prevention of HIV transmission⁷⁶ has also been demonstrated.

Carbohydrate coating can provide other benefits to dendrimers relating to their toxicity and biodistribution profiles. Reduced haemolytic toxicity, cytotoxicity, immunogenicity and antigenicity after carbohydrate coating of dendrimers have been observed.⁶³ Galactose coating of dendrimers has proven effective for liver targeting and this was successfully used to deliver primaquine phosphate⁷⁷ and chloroquine phosphate⁷⁸ to the liver, targeting the liver stage of malaria parasites.

I.1.3.3.2 Other surface modifications of dendrimers

Different modifications of the dendrimer surface are used to achieve specific desired effects. Some examples of other useful modifications include converting terminal amino groups to carboxylates using anhydrides to increase water solubility and eliminate toxicity,⁷⁹ hydrophobic amino-acid decoration for enhancing gene transfection,⁸⁰ RGD-peptide decoration for modifying cell internalization⁸¹ and folate decoration for targeting tumors.⁸²

I.1.3.4 Applications of dendrimers

Vast field of potential applications of dendrimer-based products is currently being extensively studied. Notably, dendrimers are considered useful for the development of anti-cancer, anti-inflammatory and anti-viral agents.⁸³

I.1.3.4.1 Dendrimers in cancer therapy

Passive targeting via Enhanced Permeation and Retention (EPR) effect⁸⁴ and active targeting by incorporating various targeting ligands and triggering receptor-mediated endocytosis⁸⁵ are two main features that make dendrimer-based delivery of anti-cancer agents an attractive option.

Notable examples of anti-cancer drugs that demonstrated enhanced pharmacokinetics or better outcomes using dendrimers as drug delivery vehicles include methotrexate, doxorubicin, paclitaxel, 5-fluorouracil and cisplatin.⁸³ Dendrimers, decorated with boronophenylalanin or sodium borocaptate,⁸⁶ have also been used for Boron Neutron Capture Therapy (BNCT), a targeted radiotherapy based on intracellular ¹⁰B fission that releases α -particles inside the tumor cells.⁸⁷ Another interesting application is photodynamic therapy (PDT) which is based on a combination of light, photosensitizer and oxygen.⁸⁸ Dendrimer carriers were used to improve the efficiency and selectivity of this approach.^{89,90}

I.1.3.4.2 Dendrimers in inflammation therapy

Inflammation, being an important factor in the pathophysiology of many major diseases, is a very relevant therapeutic target today. Traditionally, dendrimers were studied only as carriers for anti-inflammatory drugs,^{83,91} but lately it has been shown that many dendrimers themselves possess strong anti-inflammatory effect. This effect is present with different kinds of simple functional groups present on the surface including amine, hydroxyl and carboxylic acid.⁹²

Anti-inflammatory activity of azabisphosphonate (ABP) dendrimer⁹³ found application in treatment of rheumatoid arthritis (RA). It helps reduce levels of inflammatory cytokines, bone erosion and cartilage destruction, which suggests ABP might be an efficient nanomedicine for RA.⁹⁴ Another way to improve outcomes of RA treatment is by conjugating methotrexate, a longstanding first-line treatment drug, to PAMAM dendrimers.⁹⁵

I.1.3.4.3 Dendrimers in anti-viral therapy

Due to many problems present in the treatment of viral infections, such as human immunodeficiency virus (HIV) and influenza, more efficient treatment options need to be developed.⁹⁶

Polyanionic dendrimers have demonstrated anti-viral activity against viruses such as HIV and herpes virus, by targeting their viral life cycle in

addition to preventing the binding to the host cell.⁹⁷ Starpharma has developed sulfonated dendrimers that take advantage of these effects,⁹⁸ resulting in the world's first dendrimer-based clinical product on the market, Vivagel®.⁹⁹

Another application of dendrimers as anti-viral agents involves sialic acid (SIA) decorated dendrimers for inhibition of Influenza A virus infection. Enhanced inhibition was achieved using efficiently designed multivalent SIA conjugates of PAMAM dendrimers compared to the monomer SIA.¹⁰⁰

I.1.4 Dendrimers on the market and in clinical trials

The clinical use of dendrimers is still in its infant stage, with only one currently available product, VivaGel® by Starpharma. However, a growing number of research papers focusing on dendrimers and their applications is published each year, along with a growing interest of pharmaceutical companies for further development of dendrimer based products. There are currently at least two products undergoing clinical trials – phase 2 for DEP® docetaxel and phase 1 / 2 for DEP® cabazitaxel both by Starpharma.¹⁰¹ All of the Starpharma formulations rely on their DEP® technology dendrimers, which are poly-L-lysine based.

Beside Starpharma clinical products, some dendrimer-based laboratory agents are also available on the market. Examples of these are Stratus CS® reagent for cardiac immunoassays from Dade Behring,¹⁰²

Superfect® transfection agent from Qiagen,^{103,104} Prioject™ transfection agent from Starpharma¹⁰⁴ and an U.S. army lab anthrax-detecting agent Alert ticket™.¹⁰⁵ All of these products are based on PAMAM dendrimers.

I.2 Molecular targeting

Selectivity in medicine is best achieved by exploiting distinct features of the biological target of interest. Astonishing early progress achieved in the field of antibiotics owes this success to the fact that microbes possess extremely different features compared to human cells and there is an abundance of agents in nature that selectively affect only prokaryotic cells. Fundamentally, selectivity of these agents is achieved via specific interactions with certain molecular targets, but not others. By definition, the narrower the range of molecules that an agent interacts with, the higher is the specificity of the interaction.

Specific interaction between molecules based on noncovalent binding is termed molecular recognition.¹⁰⁶ By convention, a binding partner that is anchored to the surface of the cell is the receptor or the target, while the other partner, that binds to it, is a ligand.¹⁰⁷ Molecular recognition is used to achieve molecular targeting by directing drugs or other agents, using ligands specific to a chosen target molecule, towards those cells or tissues or other entities that contain this target molecule.

I.2.1 Antibodies

Antibodies (Abs) or immunoglobulins (Ig) are globular glycoproteins used by the immune system to recognize and neutralize pathogens. Due to their inherent role in protecting the organism from outside threats, and unique features such as high target specificity and invaluable interactions with the immune system, they have been extensively used in many therapeutic areas such as infectious diseases, cancer, immune diseases etc.¹⁰⁸

I.2.1.1 Structure and function of Abs

Abs are globular glycoproteins with molecular weight of around 150 kDa, consisting of four polypeptide chains. Two identical heavy chains (H – chains) and two identical light chains (L – chains), are interconnected via disulfide bridges. Immunoglobulins G (IgGs), named after the type of their heavy chain, are most commonly used for biomedical applications. Heavy chains of Abs are composed of three constant (C_{H1-3}) and one variable (V_H) regions, while light chains have one constant and one variable region (C_L and V_L , see Figure 6)

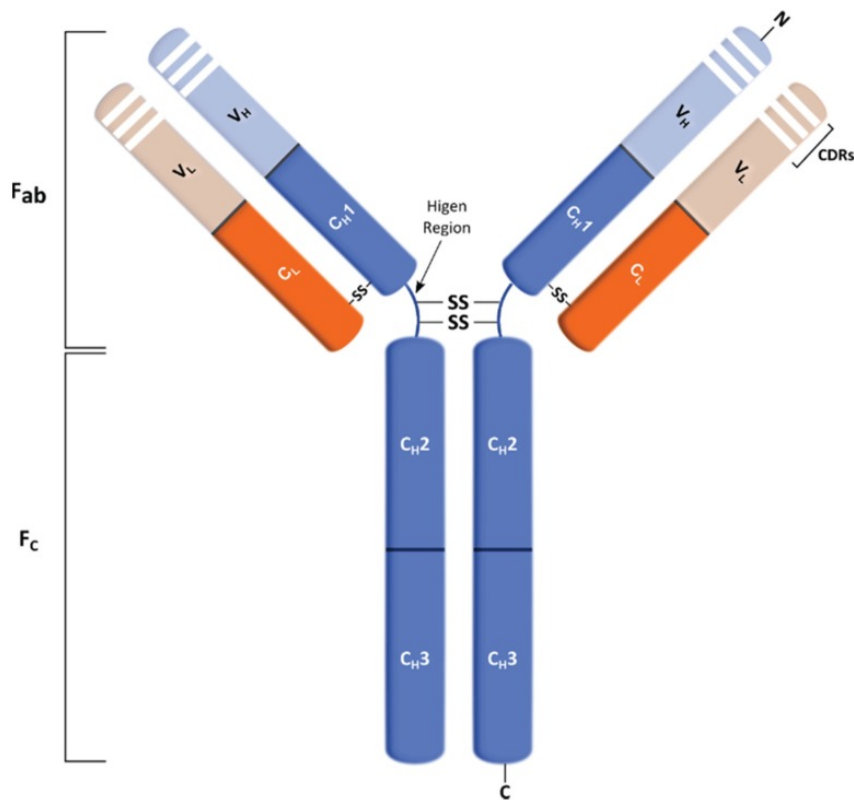


Figure 6. Structural and functional subunits of IgGs (from 109)

Functionally, Abs contain two antigen-binding fragments (Fab), which consist of variable regions V_H and V_L and constant regions C_L and C_{H1} , while the rest of the antibody makes up F_c , a “crystallizable” fragment. The variable part of Fab, dubbed also F_v , has the ability to recognize and specifically bind to various target molecules, called antigens (Ag). A huge library of amino acid sequences available in over 10^{12} different antibody molecules that a human typically produces allows recognition of a great range of diverse molecular targets.¹¹⁰

While hyper-variable complementarity-determining regions (CDRs) of F_v determine antigen binding properties of the Ab, the role of F_c is in the

interaction with the immune system. Fc either binds the Fc receptor (FcR), present on the surface of various immune cells, thereby triggering their responses, or it binds parts of the complement system, causing activation via classical pathway.¹¹⁰

I.2.1.2 Application of Abs

The main advantage of using antibodies as therapeutics is their high specificity and ability to naturally interact with components of the immune system without disrupting homeostasis. Some mechanisms of antibody action, such as toxin and virus neutralization and complement activation, and direct antimicrobial functions, such as the generation of oxidants, are independent of other host immune components. By contrast, antibody-dependent cellular cytotoxicity and opsonization are dependent on cellular and other host mediators.¹¹¹

Beside their use as therapeutics, antibodies are widely used as laboratory reagents for diagnosis, purification and many other purposes.¹⁰⁹ A large portion of current research on Abs, either as naked Abs or antibody-drug conjugates (ADCs), is focused on anti-cancer therapy (Table 2).¹¹² In addition, many Abs and ADCs specific to microbial targets can also be used for treatment and diagnosis of various infectious diseases.¹¹³⁻¹¹⁶ Examples include *Clostridium difficile* toxin neutralization,¹¹³ anti-HIV action¹¹⁵ and delivery of ionizing radiation to fungal infections.¹¹⁶

Table 2. Overview of major research of Abs as anti-cancer agents (from 112)

| mAb-based therapeutic | Structure | Characteristics of target antigen | Example of major ongoing research questions |
|----------------------------------|--|--|--|
| Antitumour mAbs | Unmodified IgG or IgG modified to mediate enhanced ADCC | Tumour-associated surface antigen | Are IgGs with enhanced affinity for Fc receptors more clinically effective than unaltered IgG? |
| Angiogenesis inhibition | Unmodified IgG | Host molecules that control angiogenesis | What is the best way to evaluate clinical response in patients treated with angiogenesis inhibitors? |
| T cell checkpoint blockade | IgG1 (blocks checkpoint and mediates ADCC) or IgG4 (blocks checkpoint without mediating extensive ADCC) | Molecules that limit the anticancer T cell response | How should we combine checkpoint blockade mAbs with each other, with other immunotherapeutics and with other anticancer agents? |
| Radioimmunotherapy | Unmodified IgG or mAb fragment | Tumour-associated antigen that is not shed or present in the circulation | How can the logistics of administering successful radioimmunotherapeutic agents be simplified to enhance their clinical utility? |
| Antibody–drug conjugate | IgG modified with cleavable linker and drug | Highly specific tumour-associated antigen that can internalize when bound by a mAb | What is the best combination of linkers and drugs with each mAb and target antigen? |
| Bispecific antibody | Variable regions from cancer-specific mAbs linked to variable regions specific for activating receptors on T cells | Tumour-associated antigen that is not commonly absent in antigen-loss-resistant cancer variants | Can effective bispecific constructs that have modified kinetics (thereby avoiding the logistic complexities of continuous infusion) be developed? |
| Chimeric antigen receptor T cell | Gene therapy approach to modifying T cells by inserting DNA coding for the mAb variable region fused to DNA coding for signalling peptides | Highly tumour-specific antigen that is not commonly absent in antigen-loss-resistant cancer variants | Can very promising preliminary results be extended to solid tumours, or will toxicity be associated even with low levels of target antigen expression by benign cells? |

ADCC, antibody-dependent cellular cytotoxicity; IgG, immunoglobulin G; mAb, monoclonal antibody.

1.2.1.3 Antibody-nanoparticle conjugates

Traditionally, Abs are considered both effectors and delivery vehicles, due to their unique biological properties. Lately, with the expansion of nanotechnology, a big number of NP-based agents have been decorated with Abs to combine their powerful molecular targeting with the properties of NPs as delivery vehicles. Ab-conjugated NPs are used either as delivery vehicles for drugs and imaging agents, or *in vitro* for various purposes such as enzyme immobilization, immunoassays, transfection, purification, etc.¹¹⁷

Just like in the case of naked Abs and ADCs, there are many examples of Ab-conjugated NPs for cancer therapy or imaging.¹¹⁸⁻¹²⁰ Among many other potential applications, we will focus here on radio-conjugated vehicles and diagnosis of infectious diseases.

I.2.1.3.1 Radio-labelled antibody-nanoparticle conjugates

Radio-labelled Abs or Ab-NP conjugates have a two-fold application as imaging agents or for radioimmunotherapy (as theranostic in case both features are combined). Radioimmunotherapy is a strategy of linking radionuclides to Abs or Ab-NP conjugates in order to specifically deliver radiation toxic to the target cell. This approach is widely used for targeting cancer cells, but it has also proven effective for use in infections.¹¹¹

Examples of nano-vehicles using Abs as targeting moieties for enhanced radioimmunotherapy include targeting anti-MUC-1-expressing tumors with ¹¹¹In labelled NPs¹²¹ and VEGF-expressing tumors with ¹³¹I labelled NPs.¹²²

Radioimmunotherapy of infectious diseases using targeted NPs has, to best of our knowledge, not been explored so far. Considering an urgent need for more efficient means to deal with drug resistance in this field, such an approach could provide potentially big benefits.

I.2.1.3.2 Antibody-nanoparticle conjugates for infection diagnosis

Fluorescent silica NPs decorated with Abs have successfully been used to detect *Mycobacterium tuberculosis*.¹²³ A rapid ELISA detection based on anti-human IgG decorated gold NPs, using a test strip, allows detection of Herpes Simplex Virus type 2 in only 15-20 minutes.¹²⁴ Magnetic NPs coated with Abs have successfully been used for detection and immunogenic separation of food-borne pathogens such as *E. coli* and *Salmonella*.¹²⁵ Also, fluorescent Ab-NP conjugates have been used for a rapid bacteria detection in human blood samples.¹²⁶

I.2.1.4 Limitations of Abs

Despite Abs being first and most widely used ligands for molecular targeting, their complex structure imposes several limitations to their use. First, eukaryotic expression systems are required for production of Abs, which renders them costly and sparse. Their large size limits their ability to penetrate tissues and bind epitopes that are not easily accessible.¹²⁷ This, in combination with the interaction with FcR, leads to long half-life, which is suboptimal for purposes such as imaging, where fast clearance is required for good contrast.¹²⁸ Due to their thermal and chemical instability and pharmaceutical formulation (often in liquid form), storage and transport conditions are restrictive, but also the conditions that can be used for their manipulation, such as solvents, temperature and pH.

Advances in protein engineering have recently allowed the development of different strategies for overcoming these limitations of Abs. Two main strategies that rely on natural immune system components include using (i) Ab fragments, that are obtained either by proteolytic digestion of Abs¹²⁹ or by *in vitro* expression,¹³⁰ and (ii) nanobodies (Nb), fragments of camelid antibodies that provide good binding properties along with small size and good stability.¹³¹ However, the immune system is not the only source of specific recognition molecules. Alternative scaffolds for specific binders that offer unprecedented advantages and customization possibilities are available nowadays.¹³²

1.2.2 Alternative scaffolds for molecular targeting

Specific binding exists in many naturally occurring proteins which can provide a starting point for the design of novel agents for molecular targeting. In order to be useful, these scaffolds should combine molecular recognition properties of Abs with further advantages, such as small size, improved stability, and easy and cheap production.¹³² They are commonly between 2 and 20 kDa in size, composed of one single polypeptide chain, stable at high temperatures and a wide range of pH, making them highly compatible with chemical synthesis, and easily produced in bacteria in large amounts.¹³³ Furthermore, good candidates for alternative scaffolds should have a robust, stable conformation, and tolerance towards amino acid

substitution and multimerization.¹³⁴ Some notable examples of these scaffolds are given in Table 3,¹³³ while a non-exhaustive list of 102 target proteins and 139 binding proteins from 20 different types of alternative scaffolds can be found in the SI of the review of Sklerk et al.¹³⁵

Table 3. Some examples of scaffolds alternative to Abs and their basic characteristics.¹³⁵⁻¹³⁷

| Scaffold name (commercial name) | Parent protein | Origin of the parent protein | Residues / S-S bridges | Structure | Randomization | Selection method | Company |
|---------------------------------|-----------------------------------|------------------------------|------------------------|--|---|--|----------------------|
| ABD | Albumin-binding domain | Bacterial | 46/0 | Three α -helices | 15 surface residues | Phage display, ribosome display | |
| Adhiron | Phytocystatin protein | Plant | ~ 100/0 | Four-strand antiparallel β -sheet core with a | Insertion of two variable peptide regions | Phage display | |
| Monobody (Adnectin) | 10th domain of human fibronectin | Human | 94/0 | β -sandwich of seven β -sheets | Residues in BC, DE, and FG loops (loop library) or in in C and D β -sheets, DE and FG loops (side and loop library) | Phage display, mRNA display, yeast display, yeast-two-hybrid | Adnexus Therapeutics |
| Affibody | Z-domain of SpA | Bacterial | 58/0 | Three α -helices | 13 residues in two helices | Phage display, ribosome display | Affibody AB |
| Affilin | γ -B-crystallin | Human | 176/0 | β -sheet | Eight residues | Phage display | SCIL Proteins |
| Affilin | Ubiquitin | Human | 76/0 | α/β | Six residues in the β -sheet | Ribosome display | SCIL Proteins |
| Affimer | Protease inhibitor Stefin A | Human | 98/0 | Threefold clustering | 12–36 residues | Phage display, yeast-two-hybrid, CIS display | Avacta Life Sciences |
| Affitin (Nanofitin) | DNA-binding protein Sac7d (Sso7d) | Archaea | 66(64)/0 | Five-stranded incomplete β -barrel and α -helix | 10-14 residues located in the β -sheet (surface library); additional elongated loop (surface and loop library) | Ribosome display | Affilogic |
| Alphabody | Triple antiparallel helices | Artificial (de novo design) | 70–100/0 | Three α -helices | 11 residues (A and C helix) | Phage display | Complex |
| Anticalin | Lipocalins | Human/insect | 160–180/0–2 | Eight-stranded β -barrel | Four loops (up to 24 AA) | Phage display | Pieris AG |

| Scaffold name (commercial name) | Parent protein | Origin of the parent protein | Residues / S-S bridges | Structure | Randomization | Selection method | Company |
|----------------------------------|--|---------------------------------------|--------------------------------------|---|--|--|----------------------|
| Armadillo repeat proteins | Armadillo (homologous to β -catenin) | Various/artificial (consensus design) | $n \times \sim 40/0$ | Three α -helices | Six residues in each internal repeat | Ribosome | |
| Atrimer / Tetranectin | C-type lectin domain CTLD3 | Human | $n \times 40/3$ S-S | Five flexible loops | 11 residues | Phage display | Anaphore |
| Avimer / Maxibody | Multimerized LDLRA module | Human/artificial (consensus design) | $n \times \sim 43/3$ S-S + Ca^{2+} | Four loops | 28 residues | Phage display | Amgen |
| Bicycle peptides | Synthetic | - | 9-15/1-2 | Two loops | - | - | Bicycle therapeutics |
| Centryn | Fn3 domains of hTenascin C (Tencon) | Human | 89/0 | β -Sheet | 13 residues | CIS display, phage display | |
| DARPin | Ankyrin repeat proteins | Human/artificial (consensus design) | $67 + n \times 33/0$ | $\alpha 2/\beta 2$ repeated | 7-8 residues in each n-repeat; additional 13 residues in elongated loop (LoopDARPin library) | Ribosome display, phage display, yeast display | Molecular Partners |
| Fynomer | SH3 domain of the human Fyn tyrosine kinase | Human | 63/0 | β -Sandwich | Six residues in two loops (RT- and n-Src-loop) | Phage display, DNA display | Covagen |
| Kunitz domain | BPTI/LAC1 D1/ITID2/APPI | Human | 58/3 S-S | α -helices, β -sheets | 1-2 loops | Phage display | DYAX |
| L35Ae 10x | 50S ribosomal RNA-binding protein | Archaea | 78/0 | Six-stranded β -barrel, 3 CDR-like loops, α -helix | 20-24 residues in loop regions; additional elongated loop | Phage display | |
| OB-fold (Obody) | OB-fold of the aspartyl tRNA | Archaea | 111/0 | Five-stranded β -barrel | 17 residues | Phage display | |
| Pronectin | 14th extracellular domain of human fibronectin | Human | 90-95/0 | Two β - sheets and three surface exposed loops | Three loops (BC, DE, FG loops) | Phage display | Protelica |
| rcSso7d | DNA-binding protein Sac7d (Sso7d) | Archaea | 62/0 | Five-stranded incomplete β -barrel and α -helix | 9 residues in the β -sheet | Yeast display | |

I.2.2.1 Selection of binders from alternative scaffolds

A traditional rational design approach of engineering interactions between molecules is not very useful in predicting binding specificity of different amino-acid sequences, due to extreme conformational complexity and a variety of interactions involved in recognition. Thus, combinatorial approaches that rely on huge libraries of random structures from which binders are selected (much like the natural process of Ab maturation) are preferable.¹³⁸ Usually, a number of amino-acids determined to be part of the binding interface are randomly mutated to provide molecules of unchanged conformation, but diverse binding specificities. Then, a target-driven selection is applied to eliminate binders that don't bind to the desired molecule. Using larger libraries improves the chances of finding proper binders, while increasing the number of cycles of selection improves specificities and affinities of selected binders.

Selection systems are based on links between the genotype and phenotype that enables amplification of selected proteins via their nucleotide sequences. Based on the way this link is established, selection systems can be classified into three groups: cell-based display, cell-free display, and non-display systems.¹³⁸

First selection systems were cell-based display systems, such as phage display¹³⁹ and yeast display.¹⁴⁰ Advantages of cell based systems include application of flow cytometry for screening and generally narrow

specificities of binders after multiple cycles of selection. However, a big limitation is library size which goes up to a maximum of 10^{10} variations.¹²⁹

Non-display systems, such as protein complementation assay (PCA),¹⁴¹ take full advantage of cellular machinery of expression bacteria, performing selections inside the cells by linking cell survival to successful binding to the target molecule. This approach allows high-throughput screening in a simple procedure, but there are still major limitations related to specificity and affinity of selected binders.¹³⁸

Cell-free display systems, being completely *in vitro* methods, combine large library sizes with very efficient and precise affinity maturation.¹⁴² A widely used cell-free display system is ribosome display, first described in 1994.¹⁴³

I.2.2.1.1 Ribosome display

Ribosome display technique relies on ternary complexes consisting of mRNA, a ribosome and the protein bound together. *In vitro* transcription of the combinatorial DNA library (10^{12} or more members) yields mRNA, which is then used for *in vitro* translation. Since no stop codon is introduced into the mRNA, the ribosome stalls at the end of the sequence without releasing the protein.¹⁴⁴ The library of ternary complexes is then exposed to the immobilized target for selection of binders. This process is repeated in

cycles, using output of each cycle, after mRNA dissociation, reverse transcription and PCR amplification, as the input of the next (Figure 7).

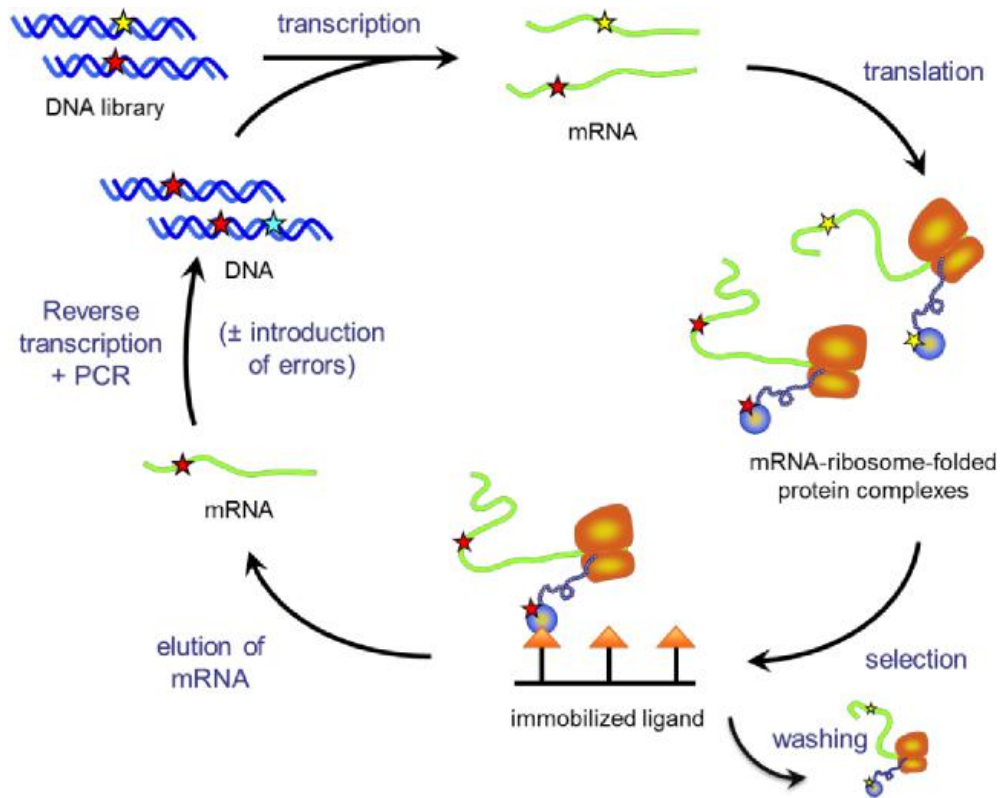


Figure 7. Schematic representation of a ribosome display selection. A DNA library is obtained in the form of a PCR product. In vitro transcription yields mRNA that is used for in vitro translation. Ribosome stalls at the end of the mRNA and does not release the encoded and properly folded protein due to an absence of a stop codon. The ternary complexes are used for affinity selection on an immobilized target. The mRNA of bound complexes is recovered, reverse transcribed and amplified by PCR. Then, the selected pools of binders can be used directly for the next cycle of ribosome display or analysis of single clones after cloning into expression vectors, which are then used for *E. coli* transformation and small-scale in vivo expression.¹⁴⁵

Selection can also be performed in solution. In that case, a biotinylated target could be used in order to subsequently immobilize complexes to the streptavidin support and wash away the unbound ones.¹⁴⁵ Finally, selected binders can be cloned into the expression vector and produced in *E. coli*.

I.2.2.2 NPs decorated with alternative-scaffold targeting moieties

Examples of NPs decorated with alternative scaffold targeting moieties include DARPin-targeted and Affibody-targeted NPs specific for Human Epidermal growth factor Receptor 2 (HER2), which is a protein marker overexpressed in breast cancer cells.¹⁴⁶

DARPin_9-29, that specifically binds HER2 molecule, has been passively adsorbed to the surface of gold NPs, yielding NPs with approximately 35 DARPin molecules attached to the surface. These targeted nanostructures have shown high affinity towards targeting and endocytosis of cancer cells, providing a promising platform for efficient targeting HER2 overexpressing tumours.¹⁴⁷

Another HER2-specific DARPin, dubbed G3, has been used to decorate 100 nm superparamagnetic NPs for enhanced MRI monitoring of HER2 expression in transplantation breast tumours.¹⁴⁸

Very small NPs, consisting of Affibodies specific for HER2 and attached to a DNA sequence, which serves as an anchor for two Affibody molecules and as a vehicle that non-covalently binds multiple copies of a small molecule drug, have been described. This innovative nanoparticle has a small size of only 95 kDa and is capable of carrying around 53 molecules of doxorubicin per complex, demonstrating selective and highly efficacious inhibition of HER2 overexpressing cancer cells.¹⁴⁹

Larger, polymeric NPs have also been decorated with a HER2 targeting Affibody. These vehicles have been shown to internalize in cancer cells. When they are used to deliver Paclitaxel to the target cells, their cytotoxicity was shown to be significantly higher compared to the free drug or the non-targeted NPs carrying the drug, confirming the adequacy of this approach for increasing selectivity and efficacy.

II. *Staphylococcus aureus*

S. aureus is a Gram-positive microbe that is consistently present in approximately one-third of the human population, while another one-third is colonized intermittently.¹⁵⁰ While it usually acts as a commensal of the human microbiota, it can become a dangerous opportunistic pathogen which is a common cause of skin and respiratory infections, as well as food poisoning.¹⁵¹ Unfortunately, the events leading to the infections, especially those leading to the transition from colonization to infection, are ill-defined *in vivo*.¹⁵²

Clinical significance of *S. aureus* today comes from the fact that this microbe is notorious for its ability to develop resistance mechanisms against virtually any antibiotic, which is correlated with higher mortality and other negative outcomes.¹⁵¹ This creates a clear need for innovative alternative strategies against it.

II.1 Clinical significance of *S. aureus*

The annual number of patients that require medical treatment of *S. aureus* infections is higher than one million, including 490.000 hospitalizations, 93.000 cases of bacteremia and 35.000 cases of sepsis and/or endocarditis,¹⁵³ resulting in more than 20.000 fatal outcomes annually.

Negative outcomes are associated to the presence of drug resistance in the infectious strain. Methicillin-resistant strains, labelled MRSA, which are typically multi-drug resistant, account for most of the cases with negative outcomes. Their resistance to methicillin and other β -lactams has the molecular basis in acquisition of the specific penicillin-binding protein, labelled PBP2a, which renders even penicillinase-resistant drugs useless.¹⁵⁴

Broadly, *S. aureus* infections can be divided into skin and soft tissue infections (SSTIs), and bloodstream infections.

II.1.1 SSTIs

Although breaches in skin following trauma or surgical procedures are related to increased risk of SSTIs, they often occur without any breach in the skin, for example through hair follicles.¹⁵¹ SSTIs manifest as purulent exudates draining from the infectious sites. Considering that around 20% of patients with SSTIs develop recurrent infections with the same strain of bacteria¹⁵⁵ it is likely that prior infection does not induce a protective immune response in this case.

Patients with compromised immune systems tend to be more susceptible to SSTIs.^{156,157} A growing body of evidence suggests a crucial role of T_H17 cells as protectors against *S. aureus* skin and lung infections, but these cells might be less important for infections of other tissues.¹⁵⁸

II.1.2 Bloodstream infections

S. aureus is a leading cause of bacteremia in United States,¹⁵⁹ resulting in a 20% 30-day mortality.¹⁶⁰ Most of these cases of bacteremia are hospital-acquired, either nosocomial or with community onset, while only 28% account for community-acquired infections. Furthermore, hospital-acquired cases tend to be more severe, with over 50% of them being due to MRSA, compared to only 14% of the community-acquired ones.¹⁶¹

Among the risk factors, by far the most important one is use of prosthetic devices such as catheters, implants and orthopedic prosthetics.¹⁶² These devices provide to the microbe direct access to bloodstream. Other risk factors include underlying medical comorbidities, intravenous drug use, immunosuppression and malignancy.¹⁶³

II.2 Molecular basis of pathogenicity and immune evasion

S. aureus has developed a formidable arsenal of factors to evade innate immunity. Crucial defense mechanisms employed against this pathogen include phagocytosis, primarily by neutrophils;¹⁶⁴ and the system of complement, capable of rapid recognition and direct killing of bacteria.¹⁶⁵ Furthermore, opsonization that occurs either by the components of the complement or IgGs facilitates neutrophil phagocytosis.¹⁶⁶ These and other immune responses are actively counteracted by a wide range of mechanisms

employed by the microbe. Figure 8 illustrates some of the most important immune evasion mechanisms of *S. aureus*.

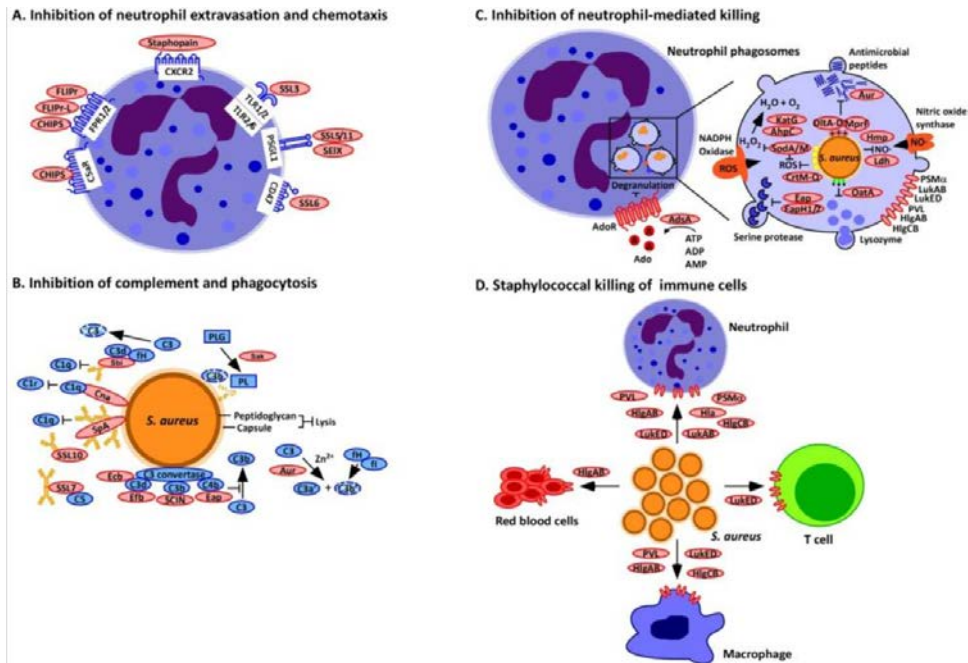


Figure 8. *S. aureus* immune evasion examples (From 167) (a) Neutrophil extravasation and chemotaxis is inhibited by *Staphylococcus aureus* through the secretion of staphylococcal superantigen-like (SSL) molecules, as well as chemotaxis inhibitory protein of *S. aureus*, formyl peptide receptor-like 1 inhibitor and staphopain. (b) Complement activation and phagocytosis of staphylococci are blocked through the secretion of inhibitory factors to interfere with opsonization. (c) *S. aureus* inhibits neutrophil-mediated killing of phagocytosed bacteria by expressing several enzymes and inhibitors such as adenosine-synthesizing enzyme staphyloxanthin, superoxide dismutase, the catalase *KatG* and alkylhydroperoxide reductase, aureolysin and others. (d) Secreted β -barrel pore forming toxins (β -PFTs), bind specific receptors on immune cells to impair immune cell functions or promote cell lysis.

II.2.1 Neutrophil extravasation and chemotaxis

Pro-inflammatory signals promote neutrophil adhesion and extravasation through capillary endothelia, seeking to migrate neutrophils towards the bacterial invaders.¹⁶⁷ However, *S. aureus* can interfere with this process through secretion of different factors that inhibit and block molecular interactions necessary for the process.

Superantigen-like proteins (SSLs) are a family of proteins heavily involved in blocking adhesion and rolling of neutrophils,¹⁶⁸ as well as their activation.¹⁶⁹ Furthermore, they activate platelets¹⁷⁰ and prevent immune cell recognition of lipoproteins and peptidoglycan of *S. aureus*.¹⁷¹ This family of proteins provides a wide range of defense to the microbe and exemplifies the diversity of mechanisms evolved by *S. aureus* in response to hosts defenses.

II.2.2 Complement activation and phagocytosis

Beside the peptidoglycan, that protects *S. aureus* as a Gram positive bacterium, from direct killing by complement, this microbe can also contain the capsular polysaccharide that protects it from efficient opsonization by complement that would lead to neutrophil phagocytosis.¹⁷²

Furthermore, several proteins are secreted by *S. aureus* to interfere with some of the crucial reactions in the complement cascade. Examples of these include Aureolysin, a secreted metalloprotease that cleaves C3 to

generate C3a and C3b factors of complement,¹⁷³ as well as Staphylococcal Complement Inhibitor, which inhibits the C3 convertase.¹⁷⁴

II.2.3 Neutrophil-mediated killing

Even when phagocytosis evasion mechanisms of *S. aureus* fail, once phagocytosed, the microbe has evolved mechanisms to survive exposure to a variety of toxic products that kill and degrade bacteria in the phagosome environment.

The microbe evades lysosome and antimicrobial-peptide mediated killing by blocking either the enzyme (lysosome) or the peptide binding to the envelope target. This is achieved via peptidoglycan acetylation, D-alanylation of teichoic acids, and lysyl- or alanyl-phosphatidylglycerol synthesis.^{167,175-177}

S. aureus expresses two pigments to protect from phagosome environment. Staphyloxanthin provides resistance against hydrogen peroxide/hydroxyl radicals,¹⁷⁸ while flavohemoglobin is a factor protecting the microbe from nitrosative stress.¹⁷⁹ In addition, a number of enzymes are expressed to protect it against these factors too.¹⁶⁷

II.2.4 Staphylococcal killing of host cells

Beside protecting itself from the immune system by evasion, *S. aureus* is also capable of inducing the killing of the innate immune cells.

The microbe secretes β -barrel pore forming toxins (β -PFTs), which bind specific receptors on immune cells to impair immune cell functions or promote cell lysis. Typical example of a β -PFT is α -hemolysin, which binds to neutrophils via its receptor ADAM10, assembling into a heptameric pore. Beside neutrophils, other β -PFTs can bind and modulate T-cells, macrophages, erythrocytes, but also epithelial cells.¹⁸⁰ Phenol-soluble modulin α is another factor secreted by *S. aureus* which is not a β -PFT, but can also lyse leukocytes.¹⁸¹

II.2.5 Other factors of pathogenicity and immune evasion

S. aureus secretes two enzymes, coagulase and Willebrand Factor-binding protein, to modulate coagulation of the host, thus protecting itself from this innate immunity response.¹⁸²

However, beside many mechanisms *S. aureus* uses to evade innate immunity, it also possess an impressive ability of evading the specific, adaptive immune responses.¹⁶⁷ Over 23 different enterotoxins and T-cell superantigens are mobilized to neutralize the T-cell adaptive immune response.¹⁸³ A central role in evading the B-cell response is played by the Staphylococcal protein A (SpA), which is the most common molecule on the surface of *S. aureus*.¹⁶⁷ It is one of the most studied virulence factors of *S. aureus* with many important functions.

II.3 SpA

SpA was initially described as an Immunoglobulin Binding Protein (IBP), considering its high affinity binding to the Fc fragments of human and mouse antibodies.¹⁸⁴ This feature has been heavily exploited for affinity purification of IgGs in laboratory work. Further studies provided detailed insight into the structure and multiple important roles of SpA in *S. aureus*.

II.3.1 Structure of SpA

SpA is highly resistant to denaturing factors, including high temperature, wide range of pH, and trypsinization.^{185,186} Its structure includes a signaling sequence (S-region), five highly homologous IgG-binding domains (E, D, A, B, and C), each consisting of 58-62 amino acids, and a C-terminal part (XM-region, around 150 amino acids).^{187,188} This C-terminal part is the highly heterogeneous part of the molecule, responsible for embedding SpA in the bacterial cell wall. SpA can either be bound to the outer layer of the cell wall, or released into the surrounding medium.¹⁸⁹

II.3.2 Roles of SpA in *S. aureus*

The IgG binding activity of SpA has been its first function to be described. Binding the Fc fragment, it enables *S. aureus* to avoid opsonization with IgGs, since they bind in the wrong orientation. It has been demonstrated in mice that a *S. aureus* strain where 4 amino acids crucial to

IgG-binding were mutated, has been unable to evade immune response and as a result was quickly phagocytosed and elicited B cell response to key virulence antigens.¹⁹⁰ Thus, SpA provides an essential immune-evasion mechanism to the microbe.

Beside binding the Fc fragment of IgGs, which provides protection from opsonization, SpA can also bind a Fab fragment of a V_H3 clan IgM antibodies, crosslinking them and promoting B-cell superantigen activity.¹⁹¹ This causes either a proliferative response that leads to the apoptotic collapse, or to a secretion of non-specific Abs that exhausts the capacity of the immune response disabling specific activation (Figure 9).¹⁶⁷

In *S. aureus*-associated osteomyelitis, it has been found that SpA is able to bind osteoblasts and inhibit *de novo* bone formation, thus demonstrating a central role of SpA in progression of this pathogenesis.¹⁹²

Another significant role of SpA is in modulating multicellular behaviors of *S. aureus*. It has been shown to participate in self-aggregation of bacterial cells and to have a related function in the second phase of biofilm development, which is the accumulation phase, characterized by cells clustering together to form the maturing biofilm community.¹⁹³ In contrast, SpA seems to play no role in the attachment of bacteria to the surfaces, as shown on the example of silastic catheters.¹⁹⁴

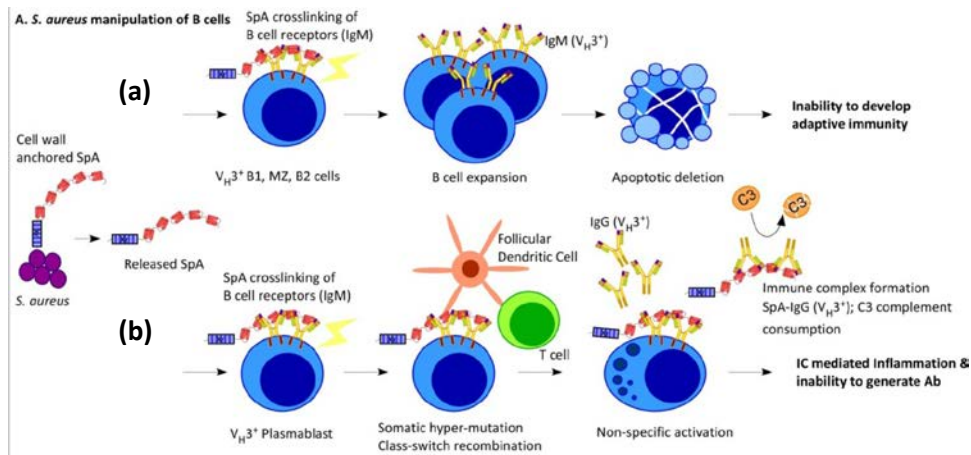


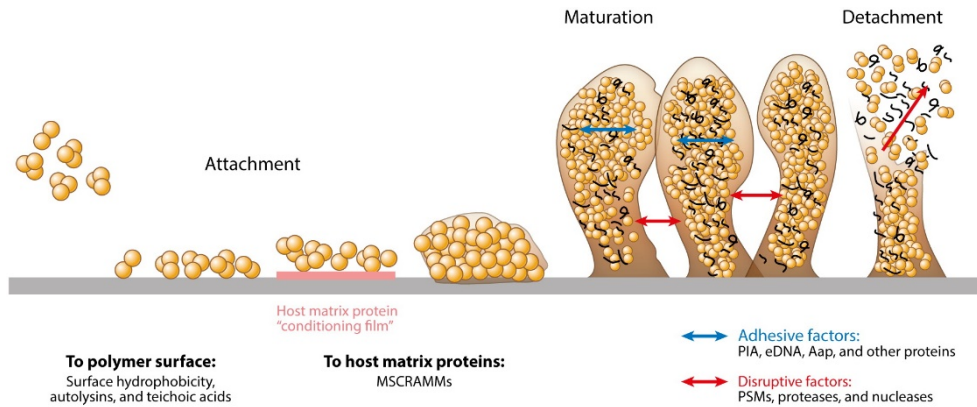
Figure 9. SpA role in B-cell response evasion (adapted from 167) (a) *S. aureus* releases SpA into host tissues, where it binds to and crosslinks V_H3 clan B cell receptors. In B1 cells, marginal zone B cells and B2 cells, SpA crosslinking is associated with proliferative expansion and apoptotic collapse. The death of these cells impedes the development of adaptive immunity during *S. aureus* infections. (b) In V_H3 plasmablasts, SpA crosslinking promotes somatic hypermutation and class switching from IgM antibodies to IgG antibodies, followed by the secretion of antibodies that are not specific for the *S. aureus* antigen.

II.4 *S. aureus* biofilms

For a long time, bacteria were considered to exist only as unicellular, self-sufficient organisms incapable of forming complex multicellular structures. However, today we know that most bacteria in nature, instead of the planktonic form, exist in complex, surface-associated communities called biofilms.¹⁹⁵ Staphylococcal biofilms are of great clinical significance, since they are the most frequent cause of biofilm-related infections, especially those related to medical devices such as catheters, artificial heart valves and prostheses, but also to wound infections and native valve endocarditis.¹⁹⁶ Furthermore, they are found to correlate with increased antibiotic resistance and virulence of bacteria.¹⁹⁷

II.4.1 Biofilm formation

Traditionally, biofilm formation is divided into three main phases: attachment, maturation, and detachment (Figure 10).^{196,198} Recent observations suggest that attachment and maturation phases might be happening simultaneously or in a perturbed order,¹⁹⁹ but they still constitute a good model since they are characterized by different molecular processes.



AR Otto M. 2013.
Annu. Rev. Med. 64:175–88

Figure 10. Biofilm formation phases (from 196). Attachment might occur either directly to a surface (such as polymer surface of an indwelling medical device) or to host matrix proteins that form a “conditioning film” on this surface. Maturation then proceeds via agglomeration of cells and formation of characteristic channels between them. The disruptive forces that are responsible for this channel creation also facilitate the last, dissemination phase. Abbreviations: Accumulation-associated protein (Aap), extracellular DNA, Microbial Surface Components Recognizing Adhesive Matrix Molecules (MSCRAMMs), Polysaccharide Intercellular Adhesin (PIA), Phenol-Soluble Modulins (PSMs).

II.4.1.1 Attachment

Primary attachment encompasses cell-to-surface interactions, which can occur between the cells and either abiotic or biotic surfaces.

Attachment to abiotic surfaces mostly relies on physicochemical characteristics of the cell surface and the abiotic surface, driven by either hydrophobic or electrostatic interactions. Specific molecules present on the surface of *Staphylococci*, such as autolysin²⁰⁰ and teichoic acids,²⁰¹ are involved in these interactions.

Completely different set of molecules is involved in attachment to biotic surfaces, such as human tissues. *Staphylococci* express a variety of molecules that bind specifically to host matrix proteins, labelled MSCRAMMs.²⁰² These molecules play a crucial role in medical-device-related biofilm infections, considering that all indwelling medical devices become covered with host matrix proteins soon after insertion.¹⁹⁶

II.4.1.2 Maturation

Maturation phase is characterized by cell-cell interactions, which are mediated by a different set of factors, including SpA. These interactions can be either adhesive or disruptive, contributing to either biofilm accumulation or formation of channels, respectively.

The most important molecule involved in the adhesive process of accumulation of biofilm mass is probably an exopolysaccharide named polysaccharide intercellular adhesin (PIA).²⁰³ Still, many strains heavily rely on other molecules such as Accumulation-associated protein (Aap)²⁰⁴ or SpA.¹⁹³

Disruptive processes that occur during the maturation phase play a role in the formation of channels,¹⁹⁸ which facilitate nutrient diffusion to deeper biofilm layers.¹⁹⁶ Furthermore, these processes facilitate detachment and dissociation of the cells that occurs in the final dissemination phase. These processes are controlled by a large set of factors, many of them related to the quorum-sensing accessory gene regulator (Agr) system.²⁰⁵ Beside the molecules involved in disruptive processes, this system is known to also control the expression of a number of other molecules involved in biofilm formation,²⁰⁶ thus indicating that the quorum-sensing phenomenon plays a central role in biofilm development.

1.4.1.3 Dissemination phase

Dissemination phase, which happens when biofilms mature and grow to a certain level, is characterized by either individual cells or clusters detaching from the biofilm and migrating to a different site. This happens in outer most layers of biofilms, as a result of disruptive forces becoming predominant. Beside dissemination of the biofilms to other sites, this

detachment allows for regrowth of the biofilm that replaces the detached biofilm mass. This process is of particular importance *in vivo*, where it contributes to infections spreading. For example, biofilms introduced via medical devices, can spread and cause more severe secondary infections following detachment from the original biofilm.¹⁹⁶

Only Phenol-Soluble Modulins (PSMs) have been shown to have a significant role in the dissemination phase *in vivo*, considering the complexities of *in vivo* biofilm assays.²⁰⁷ However, it is assumed that any factor that plays a role in the disruptive processes of the maturation phase is also important for the *in vivo* dissemination.

II.4.2 Biofilm formation assays

Biofilm formation assays can be broadly classified as indirect and direct methods. Indirect methods allow high-throughput screenings, but provide little information about the nature of formed biofilms or the particular processes that are being affected. Direct methods provide more elaborate insight at a cost of a lower output due to lengthy and labor-intensive techniques used.²⁰⁸

II.4.2.1 Indirect methods

Most commonly used indirect biofilm formation assay is a microtiter dish assay called Crystal violet (CV) assay. It is based on incubation of biofilms in the wells of a microtiter dish, followed by staining using crystal violet. A more general term “microtiter dish assay” is applied when other dyes are used for staining. After the non-attached cells are washed off, a dye is solubilized, which allows quantification of the formed biofilms. Advantages of this method are reduced price, simplicity and high throughput, which makes it useful as an initial screening method when multiple strains or diverse conditions need to be used. However, more elaborate assays need to be used to elucidate the effect that tested agents have on the particular processes that comprise biofilm formation.²⁰⁹

Many similar, simple and high-throughput assays, focusing on early stages of biofilm development have been described, relying on exopolysaccharide staining dyes,^{210,211} growth observation on solid media and other techniques.²¹²

II.4.2.2 Direct methods

Direct methods are typically more time intensive and therefore allow characterization of only a limited number of samples. However, they provide deeper insight into the particular changes that occur in the biofilm formation

process, as well as the much lower bias in estimating the impact of the tested factors.²⁰⁸

Examples of these methods include direct observation by scanning electron microscopy²¹³ or confocal laser-scanning microscopy,²¹⁴ as well as biofilm dry weight measurements.²¹⁵

III. References

1. Ehrlich, P. Beiträge zur Theorie und Praxis der histologischen Färbung. Thesis, Univ. Leipzig (1878) (in German).
2. Ehrlich, P. Aus Theorie und Praxis der Chemotherapie. *Folia Serologica* 7, 697–714 (1911) (in German).
3. Ehrlich, P. Die Wertbemessung des Diphtherie-heilserums und deren theoretische Grundlagen. *Klinisches Jahrbuch* 6, 299–326 (1897) (in German).
4. Fleming A. The discovery of penicillin. *British Medical Bulletin*. 1944 Jan 1;2(1):4-5.
5. Strebhardt K, Ullrich A. Paul Ehrlich's magic bullet concept: 100 years of progress. *Nature Reviews Cancer*. 2008 Jun;8(6):473.
6. Hoffman AS. The origins and evolution of “controlled” drug delivery systems. *Journal of Controlled Release*. 2008 Dec 18;132(3):153-63.
7. Kumar S, Aaron J, Sokolov K. Directional conjugation of antibodies to nanoparticles for synthesis of multiplexed optical contrast agents with both delivery and targeting moieties. *Nature protocols*. 2008 Feb;3(2):314.
8. El-Sayed IH, Huang X, El-Sayed MA. Surface plasmon resonance scattering and absorption of anti-EGFR antibody conjugated gold nanoparticles in cancer diagnostics: applications in oral cancer. *Nano letters*. 2005 May 11;5(5):829-34.

9. Niemelä E, Desai D, Nkizinkiko Y, Eriksson JE, Rosenholm JM. Sugar-decorated mesoporous silica nanoparticles as delivery vehicles for the poorly soluble drug celastrol enables targeted induction of apoptosis in cancer cells. *European Journal of Pharmaceutics and Biopharmaceutics*. 2015 Oct 1;96:11-21.
10. Munoz EM, Correa J, Fernandez-Megia E, Riguera R. Probing the relevance of lectin clustering for the reliable evaluation of multivalent carbohydrate recognition. *Journal of the American Chemical Society*. 2009 Nov 17;131(49):17765-7.
11. Gao H, Zhang Q, Yang Y, Jiang X, He Q. Tumor homing cell penetrating peptide decorated nanoparticles used for enhancing tumor targeting delivery and therapy. *International journal of pharmaceutics*. 2015 Jan 15;478(1):240-50.
12. Jiang X, Sha X, Xin H, Chen L, Gao X, Wang X, Law K, Gu J, Chen Y, Jiang Y, Ren X. Self-aggregated pegylated poly (trimethylene carbonate) nanoparticles decorated with c (RGDyK) peptide for targeted paclitaxel delivery to integrin-rich tumors. *Biomaterials*. 2011 Dec 1;32(35):9457-69.
13. Jin H, Pi J, Yang F, Jiang J, Wang X, Bai H, Shao M, Huang L, Zhu H, Yang P, Li L. Folate-chitosan nanoparticles loaded with ursolic acid confer anti-breast cancer activities in vitro and in vivo. *Scientific Reports*. 2016 Jul 29;6:30782.

14. Tassa C, Duffner JL, Lewis TA, Weissleder R, Schreiber SL, Koehler AN, Shaw SY. Binding affinity and kinetic analysis of targeted small molecule-modified nanoparticles. *Bioconjugate chemistry*. 2009 Dec 22;21(1):14-9.
15. Brodsky FM. Monoclonal antibodies as magic bullets. *Pharmaceutical research*. 1988 Jan 1;5(1):1-9.
16. Arruebo M, Valladares M, González-Fernández Á. Antibody-conjugated nanoparticles for biomedical applications. *Journal of Nanomaterials*. 2009 Jan 1;2009:37.
17. Owens B. Faster, deeper, smaller—the rise of antibody-like scaffolds.
18. Ventola CL. The nanomedicine revolution: Part 1: Emerging concepts. *Pharmacy and Therapeutics*. 2012 Sep;37(9):512.
19. What is Nanotechnology? | Nano. NNI (2018). Available at: <https://www.nano.gov/nanotech-101/what/definition>. (Accessed: 15th October 2018)
20. Granqvist CG, Buhrman RA, Wynn J, Sievers AJ. Far-infrared absorption in ultrafine Al particles. *Physical Review Letters*. 1976 Sep 6;37(10):625.
21. Uyeda T, Hayashi C, Tasaki A. *Ultra-Fine Particles: Exploratory Science and Technology*. Elsevier; 1995 Dec 31.
22. Kiss LB, Söderlund J, Niklasson GA, Granqvist CG. New approach to the origin of lognormal size distributions of nanoparticles. *Nanotechnology*. 1999 Mar;10(1):25.

23. Vert M, Doi Y, Hellwich KH, Hess M, Hodge P, Kubisa P, Rinaudo M, Schué F. Terminology for biorelated polymers and applications (IUPAC Recommendations 2012). *Pure and Applied Chemistry*. 2012 Jan 11;84(2):377-410.
24. Morachis JM, Mahmoud EA, Almutairi A. Physical and chemical strategies for therapeutic delivery by using polymeric nanoparticles. *Pharmacological reviews*. 2012 Apr 27:pr-111.
25. Kannan RM, Nance E, Kannan S, Tomalia DA. Emerging concepts in dendrimer-based nanomedicine: from design principles to clinical applications. *Journal of internal medicine*. 2014 Dec;276(6):579-617.
26. Nijhara R, Balakrishnan K. Bringing nanomedicines to market: regulatory challenges, opportunities, and uncertainties. *Nanomedicine: Nanotechnology, Biology and Medicine*. 2006 Jun 1;2(2):127-36.
27. Tyner K, Sadrieh N. Considerations when submitting nanotherapeutics to FDA/CDER for regulatory review. In *Characterization of nanoparticles intended for drug delivery 2011* (pp. 17-31). Humana Press.
28. Bawa R. Regulating nanomedicine-can the FDA handle it?. *Current Drug Delivery*. 2011 May 1;8(3):227-34.
29. Bellare JR. Nanotechnology and nanomedicine for healthcare: challenges in translating innovations from bench to bedside. *Journal of biomedical nanotechnology*. 2011 Feb;7(1):36-7.

30. Zhu M, Nie G, Meng H, Xia T, Nel A, Zhao Y. Physicochemical properties determine nanomaterial cellular uptake, transport, and fate. *Accounts of chemical research*. 2012 Aug 14;46(3):622-31.
31. Meng H, Yang S, Li Z, Xia T, Chen J, Ji Z, Zhang H, Wang X, Lin S, Huang C, Zhou ZH. Aspect ratio determines the quantity of mesoporous silica nanoparticle uptake by a small GTPase-dependent macropinocytosis mechanism. *ACS nano*. 2011 May 12;5(6):4434-47.
32. Rivera Gil P, Oberdörster G, Elder A, Puentes V, Parak WJ. Correlating physico-chemical with toxicological properties of nanoparticles: the present and the future. *ACS nano*. 2010 Oct 26;4(10):5527-31.
33. Ventola CL. Progress in nanomedicine: approved and investigational nanodrugs. *Pharmacy and Therapeutics*. 2017 Dec;42(12):742.
34. ClinicalTrials.gov. [Accessed October 19, 2018]. Available at: <https://clinicaltrials.gov>.
35. Ealia SA, Saravanakumar MP. A review on the classification, characterisation, synthesis of nanoparticles and their application. In IOP Conference Series: Materials Science and Engineering 2017 Nov (Vol. 263, No. 3, p. 032019). IOP Publishing.
36. Cha C, Shin SR, Annabi N, Dokmeci MR, Khademhosseini A. Carbon-based nanomaterials: multifunctional materials for biomedical engineering. *ACS nano*. 2013 Apr 5;7(4):2891-7.
37. Conniot J, Silva JM, Fernandes JG, Silva LC, Gaspar R, Brocchini S, Florindo HF, Barata TS. Cancer immunotherapy: nanodelivery

- approaches for immune cell targeting and tracking. *Frontiers in chemistry*. 2014 Nov 26;2:105.
38. Khalid M, El-Sawy HS. Polymeric nanoparticles: Promising platform for drug delivery. *International journal of pharmaceutics*. 2017 Aug 7;528(1-2):675-91.
39. Ventola CL. Progress in nanomedicine: approved and investigational nanodrugs. *Pharmacy and Therapeutics*. 2017 Dec;42(12):742.
40. Weissig V, Pettinger TK, Murdock N. Nanopharmaceuticals (part 1): products on the market. *International journal of nanomedicine*. 2014;9:4357.
41. Park JW. Liposome-based drug delivery in breast cancer treatment. *Breast Cancer Research*. 2002 Jun;4(3):95.
42. Giner-Casares JJ, Henriksen-Lacey M, Coronado-Puchau M, Liz-Marzan LM. Inorganic nanoparticles for biomedicine: where materials scientists meet medical research. *Materials Today*. 2016 Jan 1;19(1):19-28.
43. Wang YX, Hussain SM, Krestin GP. Superparamagnetic iron oxide contrast agents: physicochemical characteristics and applications in MR imaging. *European radiology*. 2001 Nov 1;11(11):2319-31.
44. García MA. Surface plasmons in metallic nanoparticles: fundamentals and applications. *Journal of Physics D: Applied Physics*. 2011 Jun 24;44(28):283001.

45. Tomalia DA, Baker H, Dewald J, Hall M, Kallos G, Martin S, Roeck J, Ryder J, Smith P. Dendritic macromolecules: synthesis of starburst dendrimers. *Macromolecules*. 1986 Sep;19(9):2466-8.
46. Carlmark A, Hawker C, Hult A, Malkoch M. New methodologies in the construction of dendritic materials. *Chemical Society Reviews*. 2009;38(2):352-62.
47. Newkome GR, Moorefield CN, Vögtle F. *Dendrimers and dendrons: concepts, syntheses, applications*. Wiley-VCH: Weinheim; 2001.
48. Kim Y, Park EJ, Na DH. Recent progress in dendrimer-based nanomedicine development. *Archives of pharmacal research*. 2018 Feb 15:1-2.
49. Kaminskis LM, Boyd BJ, Porter CJ. Dendrimer pharmacokinetics: the effect of size, structure and surface characteristics on ADME properties. *Nanomedicine*. 2011 Aug;6(6):1063-84.
50. Caminade AM, Yan D, Smith DK. Dendrimers and hyperbranched polymers. *Chemical Society Reviews*. 2015;44(12):3870-3.
51. Boas U, Heegaard PM. Dendrimers in drug research. *Chemical Society Reviews*. 2004;33(1):43-63.
52. Bosman DA, Janssen HM, Meijer EW. About dendrimers: structure, physical properties, and applications. *Chemical reviews*. 1999 Jul 14;99(7):1665-88.
53. Weener JW. *A closer look at dendrimers*. Technische Universiteit Eindhoven; 2000.

54. García-Gallego S, Hult D, Olsson JV, Malkoch M. Fluoride-Promoted Esterification with Imidazolid-Activated Compounds: A Modular and Sustainable Approach to Dendrimers. *Angewandte Chemie International Edition*. 2015 Feb 16;54(8):2416-9.
55. Hawker CJ, Fréchet JM. Preparation of polymers with controlled molecular architecture. A new convergent approach to dendritic macromolecules. *Journal of the American Chemical Society*. 1990 Oct;112(21):7638-47.
56. Brauge L, Magro G, Caminade AM, Majoral JP. First divergent strategy using two AB₂ unprotected monomers for the rapid synthesis of dendrimers. *Journal of the American Chemical Society*. 2001 Jul 11;123(27):6698-9.
57. Spindler R, Fréchet JM. Two-step approach towards the accelerated synthesis of dendritic macromolecules. *Journal of the Chemical Society, Perkin Transactions 1*. 1993(8):913-8.
58. Wooley KL, Hawker CJ, Fréchet JM. Hyperbranched macromolecules via a novel double-stage convergent growth approach. *Journal of the American Chemical Society*. 1991 May;113(11):4252-61.
59. Agashe HB, Dutta T, Garg M, Jain NK. Investigations on the toxicological profile of functionalized fifth-generation poly (propylene imine) dendrimer. *Journal of pharmacy and pharmacology*. 2006 Nov;58(11):1491-8.

60. Stasko NA, Johnson CB, Schoenfish MH, Johnson TA, Holmuhamedov EL. Cytotoxicity of polypropylenimine dendrimer conjugates on cultured endothelial cells. *Biomacromolecules*. 2007 Nov 16;8(12):3853-9.
61. Jevprasesphant R, Penny J, Jalal R, Attwood D, McKeown NB, D'emanuele A. The influence of surface modification on the cytotoxicity of PAMAM dendrimers. *International journal of pharmaceutics*. 2003 Feb 18;252(1-2):263-6.
62. Shcharbin D, Janaszewska A, Klajnert-Maculewicz B, Ziemia B, Dzmitruk V, Halets I, Loznikova S, Shcharbina N, Milowska K, Ionov M, Shakhbazov A. How to study dendrimers and dendriplexes III. Biodistribution, pharmacokinetics and toxicity in vivo. *Journal of Controlled Release*. 2014 May 10;181:40-52.
63. Jain K, Kesharwani P, Gupta U, Jain NK. Dendrimer toxicity: Let's meet the challenge. *International journal of pharmaceutics*. 2010 Jul 15;394(1-2):122-42.
64. Liu M, Kono K, Fréchet JM. Water-soluble dendritic unimolecular micelles:: Their potential as drug delivery agents. *Journal of Controlled Release*. 2000 Mar 1;65(1-2):121-31.
65. Stevelmans S, Van Hest JC, Jansen JF, Van Boxtel DA, De Brabander-van den Berg EM, Meijer EW. Synthesis, Characterization, and Guest– Host Properties of Inverted Unimolecular Dendritic Micelles. *Journal of the American Chemical Society*. 1996 Aug 7;118(31):7398-9.

66. Saovapakhiran A, D'Emanuele A, Attwood D, Penny J. Surface modification of PAMAM dendrimers modulates the mechanism of cellular internalization. *Bioconjugate chemistry*. 2009 Mar 9;20(4):693-701.
67. Kaminskas LM, Wu Z, Barlow N, Krippner GY, Boyd BJ, Porter CJ. Partly-PEGylated Poly-L-lysine dendrimers have reduced plasma stability and circulation times compared with fully PEGylated dendrimers. *Journal of pharmaceutical sciences*. 2009 Oct;98(10):3871-5.
68. Chen RH, Abuchowski A, Van Es T, Palczuk NC, Davis FF. Properties of two urate oxidases modified by the covalent attachment of poly (ethylene glycol). *Biochimica et Biophysica Acta (BBA)-Enzymology*. 1981 Aug 13;660(2):293-8.
69. Khambete H, Gautam SP, Karthikeyan C, Ramteke S, Moorthy NH, Trivedi P. A new approach for PEGylation of dendrimers. *Bioorganic & medicinal chemistry letters*. 2010 Jul 15;20(14):4279-81.
70. Bhadra D, Bhadra S, Jain S, Jain NK. A PEGylated dendritic nanoparticulate carrier of fluorouracil. *International journal of pharmaceutics*. 2003 May 12;257(1-2):111-24.
71. Imberty A, Chabre YM, Roy R. Glycomimetics and glycodendrimers as high affinity microbial anti-adhesins. *Chemistry—A European Journal*. 2008 Aug 28;14(25):7490-9.
72. Thompson JP, Schengrund CL. Oligosaccharide-derivatized dendrimers: defined multivalent inhibitors of the adherence of the cholera toxin B

- subunit and the heat labile enterotoxin of *E. coli* to GM1. Glycoconjugate journal. 1997 Nov 1;14(7):837-45.
73. Pukin AV, Branderhorst HM, Sisu C, Weijers CA, Gilbert M, Liskamp RM, Visser GM, Zuilhof H, Pieters RJ. Strong inhibition of cholera toxin by multivalent GM1 derivatives. ChemBioChem. 2007 Sep 3;8(13):1500-3.
74. Johansson EM, Crusz SA, Kolomiets E, Buts L, Kadam RU, Cacciarini M, Bartels KM, Diggle SP, Cámara M, Williams P, Loris R. Inhibition and dispersion of *Pseudomonas aeruginosa* biofilms by glycopeptide dendrimers targeting the fucose-specific lectin LecB. Chemistry & biology. 2008 Dec 22;15(12):1249-57.
75. Klementieva O, Benseny-Cases N, Gella A, Appelhans D, Voit B, Cladera J. Dense shell glycodendrimers as potential nontoxic anti-amyloidogenic agents in alzheimer's disease. Amyloid–dendrimer aggregates morphology and cell toxicity. Biomacromolecules. 2011 Oct 14;12(11):3903-9.
76. Garcia-Vallejo JJ, Koning N, Ambrosini M, Kalay H, Vuist I, Sarrami-Forooshani R, Geijtenbeek TB, van Kooyk Y. Glycodendrimers prevent HIV transmission via DC-SIGN on dendritic cells. International immunology. 2013 Jan 4;25(4):221-33.
77. Bhadra D, Yadav AK, Bhadra S, Jain NK. Glycodendrimeric nanoparticulate carriers of primaquine phosphate for liver targeting. International journal of pharmaceutics. 2005 May 13;295(1-2):221-33.

78. Agrawal P, Gupta U, Jain NK. Glycoconjugated peptide dendrimers-based nanoparticulate system for the delivery of chloroquine phosphate. *Biomaterials*. 2007 Aug 1;28(22):3349-59.
79. Zhuo RX, Du B, Lu ZR. In vitro release of 5-fluorouracil with cyclic core dendritic polymer. *Journal of controlled release*. 1999 Feb 22;57(3):249-57.
80. Kono K, Akiyama H, Takahashi T, Takagishi T, Harada A. Transfection activity of polyamidoamine dendrimers having hydrophobic amino acid residues in the periphery. *Bioconjugate chemistry*. 2005 Jan 19;16(1):208-14.
81. Yang H, Kao WJ. Synthesis and characterization of nanoscale dendritic RGD clusters for potential applications in tissue engineering and drug delivery. *International journal of nanomedicine*. 2007 Mar;2(1):89.
82. Singh P, Gupta U, Asthana A, Jain NK. Folate and folate- PEG- PAMAM Dendrimers: synthesis, characterization, and targeted anticancer drug delivery potential in tumor bearing mice. *Bioconjugate chemistry*. 2008 Oct 25;19(11):2239-52.
83. Kim Y, Park EJ, Na DH. Recent progress in dendrimer-based nanomedicine development. *Archives of pharmacal research*. 2018 Feb 15:1-2.
84. Maeda H. Polymer therapeutics and the EPR effect. *Journal of drug targeting*. 2017;25(9-10):781.

85. Medina SH, El-Sayed ME. Dendrimers as carriers for delivery of chemotherapeutic agents. *Chemical reviews*. 2009 Jun 17;109(7):3141-57.
86. Michiue H, Sakurai Y, Kondo N, Kitamatsu M, Bin F, Nakajima K, Hirota Y, Kawabata S, Nishiki TI, Ohmori I, Tomizawa K. The acceleration of boron neutron capture therapy using multi-linked mercaptoundecahydrododecaborate (BSH) fused cell-penetrating peptide. *Biomaterials*. 2014 Mar 1;35(10):3396-405.
87. Barth RF, Coderre JA, Vicente MG, Blue TE. Boron neutron capture therapy of cancer: current status and future prospects. *Clinical Cancer Research*. 2005 Jun 1;11(11):3987-4002.
88. Hong S, Choi Y. Mesoporous silica-based nanoplatfoms for the delivery of photodynamic therapy agents. *Journal of Pharmaceutical Investigation*. 2018:1-5.
89. Narsireddy A, Vijayashree K, Adimoolam MG, Manorama SV, Rao NM. Photosensitizer and peptide-conjugated PAMAM dendrimer for targeted in vivo photodynamic therapy. *International journal of nanomedicine*. 2015;10:6865.
90. Schumann C, Taratula O, Khalimonchuk O, Palmer AL, Cronk LM, Jones CV, Escalante CA, Taratula O. ROS-induced nanotherapeutic approach for ovarian cancer treatment based on the combinatorial effect of photodynamic therapy and DJ-1 gene suppression. *Nanomedicine: Nanotechnology, Biology and Medicine*. 2015 Nov 1;11(8):1961-70.

91. Koç FE, Şenel M. Solubility enhancement of non-steroidal anti-inflammatory drugs (NSAIDs) using polypolypropylene oxide core PAMAM dendrimers. *International journal of pharmaceutics*. 2013 Jul 15;451(1-2):18-22.
92. Chauhan AS, Diwan PV, Jain NK, Tomalia DA. Unexpected in vivo anti-inflammatory activity observed for simple, surface functionalized poly (amidoamine) dendrimers. *Biomacromolecules*. 2009 Apr 6;10(5):1195-202.
93. Bosch X. Dendrimers to treat rheumatoid arthritis. *ACS nano*. 2011 Aug 31;5(9):6779-85.
94. Hayder M, Poupot M, Baron M, Nigon D, Turrin CO, Caminade AM, Majoral JP, Eisenberg RA, Fournié JJ, Cantagrel A, Poupot R. A phosphorus-based dendrimer targets inflammation and osteoclastogenesis in experimental arthritis. *Science Translational Medicine*. 2011 May 4;3(81):81ra35-.
95. Thomas TP, Goonewardena SN, Majoros IJ, Kotlyar A, Cao Z, Leroueil PR, Baker Jr JR. Folate-targeted nanoparticles show efficacy in the treatment of inflammatory arthritis. *Arthritis & Rheumatism*. 2011 Sep;63(9):2671-80.
96. Singh L, Kruger HG, Maguire GE, Govender T, Parboosing R. The role of nanotechnology in the treatment of viral infections. *Therapeutic advances in infectious disease*. 2017 Jul;4(4):105-31.

97. Gajbhiye V, Palanirajan VK, Tekade RK, Jain NK. Dendrimers as therapeutic agents: a systematic review. *Journal of Pharmacy and Pharmacology*. 2009 Aug;61(8):989-1003.
98. Witvrouw M, Fikkert V, Pluymers W, Matthews B, Mardel K, Schols D, Raff J, Debyser Z, De Clercq E, Holan G, Pannecouque C. Polyanionic (ie, polysulfonate) dendrimers can inhibit the replication of human immunodeficiency virus by interfering with both virus adsorption and later steps (reverse transcriptase/integrase) in the virus replicative cycle. *Molecular pharmacology*. 2000 Nov 1;58(5):1100-8.
99. Price CF, Tyssen D, Sonza S, Davie A, Evans S, Lewis GR, Xia S, Spelman T, Hodsman P, Moench TR, Humberstone A. SPL7013 Gel (VivaGel®) retains potent HIV-1 and HSV-2 inhibitory activity following vaginal administration in humans. *PLoS One*. 2011 Sep 15;6(9):e24095.
100. Kwon SJ, Na DH, Kwak JH, Douaisi M, Zhang F, Park EJ, Park JH, Youn H, Song CS, Kane RS, Dordick JS. Nanostructured glycan architecture is important in the inhibition of influenza A virus infection. *Nature nanotechnology*. 2017 Jan;12(1):48.
101. Current clinical trials | Starpharma (2018). Available at: https://starpharma.com/about_us/clinical_trials. (Accessed: 14th November 2018)
102. SINGH P. Dendrimers and their applications in immunoassays and clinical diagnostics. *Biotechnology and applied biochemistry*. 2007;48:1-9.

103. Hill SW, Heidecker G. Transfection of hematopoietic cells in suspension using an activated-dendrimer reagent. *Qiagen News. Sect.* 1998:8-10.
104. Liu H, Wang H, Yang W, Cheng Y. Disulfide cross-linked low generation dendrimers with high gene transfection efficacy, low cytotoxicity, and low cost. *Journal of the American Chemical Society.* 2012 Oct 10;134(42):17680-7.
105. Spangler BD, Spangler CW, inventors; Montana State University, assignee. Biosensors utilizing dendrimer-immobilized ligands and there use thereof. United States patent US 7,138,121. 2006 Nov 21.
106. Gellman SH. Introduction: molecular recognition.
107. Mammen M, Choi SK, Whitesides GM. Polyvalent interactions in biological systems: implications for design and use of multivalent ligands and inhibitors. *Angewandte Chemie International Edition.* 1998 Nov 2;37(20):2754-94.
108. Mahmuda A, Bande F, Al-Zihiry KJ, Abdulhaleem N, Majid RA, Hamat RA, Abdullah WO, Unyah Z. Monoclonal antibodies: A review of therapeutic applications and future prospects. *Tropical Journal of Pharmaceutical Research.* 2017;16(3):713-22.
109. Loureiro L, Carrascal M, Barbas A, Ramalho J, Novo C, Delannoy P, Videira P. Challenges in antibody development against Tn and Sialyl-Tn antigens. *Biomolecules.* 2015 Aug 11;5(3):1783-809.
110. Alberts B, Johnson A, Lewis J, Walter P, Raff M, Roberts K. *Molecular Biology of the Cell 4th Edition: International Student Edition.*

111. Casadevall A, Dadachova E, Pirofski LA. Passive antibody therapy for infectious diseases. *Nature Reviews Microbiology*. 2004 Sep;2(9):695.
112. Weiner GJ. Building better monoclonal antibody-based therapeutics. *Nature Reviews Cancer*. 2015 Jun;15(6):361.
113. Lowy I, Molrine DC, Leav BA, Blair BM, Baxter R, Gerding DN, Nichol G, Thomas Jr WD, Leney M, Sloan S, Hay CA. Treatment with monoclonal antibodies against *Clostridium difficile* toxins. *New England Journal of Medicine*. 2010 Jan 21;362(3):197.
114. Casadevall A, Dadachova E, Pirofski LA. Passive antibody therapy for infectious diseases. *Nature Reviews Microbiology*. 2004 Sep;2(9):695.
115. Till MA, Zolla-Pazner S, Gorny MK, Patton JS, Uhr JW, Vitetta ES. Human immunodeficiency virus-infected T cells and monocytes are killed by monoclonal human anti-gp41 antibodies coupled to ricin A chain. *Proceedings of the National Academy of Sciences*. 1989 Mar 1;86(6):1987-91.
116. Dadachova E, Nakouzi A, Bryan RA, Casadevall A. Ionizing radiation delivered by specific antibody is therapeutic against a fungal infection. *Proceedings of the National Academy of Sciences*. 2003 Sep 16;100(19):10942-7.
117. Arruebo M, Valladares M, González-Fernández Á. Antibody-conjugated nanoparticles for biomedical applications. *Journal of Nanomaterials*. 2009 Jan 1;2009:37.

118. El-Sayed IH, Huang X, El-Sayed MA. Surface plasmon resonance scattering and absorption of anti-EGFR antibody conjugated gold nanoparticles in cancer diagnostics: applications in oral cancer. *Nano letters*. 2005 May 11;5(5):829-34.
119. Yang L, Mao H, Wang YA, Cao Z, Peng X, Wang X, Duan H, Ni C, Yuan Q, Adams G, Smith MQ. Single chain epidermal growth factor receptor antibody conjugated nanoparticles for in vivo tumor targeting and imaging. *Small*. 2009 Jan 19;5(2):235-43.
120. Chen F, Hong H, Zhang Y, Valdovinos HF, Shi S, Kwon GS, Theuer CP, Barnhart TE, Cai W. In vivo tumor targeting and image-guided drug delivery with antibody-conjugated, radiolabeled mesoporous silica nanoparticles. *ACS nano*. 2013 Oct 1;7(10):9027-39.
121. Natarajan A, Xiong CY, Gruettner C, DeNardo GL, DeNardo SJ. Development of multivalent radioimmunonanoparticles for cancer imaging and therapy. *Cancer biotherapy & radiopharmaceuticals*. 2008 Feb 1;23(1):82-91.
122. Chen J, Wu H, Han D, Xie C. Using anti-VEGF McAb and magnetic nanoparticles as double-targeting vector for the radioimmunotherapy of liver cancer. *Cancer letters*. 2006 Jan 18;231(2):169-75.
123. Qin D, He X, Wang K, Zhao XJ, Tan W, Chen J. Fluorescent nanoparticle-based indirect immunofluorescence microscopy for detection of *Mycobacterium tuberculosis*. *BioMed Research International*. 2007;2007.

124. Laderman EI, Whitworth E, Dumauual E, Jones M, Hudak A, Hogrefe W, Carney J, Groen J. Rapid, sensitive, and specific lateral-flow immunochromatographic point-of-care device for detection of herpes simplex virus type 2-specific immunoglobulin G antibodies in serum and whole blood. *Clinical and Vaccine Immunology*. 2008 Jan 1;15(1):159-63.
125. Qin L, Vermesh O, Shi Q, Heath JR. Self-powered microfluidic chips for multiplexed protein assays from whole blood. *Lab on a Chip*. 2009;9(14):2016-20.
126. Gao J, Li L, Ho PL, Mak GC, Gu H, Xu B. Combining fluorescent probes and biofunctional magnetic nanoparticles for rapid detection of bacteria in human blood. *Advanced materials*. 2006 Dec 4;18(23):3145-8.
127. Mintz CS, Crea R. Protein scaffolds. *BioProcess International*. 2013 Feb;11:40-8.
128. Schmidt MM, Wittrup KD. A modeling analysis of the effects of molecular size and binding affinity on tumor targeting. *Molecular cancer therapeutics*. 2009 Oct 1;8(10):2861-71.
129. Friedman M, Ståhl S. Engineered affinity proteins for tumour-targeting applications. *Biotechnology and applied biochemistry*. 2009 May 1;53(1):1-29.
130. Holliger P, Hudson PJ. Engineered antibody fragments and the rise of single domains. *Nature biotechnology*. 2005 Sep;23(9):1126.

131. Goldman ER, Anderson GP, Liu JL, Delehanty JB, Sherwood LJ, Osborn LE, Cummins LB, Hayhurst A. Facile generation of heat-stable antiviral and antitoxin single domain antibodies from a semisynthetic llama library. *Analytical chemistry*. 2006 Dec 15;78(24):8245-55.
132. Gebauer M, Skerra A. Engineered protein scaffolds as next-generation antibody therapeutics. *Current opinion in chemical biology*. 2009 Jun 1;13(3):245-55.
133. Owens B. Faster, deeper, smaller—the rise of antibody-like scaffolds.
134. Nygren PÅ, Skerra A. Binding proteins from alternative scaffolds. *Journal of immunological methods*. 2004 Jul 1;290(1-2):3-28.
135. Škrlec K, Štrukelj B, Berlec A. Non-immunoglobulin scaffolds: a focus on their targets. *Trends in biotechnology*. 2015 Jul 1;33(7):408-18.
136. Traxlmayr MW, Kiefer JD, Srinivas RR, Lobner E, Tisdale AW, Mehta NK, Yang NJ, Tidor B, Wittrup KD. Strong enrichment of aromatic residues in binding sites from a charge-neutralized hyperthermostable Sso7d scaffold library. *Journal of Biological Chemistry*. 2016 Aug 30;jbc-M116.
137. Lomonosova AV, Ulitin AB, Kazakov AS, Mirzabekov TA, Permyakov EA, Permyakov SE. Derivative of Extremophilic 50S Ribosomal Protein L35Ae as an Alternative Protein Scaffold. *PloS one*. 2017 Jan 19;12(1):e0170349.
138. Grönwall C, Ståhl S. Engineered affinity proteins—generation and applications. *Journal of biotechnology*. 2009 Mar 25;140(3-4):254-69.

139. Barbas CF, Kang AS, Lerner RA, Benkovic SJ. Assembly of combinatorial antibody libraries on phage surfaces: the gene III site. *Proceedings of the National Academy of Sciences*. 1991 Sep 15;88(18):7978-82.
140. Boder ET, Wittrup KD. Yeast surface display for screening combinatorial polypeptide libraries. *Nature biotechnology*. 1997 Jun;15(6):553.
141. Koch H, Gräfe N, Schiess R, Plückthun A. Direct selection of antibodies from complex libraries with the protein fragment complementation assay. *Journal of molecular biology*. 2006 Mar 24;357(2):427-41.
142. Roberts RW. Totally in vitro protein selection using mRNA-protein fusions and ribosome display. *Current opinion in chemical biology*. 1999 Jun;3(3):268-73.
143. Mattheakis LC, Bhatt RR, Dower WJ. An in vitro polysome display system for identifying ligands from very large peptide libraries. *Proceedings of the National Academy of Sciences*. 1994 Sep 13;91(19):9022-6.
144. Zahnd C, Amstutz P, Plückthun A. Ribosome display: selecting and evolving proteins in vitro that specifically bind to a target. *Nature methods*. 2007 Mar;4(3):269.
145. Plückthun A. Ribosome display: a perspective. In *Ribosome display and related technologies 2012* (pp. 3-28). Springer, New York, NY.
146. van de Vijver MJ, Peterse JL, Mooi WJ, Wisman P, Lomans J, Dalesio O, Nusse R. Neu-protein overexpression in breast cancer. *New England Journal of Medicine*. 1988 Nov 10;319(19):1239-45.

147. Deyev S, Proshkina G, Ryabova A, Tavanti F, Menziani MC, Eidelstein G, Avishai G, Kotlyar A. Synthesis, Characterization, and Selective Delivery of DARPIn–Gold Nanoparticle Conjugates to Cancer Cells. *Bioconjugate chemistry*. 2017 Aug 22;28(10):2569-74.
148. Li DL, Tan JE, Tian Y, Huang S, Sun PH, Wang M, Han YJ, Li HS, Wu HB, Zhang XM, Xu YK. Multifunctional superparamagnetic nanoparticles conjugated with fluorescein-labeled designed ankyrin repeat protein as an efficient HER2-targeted probe in breast cancer. *Biomaterials*. 2017 Dec 1;147:86-98.
149. Zhang Y, Jiang S, Zhang D, Bai X, Hecht SM, Chen S. DNA–affibody nanoparticles for inhibiting breast cancer cells overexpressing HER2. *Chemical Communications*. 2017;53(3):573-6.
150. Alexis F, Basto P, Levy-Nissenbaum E, Radovic-Moreno AF, Zhang L, Pridgen E, Wang AZ, Marein SL, Westerhof K, Molnar LK, Farokhzad OC. HER-2-Targeted Nanoparticle–Affibody Bioconjugates for Cancer Therapy. *ChemMedChem: Chemistry Enabling Drug Discovery*. 2008 Dec 15;3(12):1839-43.
151. David MZ, Daum RS. Community-associated methicillin-resistant *Staphylococcus aureus*: epidemiology and clinical consequences of an emerging epidemic. *Clinical microbiology reviews*. 2010 Jul 1;23(3):616-87.
152. van Belkum A, Melles DC, Nouwen J, van Leeuwen WB, van Wamel W, Vos MC, Wertheim HF, Verbrugh HA. Co-evolutionary aspects of human

- colonisation and infection by *Staphylococcus aureus*. *Infection, Genetics and Evolution*. 2009 Jan 1;9(1):32-47.
153. Klevens RM, Morrison MA, Nadle J, Petit S, Gershman K, Ray S, Harrison LH, Lynfield R, Dumyati G, Townes JM, Craig AS. Invasive methicillin-resistant *Staphylococcus aureus* infections in the United States. *Jama*. 2007 Oct 17;298(15):1763-71.
154. Hartman BJ, Tomasz AL. Low-affinity penicillin-binding protein associated with beta-lactam resistance in *Staphylococcus aureus*. *Journal of bacteriology*. 1984 May 1;158(2):513-6.
155. Sreeramoju P, Porbandarwalla NS, Arango J, Latham K, Dent DL, Stewart RM, Patterson JE. Recurrent skin and soft tissue infections due to methicillin-resistant *Staphylococcus aureus* requiring operative debridement. *The American Journal of Surgery*. 2011 Feb 1;201(2):216-20.
156. Heyworth PG, Cross AR, Curnutte JT. Chronic granulomatous disease. *Current opinion in immunology*. 2003 Oct 1;15(5):578-84.
157. Milner JD, Brenchley JM, Laurence A, Freeman AF, Hill BJ, Elias KM, Kanno Y, Spalding C, Elloumi HZ, Paulson ML, Davis J. Impaired T H 17 cell differentiation in subjects with autosomal dominant hyper-IgE syndrome. *Nature*. 2008 Apr;452(7188):773.
158. Frank KM, Zhou T, Moreno-Vinasco L, Hollett B, Garcia JG, Wardenburg JB. Host response signature to *Staphylococcus aureus* α -hemolysin

- implicates pulmonary Th17 response. *Infection and immunity*. 2012 Jun 25:IAI-00191.
159. Holland TL, Arnold C, Fowler VG. Clinical management of *Staphylococcus aureus* bacteremia: a review. *Jama*. 2014 Oct 1;312(13):1330-41.
160. Van Hal SJ, Jensen SO, Vaska VL, Espedido BA, Paterson DL, Gosbell IB. Predictors of mortality in *Staphylococcus aureus* bacteremia. *Clinical microbiology reviews*. 2012 Apr 1;25(2):362-86.
161. Friedman ND, Kaye KS, Stout JE, McGarry SA, Trivette SL, Briggs JP, Lamm W, Clark C, MacFarquhar J, Walton AL, Reller LB. Health care-associated bloodstream infections in adults: a reason to change the accepted definition of community-acquired infections. *Annals of internal medicine*. 2002 Nov 19;137(10):791-7.
162. Jensen AG, Wachmann CH, Poulsen KB, Espersen F, Scheibel J, Skinhøj P, Frimodt-Møller N. Risk factors for hospital-acquired *Staphylococcus aureus* bacteremia. *Archives of internal medicine*. 1999 Jul 12;159(13):1437-44.
163. Musher DM, Lamm N, Darouiche RO, Young EJ, Hamill RJ, Landon GC. The current spectrum of *Staphylococcus aureus* infection in a tertiary care hospital. *Medicine*. 1994 Jul;73(4):186-208.
164. Spaan AN, Surewaard BG, Nijland R, van Strijp JA. Neutrophils versus *Staphylococcus aureus*: a biological tug of war. *Annual review of microbiology*. 2013 Sep 8;67:629-50.

165. Müller-Eberhard HJ. Molecular organization and function of the complement system. *Annual review of biochemistry*. 1988 Jul;57(1):321-47.
166. Berends ET, Kuipers A, Ravesloot MM, Urbanus RT, Rooijackers SH. Bacteria under stress by complement and coagulation. *FEMS microbiology reviews*. 2014 Nov 1;38(6):1146-71.
167. Thammavongsa V, Kim HK, Missiakas D, Schneewind O. Staphylococcal manipulation of host immune responses. *Nature Reviews Microbiology*. 2015 Sep;13(9):529.
168. Bestebroer J, Poppelier MJ, Ulfman LH, Lenting PJ, Denis CV, van Kessel KP, van Strijp JA, de Haas CJ. Staphylococcal superantigen-like 5 binds PSGL-1 and inhibits P-selectin-mediated neutrophil rolling. *Blood*. 2007 Apr 1;109(7):2936-43.
169. Bestebroer J, van Kessel KP, Azouagh H, Walenkamp AM, Boer IG, Romijn RA, van Strijp JA, de Haas CJ. Staphylococcal SSL5 inhibits leukocyte activation by chemokines and anaphylatoxins. *Blood*. 2009 Jan 8;113(2):328-37.
170. De Haas CJ, Weeterings C, Vughs MM, De Groot PG, Van Strijp JA, Lisman T. Staphylococcal superantigen-like 5 activates platelets and supports platelet adhesion under flow conditions, which involves glycoprotein Iba and α IIb β 3. *Journal of Thrombosis and Haemostasis*. 2009 Nov;7(11):1867-74.

171. Yokoyama R, Itoh S, Kamoshida G, Takii T, Fujii S, Tsuji T, Onozaki K. Staphylococcal superantigen-like protein 3 binds to toll like receptor 2 extracellular domain and inhibits cytokine production induced by *S. aureus*, cell wall component or lipopeptides in murine macrophages. *Infection and immunity*. 2012 Jun 4:IAI-00399.
172. O'Riordan K, Lee JC. Staphylococcus aureus capsular polysaccharides. *Clinical microbiology reviews*. 2004 Jan 1;17(1):218-34.
173. Laarman AJ, Ruyken M, Malone CL, van Strijp JA, Horswill AR, Rooijackers SH. Staphylococcus aureus metalloprotease aureolysin cleaves complement C3 to mediate immune evasion. *The Journal of Immunology*. 2011 Apr 18:1002948.
174. Rooijackers SH, Ruyken M, Roos A, Daha MR, Presanis JS, Sim RB, Van Wamel WJ, Van Kessel KP, Van Strijp JA. Immune evasion by a staphylococcal complement inhibitor that acts on C3 convertases. *Nature immunology*. 2005 Sep;6(9):920.
175. Bera A, Herbert S, Jakob A, Vollmer W, Götz F. Why are pathogenic staphylococci so lysozyme resistant? The peptidoglycan O-acetyltransferase OatA is the major determinant for lysozyme resistance of Staphylococcus aureus. *Molecular microbiology*. 2005 Feb;55(3):778-87.
176. Peschel A, Otto M, Jack RW, Kalbacher H, Jung G, Götz F. Inactivation of the *dlt* Operon in Staphylococcus aureus Confers Sensitivity to

- Defensins, Protegrins, and Other Antimicrobial Peptides. *Journal of Biological Chemistry*. 1999 Mar 26;274(13):8405-10.
177. Ernst CM, Peschel A. Broad-spectrum antimicrobial peptide resistance by MprF-mediated aminoacylation and flipping of phospholipids. *Molecular microbiology*. 2011 Apr 1;80(2):290-9.
178. Liu GY, Essex A, Buchanan JT, Datta V, Hoffman HM, Bastian JF, Fierer J, Nizet V. *Staphylococcus aureus* golden pigment impairs neutrophil killing and promotes virulence through its antioxidant activity. *Journal of Experimental Medicine*. 2005 Jul 18;202(2):209-15.
179. Richardson AR, Libby SJ, Fang FC. A nitric oxide-inducible lactate dehydrogenase enables *Staphylococcus aureus* to resist innate immunity. *Science*. 2008 Mar 21;319(5870):1672-6.
180. Heuck AP, Tweten RK, Johnson AE. β -Barrel pore-forming toxins: intriguing dimorphic proteins. *Biochemistry*. 2001 Aug 7;40(31):9065-73.
181. Surewaard BG, De Haas CJ, Vervoort F, Rigby KM, DeLeo FR, Otto M, Van Strijp JA, Nijland R. Staphylococcal alpha-phenol soluble modulins contribute to neutrophil lysis after phagocytosis. *Cellular microbiology*. 2013 Aug;15(8):1427-37.
182. McCarthy AJ, Lindsay JA. Genetic variation in *Staphylococcus aureus* surface and immune evasion genes is lineage associated: implications for vaccine design and host-pathogen interactions. *BMC microbiology*. 2010 Dec;10(1):173.

183. Fraser JD, Proft T. The bacterial superantigen and superantigen-like proteins. *Immunological reviews*. 2008 Oct;225(1):226-43.
184. Jones RC, Deck J, Edmondson RD, Hart ME. Relative quantitative comparisons of the extracellular protein profiles of *Staphylococcus aureus* UAMS-1 and its *sarA*, *agr*, and *sarA agr* regulatory mutants using one-dimensional polyacrylamide gel electrophoresis and nanocapillary liquid chromatography coupled with tandem mass spectrometry. *Journal of bacteriology*. 2008 Aug 1;190(15):5265-78.
185. SJÖDAHL J. Repetitive Sequences in Protein A from *Staphylococcus aureus*: Arrangement of Five Regions within the Protein, Four being Highly Homologous and Fc-Binding. *European journal of biochemistry*. 1977 Mar;73(2):343-51.
186. Björk I, Petersson BÅ, Sjöquist J. Some physicochemical properties of protein A from *Staphylococcus aureus*. *European Journal of Biochemistry*. 1972 Sep;29(3):579-84.
187. Löfkvist T, Sjöquist J. CHEMICAL AND SEROLOGICAL ANALYSIS OF ANTIGEN PREPARATIONS FROM STAPHYLOCOCCUS AUREUS: A Comparison Between the Products Obtained by Verwey's and Jensen's Techniques. *Acta Pathologica Microbiologica Scandinavica*. 1962 Nov;56(3):295-304.
188. Moks T, ABRAHMSÉN L, NILSSON B, Hellman U, SJÖQUIST J, Uhlen M. Staphylococcal protein A consists of five IgG-binding domains. *European journal of biochemistry*. 1986 May;156(3):637-43.

189. Ton-That H, Liu G, Mazmanian SK, Faull KF, Schneewind O. Purification and characterization of sortase, the transpeptidase that cleaves surface proteins of *Staphylococcus aureus* at the LPXTG motif. *Proceedings of the National Academy of Sciences*. 1999 Oct 26;96(22):12424-9.
190. Falugi F, Kim HK, Missiakas DM, Schneewind O. Role of protein A in the evasion of host adaptive immune responses by *Staphylococcus aureus*. *MBio*. 2013 Nov 1;4(5):e00575-13.
191. Goodyear CS, Silverman GJ. Death by a B cell superantigen: in vivo VH-targeted apoptotic supraclonal B cell deletion by a staphylococcal toxin. *Journal of Experimental Medicine*. 2003 May 5;197(9):1125-39.
192. Widaa A, Claro T, Foster TJ, O'Brien FJ, Kerrigan SW. *Staphylococcus aureus* protein A plays a critical role in mediating bone destruction and bone loss in osteomyelitis. *PloS one*. 2012 Jul 11;7(7):e40586.
193. Merino N, Toledo-Arana A, Vergara-Irigaray M, Valle J, Solano C, Calvo E, Lopez JA, Foster TJ, Penadés JR, Lasa I. Protein A-mediated multicellular behavior in *Staphylococcus aureus*. *Journal of bacteriology*. 2009 Feb 1;191(3):832-43.
194. Henry-Stanley MJ, Shepherd MM, Wells CL, Hess DJ. Role of *Staphylococcus aureus* Protein A in Adherence to Silastic Catheters¹. *Journal of Surgical Research*. 2011 May 1;167(1):9-13.
195. Davey ME, O'toole GA. Microbial biofilms: from ecology to molecular genetics. *Microbiology and molecular biology reviews*. 2000 Dec 1;64(4):847-67.

196. Otto M. Staphylococcal infections: mechanisms of biofilm maturation and detachment as critical determinants of pathogenicity. *Annual review of medicine*. 2013 Jan 14;64:175-88.
197. Singh S, Singh SK, Chowdhury I, Singh R. Understanding the mechanism of bacterial biofilms resistance to antimicrobial agents. *The open microbiology journal*. 2017;11:53.
198. O'Toole G, Kaplan HB, Kolter R. Biofilm formation as microbial development. *Annual Reviews in Microbiology*. 2000 Oct;54(1):49-79.
199. Kragh KN, Hutchison JB, Melaugh G, Rodesney C, Roberts AE, Irie Y, Jensen PØ, Diggle SP, Allen RJ, Gordon V, Bjarnsholt T. Role of multicellular aggregates in biofilm formation. *MBio*. 2016 May 4;7(2):e00237-16.
200. Heilmann C, Hussain M, Peters G, Götz F. Evidence for autolysin-mediated primary attachment of *Staphylococcus epidermidis* to a polystyrene surface. *Molecular microbiology*. 1997 Jun;24(5):1013-24.
201. Gross M, Cramton SE, Götz F, Peschel A. Key role of teichoic acid net charge in *Staphylococcus aureus* colonization of artificial surfaces. *Infection and immunity*. 2001 May 1;69(5):3423-6.
202. Patti JM, Allen BL, McGavin MJ, Hook M. MSCRAMM-mediated adherence of microorganisms to host tissues. *Annual Reviews in Microbiology*. 1994 Oct;48(1):585-617.
203. Mack D, Fischer W, Krokotsch A, Leopold K, Hartmann R, Egge H, Laufs R. The intercellular adhesin involved in biofilm accumulation of

- Staphylococcus epidermidis is a linear beta-1, 6-linked glucosaminoglycan: purification and structural analysis. *Journal of bacteriology*. 1996 Jan 1;178(1):175-83.
204. Conrady DG, Brescia CC, Horii K, Weiss AA, Hasset DJ, Herr AB. A zinc-dependent adhesion module is responsible for intercellular adhesion in staphylococcal biofilms. *Proceedings of the National Academy of Sciences*. 2008 Dec 9;105(49):19456-61.
205. Yarwood JM, Bartels DJ, Volper EM, Greenberg EP. Quorum sensing in *Staphylococcus aureus* biofilms. *Journal of bacteriology*. 2004 Mar 15;186(6):1838-50.
206. Yarwood JM, Schlievert PM. Quorum sensing in *Staphylococcus* infections. *The Journal of clinical investigation*. 2003 Dec 1;112(11):1620-5.
207. Periasamy S, Joo HS, Duong AC, Bach TH, Tan VY, Chatterjee SS, Cheung GY, Otto M. How *Staphylococcus aureus* biofilms develop their characteristic structure. *Proceedings of the National Academy of Sciences*. 2012 Jan 24;109(4):1281-6.
208. Schmutzler K, Schmid A, Buehler K. A three-step method for analysing bacterial biofilm formation under continuous medium flow. *Applied microbiology and biotechnology*. 2015 Jul 1;99(14):6035-47.
209. O'Toole GA. Microtiter dish biofilm formation assay. *Journal of visualized experiments: JoVE*. 2011(47).

210. Hammar MA, Bian Z, Normark S. Nucleator-dependent intercellular assembly of adhesive curli organelles in *Escherichia coli*. *Proceedings of the National Academy of Sciences*. 1996 Jun 25;93(13):6562-6.
211. O'Shea TM, Klein AH, Geszvain K, Wolfe AJ, Visick KL. Diguanylate cyclases control magnesium-dependent motility of *Vibrio fischeri*. *Journal of bacteriology*. 2006 Dec 1;188(23):8196-205.
212. Rashid MH, Kornberg A. Inorganic polyphosphate is needed for swimming, swarming, and twitching motilities of *Pseudomonas aeruginosa*. *Proceedings of the National Academy of Sciences*. 2000 Apr 25;97(9):4885-90.
213. Eighmy TT, Maratea D, Bishop PL. Electron microscopic examination of wastewater biofilm formation and structural components. *Applied and environmental microbiology*. 1983 Jun 1;45(6):1921-31.
214. Lawrence JR, Korber DR, Hoyle BD, Costerton JW, Caldwell DE. Optical sectioning of microbial biofilms. *Journal of bacteriology*. 1991 Oct 1;173(20):6558-67.
215. Gross R, Hauer B, Otto K, Schmid A. Microbial biofilms: new catalysts for maximizing productivity of long-term biotransformations. *Biotechnology and bioengineering*. 2007 Dec 15;98(6):1123-34.

Chapter II:

Objectives

Objectives

Conferring “smartness” to nanoparticles by functionalizing them with targeting ligands provides a platform with enhanced multivalent binding, along with the possibility of carrying therapeutic, diagnostic or imaging agents.¹

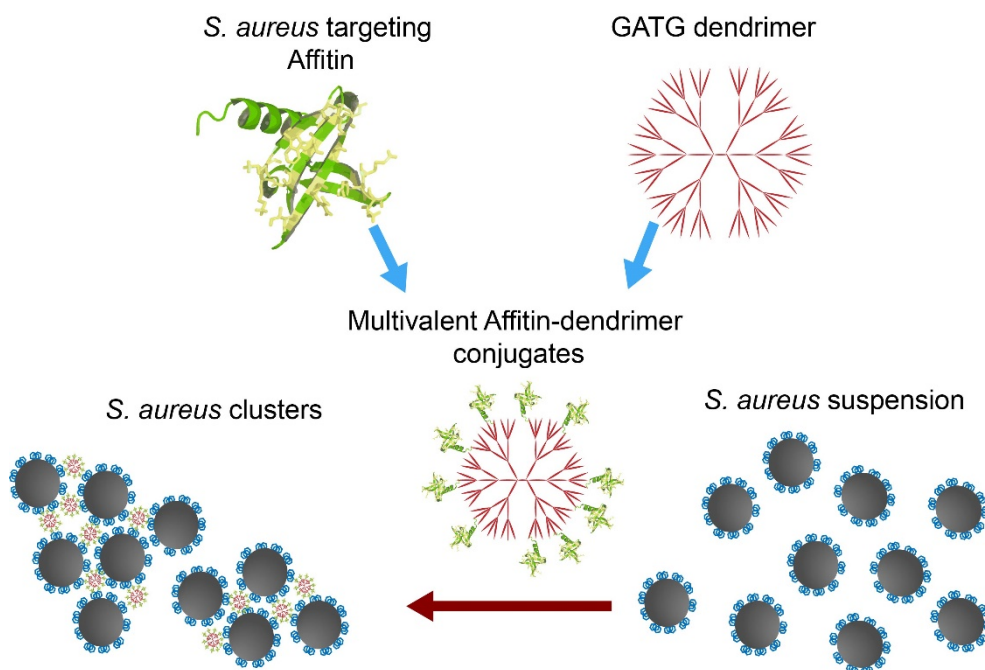
Due to limitations of antibodies related to their large size, intricate structure, instability and high production costs, other targeting ligands such as Affitins become an attractive alternative. Affitins are engineered affinity proteins, developed and extensively studied by the group of Dr. Barbara Mouratou. Along with affinities and specificities comparable to those of antibodies, Affitins possess 20-fold smaller size, simple one-chain structure and high thermal and chemical stability. Furthermore, they are obtained through a powerful target-driven selection by ribosome display, followed by an easy and cheap production in *E. coli*.^{2,3}

Dendrimers are monodisperse, unimolecular nanoparticles that introduce small-molecule level of control into the design of nanostructures. Group of Dr. Eduardo Fernandez-Megia has experience with Gallic acid-triethylene glycol (GATG) dendrimers, a class characterized by their straightforward synthesis, high tunability and abundance of clickable azide groups on the surface.⁴⁻⁷

We hypothesized that combining the powerful targeting properties of Affitins with the versatility and multivalency of GATG dendrimers as

scaffolds could provide robust nanoscale devices for biomedical application in fields such as infectious diseases. With this aim, we set the following objectives:

1. To develop a site-specific conjugation method for preparing Affitin-dendrimer conjugates that will allow for fine-tuning of size, multivalency, surface functionalization and recognition properties (Chapter III).
2. To use the obtained conjugates for targeting *Staphylococcus aureus* in a highly specific manner and assess their potential to modulate complex multicellular behaviors, such as agglutination and biofilm formation, due to enhanced multivalent interactions (Chapter IV).



References

1. D Friedman A, E Claypool S, Liu R. The smart targeting of nanoparticles. *Current pharmaceutical design*. 2013 Oct 1;19(35):6315-29.
2. Mouratou B, Schaeffer F, Guilvout I, Tello-Manigne D, Pugsley AP, Alzari PM, Pecorari F. Remodeling a DNA-binding protein as a specific in vivo inhibitor of bacterial secretin PulD. *Proceedings of the National Academy of Sciences*. 2007 Nov 13;104(46):17983-8.
3. Béhar G, Renodon-Cornière A, Mouratou B, Pecorari F. Affitins as robust tailored reagents for affinity chromatography purification of antibodies and non-immunoglobulin proteins. *Journal of Chromatography A*. 2016 Apr 8;1441:44-51.
4. Sousa-Herves A, Novoa-Carballal R, Riguera R, Fernandez-Megia E. GATG dendrimers and PEGylated block copolymers: from synthesis to bioapplications. *The AAPS journal*. 2014 Sep 1;16(5):948-61.
5. Fernandez-Megia E, Correa J, Rodríguez-Meizoso I, Riguera R. A click approach to unprotected glycodendrimers. *Macromolecules*. 2006 Mar 21;39(6):2113-20.
6. Amaral SP, Fernandez-Villamarin M, Correa J, Riguera R, Fernandez-Megia E. Efficient multigram synthesis of the repeating unit of gallic acid-triethylene glycol dendrimers. *Organic letters*. 2011 Aug 5;13(17):4522-5.

7. Amaral SP, Tawara MH, Fernandez-Villamarin M, Borrajo E, Martínez-Costas J, Vidal A, Riguera R, Fernandez-Megia E. Tuning the Size of Nanoassemblies: A Hierarchical Transfer of Information from Dendrimers to Polyion Complexes. *Angewandte Chemie International Edition*. 2018 May 4;57(19):5273-7.

Chapter III:

Synthesis and characterization of Affitin-dendrimer conjugates
for multivalent targeting of *Staphylococcus aureus* Protein A

Table of Contents

| | |
|---|------------|
| I. Introduction | 109 |
| I.1 Affitins..... | 109 |
| I.1.1 Affitin development..... | 110 |
| I.1.2 Affitin applications..... | 111 |
| I.1.3 Affitin C5..... | 114 |
| I.2 GATG dendrimers..... | 116 |
| I.2.1 Synthesis of GATG dendrimers..... | 116 |
| I.2.2 Applications of GATG dendrimers..... | 117 |
| I.3 Affitin-dendrimer conjugation..... | 122 |
| I.3.1 Azide-alkyne cycloaddition..... | 122 |
| II. Materials and methods | 125 |
| II.1 Materials..... | 125 |
| II.2 Bacterial strains and oligonucleotides..... | 126 |
| II.3 Production and purification of proteins..... | 126 |
| II.3.1 C5-SH plasmid construction..... | 126 |
| II.3.2 Production and purification of Affitins C5 and C5-SH..... | 127 |
| II.3.3 Production and purification of biotinylated C5 and SpA domain A..... | 127 |
| II.4 ELISA..... | 128 |
| II.5 Preparation of conjugates..... | 129 |
| II.5.1 C5-BCN synthesis..... | 129 |
| II.5.2 2[Gn]-FITC synthesis..... | 132 |
| II.5.3 2[Gn]-[C5] synthesis..... | 139 |
| II.6 Surface plasmon resonance..... | 145 |
| III. Results and discussion | 148 |
| III.1 Making Affitin C5 “clickable”..... | 148 |
| III.2 Surface engineering of 2[Gn]-FITC..... | 150 |
| III.3 Affitin-dendrimer conjugates..... | 151 |
| III.4 Surface plasmon resonance..... | 154 |
| IV. Acknowledgements | 159 |
| V. References | 160 |

I. Introduction

I.1 Affitins

Archaeal DNA-binding proteins, whose natural role is to pack and stabilize DNA of archaea in the extreme conditions they live in, have an important place among the range of available protein scaffolds. They are characterized by high robustness, small size and simple structure, which also results in high thermal and chemical stability, as required by their natural function, which make them attractive candidates for the development of engineered affinity binding proteins. The first successful use of archaeal proteins for the generation of artificial affinity reagents – Affitins, was described by the group of Mouratou in 2007.^{1,2}

Affitins (commercially available as Nanofitins) are derived from archaeal proteins Sac7d from *Sulfolobus acidocaldarius*³ and Sso7d *Sulfolobus solfataricus*,⁴ both being hyperthermophilic and acidophilic bacteria. Both of these proteins consist of a single polypeptide chain (66 amino acids for Sac7d and 64 for Sso7d) that contains no disulfide bridges (Figure 1) and are extremely stable thermally ($T_m = 90.4^\circ\text{C}$ for Sac7d and 100.2°C for Sso7d)^{5,6} and chemically, in a pH range from 0 to at least 12.^{7,8} Recently, another archaeal scaffold protein, Aho7c, for Affitin development has been reported by our group.⁹

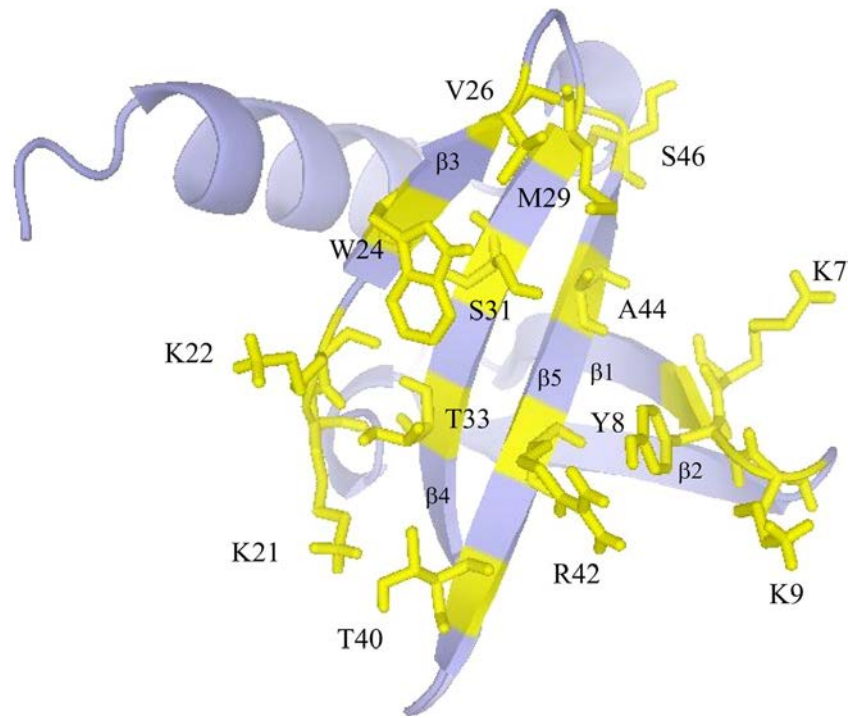


Figure 1 Schematic representation of wild-type *Sac7d*, with residues involved in DNA binding shown in yellow (from 1)

I.1.1 Affitin development

Affitins are obtained through a target-driven, fully *in vitro* selection process based on ribosome display technique. First, 14 amino acids located in the DNA binding sites of scaffold proteins are randomized, providing large DNA libraries. Alternative library design randomizes 10 amino acids, some of which are outside of the DNA binding site, further expanding on the range of potential binders.⁷ Then, these libraries are exposed to the chosen target

in a number of selection rounds via ribosome display, until only very strong and specific binders are enriched. Finally, selected binders are produced in *E. coli* and thoroughly characterized.¹

Affitin binders with nanomolar and subnanomolar affinities, specific for very different molecular targets, such as bacterial protein PulD,^{1,10,11} glycosidases (chicken egg lysozyme and CelD),^{12,13} human IgGs,^{7,14} tumor-associated markers CD138¹⁵ and EpCAM⁹ and *S. aureus* protein A (SpA)¹⁶ were isolated and characterized using the described approach. These Affitins retain favorable properties of original archaeal proteins, such as high thermal and chemical stability and high-yield production in *E. coli*, along with very narrow specificities and high affinities for their targets, that compare well with those of antibodies.

1.1.2 Affitin applications

Applications of Affitins for different purposes have been demonstrated, such as immunolocalization, enzyme inhibition, biosensing, affinity chromatography, magnetic fishing and tumor imaging (Figure 2).

PulD targeting Affitins have been fused to the green fluorescent protein (GFP). This fusion was used as a reporter for determining the localization of wild type PulD in *E. coli*, which suggested that GFP-tagged Affitins can be used as immunolocalization agents.¹¹

Applications

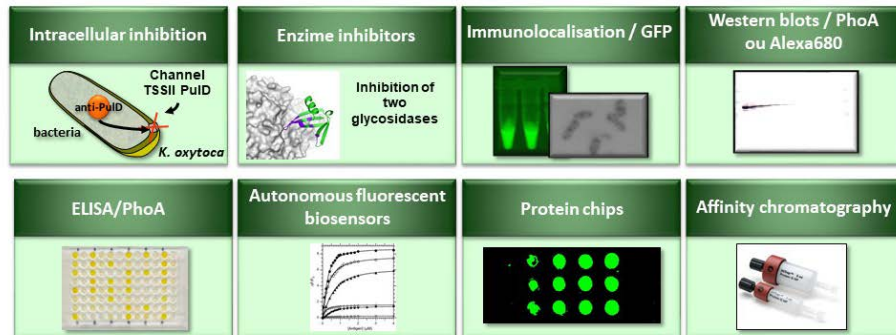


Figure 2. Applications of Affitins

Specific inhibition of two different glycosidases, CelD from *Clostridium thermocellum* and lysosome from hen egg, was achieved using Affitins developed for these targets, confirming the potential of Affitins as specific inhibitors of other enzymes.¹²

Biosensors based on Affitins and DARPins that combine specific binding with the detection signal in a single molecule have been demonstrated for particular targets. The strategy is based on exploiting an inserted Cysteine residue to chemically introduce a fluorophore in a site specific manner. Fluorescence quenching would be induced by the binding to the target, providing instantaneous analytical signal of the interaction.¹⁷

The most extensively demonstrated application of Affitins could be as reagents for Affinity chromatography, where their high specificity and

robustness allows them to sustain harsh regeneration procedures of the column. Agarose affinity columns for human IgGs, bacterial PulD and hen egg white lysozyme were demonstrated to be highly specific for their respective target, providing high degrees of protein purity and recovery, even in the presence of media, ascites or bacterial lysates. These columns could be reused with up to 90% of their initial capacity after 25 purification/cleaning cycles, while the degree of purity of IgG after the Affitin-based column was well comparable to that of a Protein A column.¹⁸

An alternative affinity-purification method based on magnetic nanoparticles (MNPs) has been successfully used for purification of IgG and lysozyme.¹⁹

A biodistribution study of Affitins demonstrated fast clearance without accumulation, compatible for radioimaging of tumors with short half-life isotopes such as ⁶⁸Ga.¹⁴ A first tumor-specific Affitin targeting CD138, showed the same fast clearance and accumulation in the tumor tissue in mice carrying subcutaneous human MDN myeloma tumors, demonstrating suitability for this kind of application.

An Affitin for another tumor marker, EpCAM, has been developed from a new scaffold Aho7c. This Affitin has been successfully used to decorate LNPs and target them towards the EpCAM expressing cells. Unfortunately, the high specificity that this Affitin achieved towards the molecular target was somewhat lost in the experiments with cell cultures.²⁰

I.1.3 Affitin C5

We have recently described an Affitin molecule, named C5, with narrow specificity and high affinity for *S. aureus*.¹⁶ Derived from Sac7d, it contains 66 amino acids in its sequence, none of which are Cysteine residues. We have shown that Affitin C5 recognizes *S. aureus* exclusively, with 0% false positives or negatives, among dozens of strains, including clinical ones. Molecular target was determined to be SpA, which was bound by C5 with an overall affinity of 170 nM, as determined by Bio-Layer Interferometry (BLI). Further elucidation identified that this binding occurs primarily at domains A (107 nM) and D (231 nM) of SpA molecule, while no binding was observed with other three domains of the protein.

Affitin C5 retains the high thermostability of the scaffold ($T_m=77.0^\circ\text{C}$), while retaining the binding properties after prolonged storage in borate buffer pH=10.5. Furthermore, fusions of Affitin C5 with bacterial phosphatase A (PhoA) and green fluorescent protein (GFP) have been obtained with unaffected activity.

Affitin C5 has been successfully used for fluorescent labelling of *S. aureus* cells (Figure 3), as well as cell capture by paramagnetic beads.

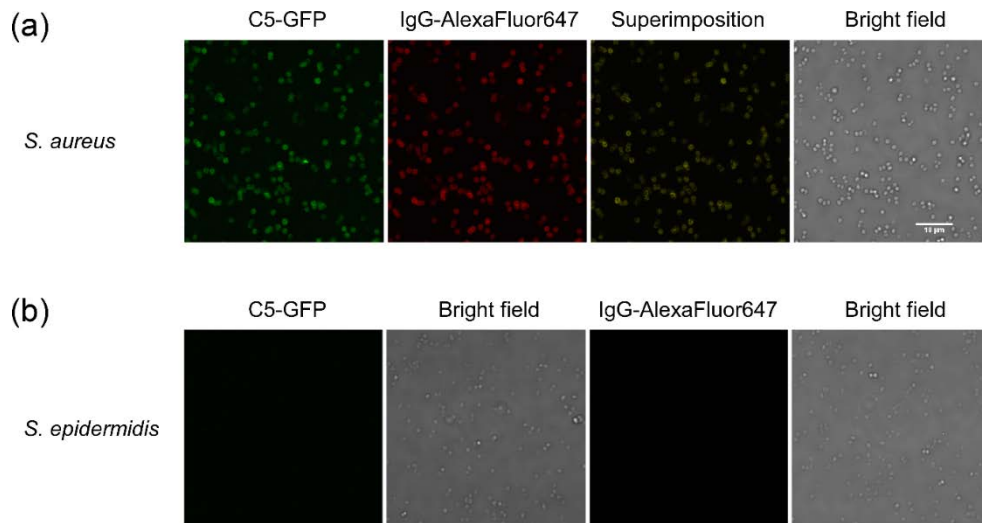


Figure 3. *S. aureus* strain detected by fluorescence microscopy. (a) C5-GFP and Ig-AlexaFluor647 were used simultaneously to probe *S. aureus* ST25 strain. (b) *S. epidermidis* strain was used to verify that the fluorescence signals seen with the two probes were specific of *S. aureus* (from 16).

I.2 GATG dendrimers

Gallic acid-triethylene glycol (GATG) dendrimers are a family of dendritic structures first described by the group of Roy,^{21,22} composed of a repeating unit that contains a gallic acid core and hydrophilic triethylene glycol arms with terminal azide groups. Such structure of the repeating unit and chemical versatility of azides are exploited for dendrimer synthesis and functionalization, providing unique advantages to GATG dendrimers compared to other dendritic architectures, such as high monodispersity and no structural defects, facile and fast synthesis and high customizability.²³

I.2.1 Synthesis of GATG dendrimers

Initial efforts to synthesize GATG dendrimers were limited by low availability of the repeating unit.^{21,22} In 2006, an improved preparation of the repeating unit was described by the group of Fernandez-Megia for cost-effective production,²⁴ while further improvement of the method allowed obtaining quantities larger than 100 g, with excellent overall yield and purity.²⁵ Very efficient divergent synthesis of $N[Gn]-N_3$ (where N is the valency of the core, and n is the generation number) dendrimers has been achieved up to generation 4 for 2[Gn] and 3[Gn] dendrimers, containing between 6 and 243 terminal azide groups (Figure 4).²⁶

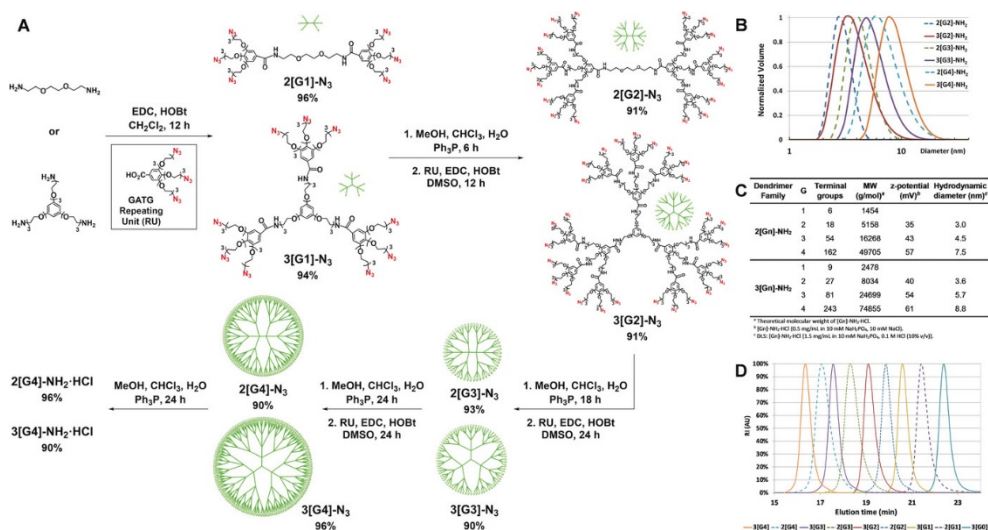


Figure 4. A) Synthesis of 2[Gn] and 3[Gn] dendrimers. B) DLS size distribution of [Gn]-NH₂·HCl. C) Structural data of dendrimers. D) GPC elugrams of [Gn]-N₃ (THF) (from 26).

Synthesis of GATG dendrimers involves a simple divergent sequence. Activation step is performed by azide reduction (Ph₃P, 90-100%), while a subsequent growth step involves an amide coupling of the resulting terminal amino groups with the repeating unit (EDC, HOBT, 93-96%). 2[Gn] and 3[Gn] dendrimers are obtained with high yield, good purity and monodispersity.²⁶

1.2.2 Applications of GATG dendrimers

Diverse applications of GATG dendrimers and their PEGylated block copolymers have been reported (Figure 5).

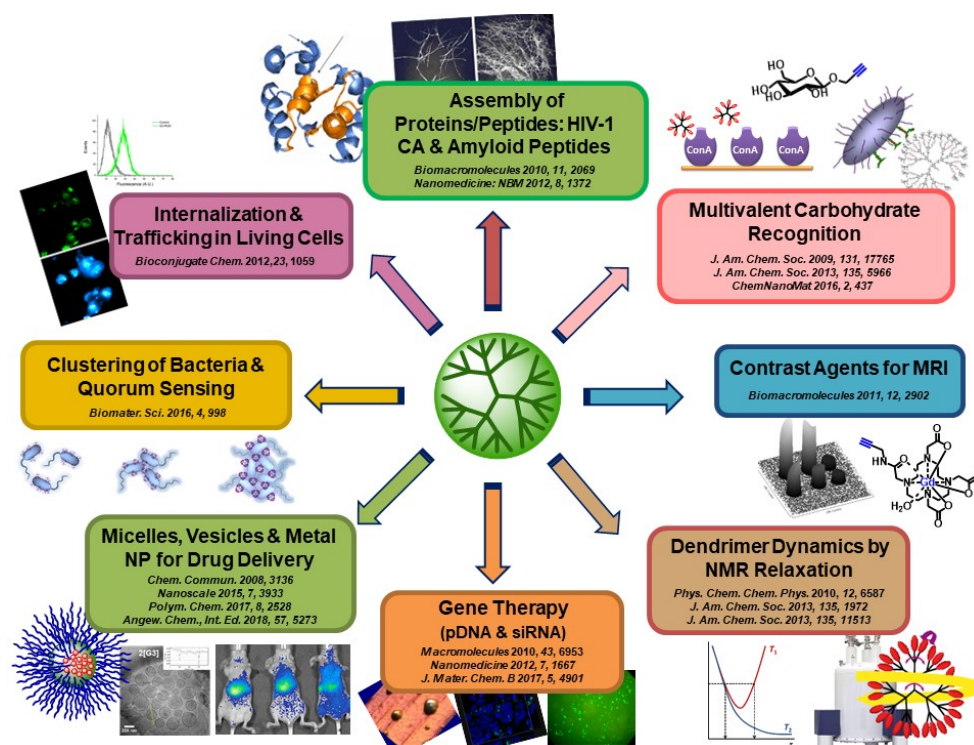


Figure 5. Applications of GATG dendrimers

An extensively explored application of GATG dendrimers is in preparation of PEGylated block copolymers. Cellular internalization of these structures has been studied,²⁷ elucidating their potential as delivery vehicles. They have also been used to template the preparation of metal NPs,²⁸ and to prepare drug delivery vehicles, such as polyion complex (PIC) micelles²⁹⁻³¹ and dendriplexes for gene therapy.^{23,32-34} In a more recent contribution, the generation of GATG dendrimers was revealed to be a powerful tool in controlling the size and biodistribution of PIC assemblies. Using combinatorial screening of oppositely charged dendrimers and linear PEGylated copolymers, a dendrimer-to-PIC hierarchical transfer of structural

information was revealed with PIC diameters that increased from 80 to 500 nm upon decreasing the dendrimer generation. The increase in size, accompanied by a micelle-to-vesicle transition, is interpreted according to a cone- to rod-shaped progression in the architecture of the unit PIC. This precise size tuning enabled dendritic PICs to act as nanorulers for controlled biodistribution.²⁶

Non-PEGylated GATG dendrimers have been shown to have potential use as anti-HIV drugs targeting the capsid assembly, when decorated with peripheral benzoate groups,³⁵ as well as a potential anti-Alzheimer's agent, in the form of morpholine-decorated dendrimers.³⁶ Furthermore, their enhanced relaxivity as contrast agents for Magnetic Resonance Imaging (MRI) has been demonstrated by peripheral decoration with Gd-DO3A chelates.³⁷

The multivalent presentation of ligands on GATG dendrimers has been exploited to study the nature of the lectin-carbohydrate recognition, which is based on weak monovalent interactions enhanced via multivalency. Different generations of dendrimers, decorated with monosaccharides, provided a precise nanoscale tool for gaining insight into the nature of these multivalent interactions.^{38,39}

Surface Plasmon Resonance (SPR) is a label-free technique that allows real-time monitoring of molecular binding events. Signal obtained from SPR, usually given as arbitrary Resonance Units (RU), represents the

local refractive index change on the surface of the SPR chip. This signal, in the conditions of constant temperature and incident light, is directly proportional to the number of molecules bound to the sensor surface.⁴⁰ Kinetic models that describe SPR sensograms of monovalent interactions are well established, since the nature of monovalent binding is not dependent on the density of the immobilized ligand, but only on the concentration of binding partners. These models are readily available in the commercial software of SPR instruments and they describe kinetics of monovalent interactions well. However, there is a growing need for robust characterization of multivalent interactions and establishment of parameters that describe them well. To this end, group of Fernandez-Megia has developed an SPR method which focuses on the analysis of early association and late dissociation phases of sensograms when high-affinity, multivalent binding modes prevail over the monovalent binding, due to high concentration of free receptors available on chip (Figure 6). This provided a generalized approach to characterizing the role of multivalency-enhanced binding mechanisms by obtaining kinetic parameters of such binding.⁴¹

More recently, cationic GATG dendrimers have been used as tools to agglutinate bacteria. It has been shown on *Vibrio harveyi* as a model organism that cationic GATG dendrimers efficiently agglutinate bacteria in a generation-dependent manner. Furthermore, this agglutination induced a quorum-sensing controlled luminescence, probably by maintaining a high

concentration of quorum sensing signals inside the cell clusters, while increasing the permeability of microbial outer membranes.⁴²

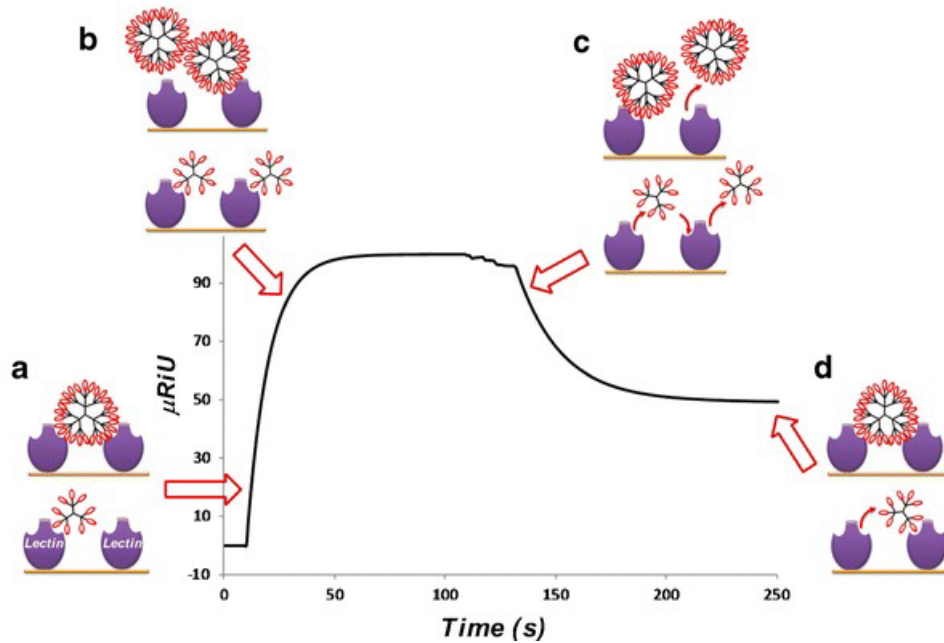


Figure 6. Schematic representation of the dynamic binding heterogeneity of surface-bound experiments between lectin clusters and glycodendrimers: **(a)** Initial binding of glycodendrimers to the lectin cluster with potential stabilization via chelate mechanism depending on glycodendrimer size and lectin cluster density. **(b)** At longer association times, competition between dendrimers for lectin complexation increases, promoting monovalent interactions primarily stabilized via rebinding effects. **(c)** An initial fast dissociation of glycodendrimers bound with low affinity is followed by **(d)** a slower dissociation due to stabilization by rebinding and potential chelate effects (From 41)

I.3 Affitin-dendrimer conjugation

Conjugation of proteins to NPs is of increasing interest in biomedicine.⁴³ A commonly used approach for attaching proteins to nanoparticles is through non-covalent interactions, which has its limitations such as possible dissociation and lack of control over the orientation. In contrast, different strategies for covalent conjugation allow very stable links to be formed in a site-specific manner. Site-specific conjugation requires a unique chemical handle to be introduced to a targeted site in the protein. Common strategies include incorporation of unnatural amino acids,⁴⁴ enzymatic modifications, such as sortase-mediated ligation,⁴⁵ and chemical modifications, such as site-selective lysine modifications⁴⁶ and thiol coupling.⁴⁷

I.3.1 Azide-alkyne cycloaddition

The concept of click chemistry, introduced in 2001 by Kolb, Finn and Shapless,⁴⁸ encompasses a set of reactions that must be modular, stereospecific and wide in scope, while giving very high yields and generating only inoffensive byproducts that can be removed by nonchromatographic methods. The greatest exponent among the entire proposed collection of click chemistry reaction has been the Huisgen 1,3-dipolar azide-alkyne cycloaddition (AAC).⁴⁹

The discovery of the Cu¹-catalyzed variant of this reaction (CuAAC) has extended its application into the fields of chemistry, polymer science and biology.⁵⁰ However, use of copper in the context of biomolecules presented limitations such as structural damage to biomolecules, as well as often limiting speed of reactions at low micromolar concentrations required for many bioconjugation reactions. Another Cu-free variant, a strain-promoted azide-alkyne cycloaddition, has been described by Bertozzi and co-workers, addressing some of the issues of CuAAC (Figure 7).^{50,51}

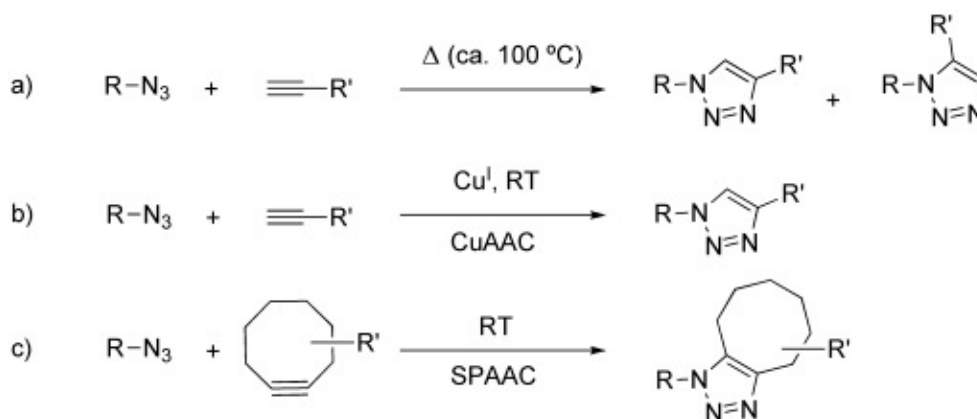


Figure 7. (from 50) (a) Huisgen 1,3-dipolar azide alkyne cycloaddition (AAC) (b) Cu¹-catalyzed variant (CuAAC) (c) Strain-promoted variant (SPAAC)

Here, we set out to develop a robust conjugation method that could allow site-selective attachment of Affitins onto GATG dendrimers. We chose a thiol-coupling strategy for site-specific modification of Affitin C5, exploiting the lack of cysteine residues as an engineering advantage. A chemical handle containing bicyclononyne (BCN), a click chemistry (SPAAC)^{50,51} partner to the

azide groups present on the surface of GATG dendrimers, was selected for an initial functionalization of the Affitin via Michael addition exploiting the site-selective incorporation of a unique thiol group (cysteine) at the C-terminal position. Such a strategy converts the Affitin into a “clickable” partner for the dendrimer surface (Figure 8).

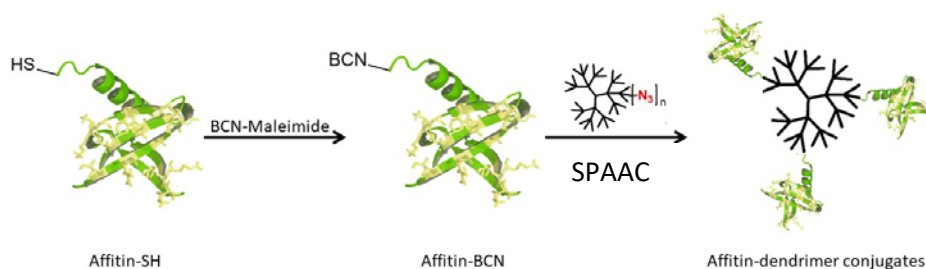


Figure 8. Synthesis scheme of Affitin-dendrimer conjugates

The rational design of targeted nanoparticles is an important factor that contributes to making a platform attractive. An important criterion to meet is customizability and control over important design parameters. We report the preparation of four distinct populations of conjugates that allows control of physicochemical properties, such as size, surface functionalization and multivalency. Obtained conjugates combine versatility and multivalency of GATG dendrimers and specific targeting properties of Affitins, providing a robust, customizable platform useful for a range of applications.

II. Materials and methods

II.1 Materials

BCN-Mal was purchased from Synaffix as a preparation kit. 2[G3]-N3 and 2[G4]-N3 were prepared following previously reported procedures from our laboratory.²⁶ Enzymes for molecular biology and DNA ladders were purchased from Thermo Fischer Scientific, oligonucleotides from Eurofins. All other reagents were purchased from commercial sources and used without further purification. Ultrafiltration was performed on Amicon stirred cells with Amicon YM10 and YM3 membranes. Nuclear Magnetic Resonance (NMR) spectra were recorded on Bruker DRX 500 MHz in D₂O. Chemical shifts were reported in ppm (δ units) downfield from the HOD signal. Mass spectra of BCN-Mal were obtained on an Agilent G1956A 1100 LC/MSD system. MALDI-TOF mass spectra were recorded on an Applied Biosystems MDS SCIEX 4800 MALDI-TOF/TOF using either 2,5-dihydroxybenzoic acid (DHB) or sinapic acid (SA) as matrix and operating in linear mode. Size-exclusion chromatography (SEC) was performed on BioLogic DuoFlow chromatography system using either Superdex 75 or Superdex 200 filtration columns (GE Healthcare). DLS measurements were carried out on a Malvern Nano ZS (Malvern Instruments, U.K.) operating at 633 nm with a 173° scattering angle, at 25 °C. Mean diameters were obtained from the volume particle size distribution provided by Malvern Zetasizer Software. UV-Vis spectra were recorded on a NanoDrop 2000c

device (Thermo Scientific), using either the drop method or the cuvettes. SPR experiments were performed on a Biacore 3000 instrument.

II.2 Bacterial strains and oligonucleotides

Escherichia coli DH5α Iq and *Escherichia coli DH5α-BirA* were used for expression of the non-biotinylated and biotinylated proteins, respectively.

Oligonucleotides:

SC_F: 5'-ACCATCACGGATCCGTCAAGGTGAAATTC-3'

H4-C-ter-R: 5'-TTAATTAAGCTTTCATTAGCAGCCCTTTTTCTCGCGTCCGCAC-3'

II.3 Production and purification of proteins

II.3.1 C5-SH plasmid construction

In this study, a unique cysteine residue was introduced at the C-terminus of C5 Affitin to allow coupling via thiol chemistry. Plasmid pFP1001 containing the sequence of C5 Affitin was used as template for in vitro mutagenesis.¹⁶ The C5 gene was amplified by the polymerase chain reaction using the SC_F and H4-C-ter-R oligonucleotides as primers. The resulting PCR product was inserted into the BamHI and HindIII restriction sites of the pFP1001 vector.

II.3.2 Production and purification of Affitins C5 and C5-SH

Affitins C5 and C5-SH were produced by modifying a method described previously.¹⁰ Briefly, 5 mL of an overnight preculture of *E. coli* *DH5 α lq* transformed with pFP1001/C5³ or pFP1001/C5-SH (LB + 0.1 mg/mL ampicillin + 1% glucose, 37 °C) was used to inoculate 1L of production culture (2xYT + ampicillin + 0.1% glucose, 37 °C). When OD600 reached 1.0, expression was induced with 0.5 mM IPTG and cultures were shaken for 19 h at 30 °C. Cells were then centrifuged and pellets were washed and resuspended in PBS (2,7mM KCl, 10mM Na₂HPO₄, 2mM KH₂PO₄, 150 mM NaCl, pH 7.4), containing 25 mM imidazole. Cells were lysed by sonication (5 min at 10W) and the debris removed by centrifugation. Affitins were purified first by immobilized metal ion affinity chromatography (IMAC) on a 5 mL HiTrap column using PBS containing 250 mM imidazole, pH 7.4 for elution and then by size-exclusion chromatography (SEC) on a Superdex 75 26/60 gel filtration column (GE Healthcare) using PBS, pH 7.4. Protein concentration was determined by UV absorption at 280 nm in PBS pH 7.4, using a calculated Molar Extinction coefficient of 15340 M⁻¹ cm⁻¹ for the monomeric form.

II.3.3 Production and purification of biotinylated C5 and SpA domain A

Biotinylated and non-biotinylated subdomain A of extracellular region of SpA, used for SPR, as well as biotinylated Affitin C5 used for ELISA,

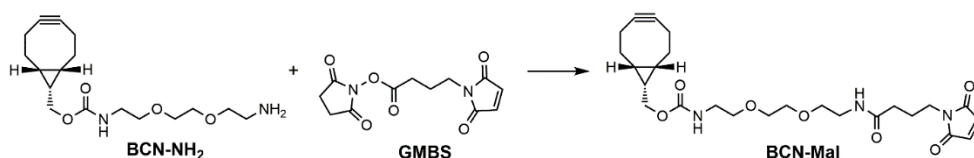
were obtained using the pFP1301 plasmid in either *E.coli DH5 α -BirA* (biotinylated) or *E.coli DH5 α* (non-biotinylated) cells, as described previously.¹⁶

II.4 ELISA

Modified Affitin C5-SH was tested against the biotinylated Affitin C5 by ELISA in order to verify that it retains the activity of C5. SpA domain A (10 μ g/mL) was coated on a Maxisorb plate (Nunc) for 2h at 25°C with shaking. After washing 3 times with PBS, wells were saturated with PBS-Caseine 1% for 2h, followed by washing 6 times with PBS-Tween 0.1% (which is repeated in each subsequent washing step). C5-SH dilutions (10 μ M-0.6nM) were made with PBS-Tween 0.1% directly in the wells and incubated for 1h, followed by a washing step. Biotinylated C5 (78,1 nM) was then added to all the wells, incubated for 1h, followed by another washing step. Finally, detection was performed using streptavidin conjugated HorseRadish Peroxidase (HRP), incubated for 1h, followed by a washing step, and a subsequent addition of the HRP substrate o-phenylenediamine (1 mg/ml in a buffer containing 0.05 M citric acid and 0.05% hydrogen peroxide (Sigma)). Once the color develops in the wells, signal is measured at 450 nm. The experiment was done in triplicate, using non-coated wells as a negative control.

II.5 Preparation of conjugates

II.5.1 C5-BCN synthesis



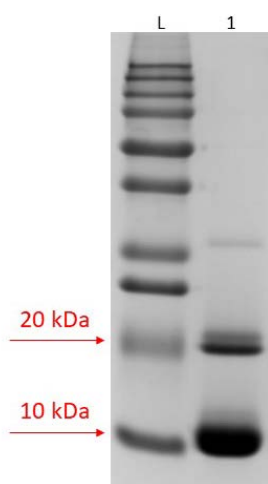
BCN-Mal. 4-Maleimidobutyric acid N-hydroxysuccinimide ester (58.9 mg, 210 μmol , GMBS) was added to a stirred solution of BCN-NH₂ (88.7 mg, 273 μmol) in DMSO (0.91 mL). The resulting solution was stirred at rt under Ar, protected from light. The reaction was followed to completion (disappearance of GMBS, 2 h) by TLC (silica, EtOAc) and ESI-MS (no signals due to GMBS and appearance of peaks at m/z 490.3 and 512.3 assigned to [BCN-Mal+H]⁺ and [BCN-Mal+Na]⁺, respectively).

C5-BCN. TCEP (47 mg, 164 μmol ; 3000 mol % per C5-SH) was added to a stirred solution of C5-SH (50 mg, 5.47 μmol) in PBS-EDTA (49.2 mL; PBS pH 7.4 + 10 mM EDTA). The resulting solution was stirred at rt under Ar for 1 h to reduce the disulfide bridge present in C5-S dimers. During this time, a freshly prepared solution of BCN-Mal (as described above) was diluted with DMSO to a final volume of 6.1 mL. Then, 5.5 mL of this solution (equivalent to 80.4 mg of BCN-Mal, 164 μmol ; 3000 mol % per C5-SH) was added dropwise to the C5-SH solution. The reaction mixture was stirred at rt under Ar for 24 h, protected from light before being filtered through a cotton plug

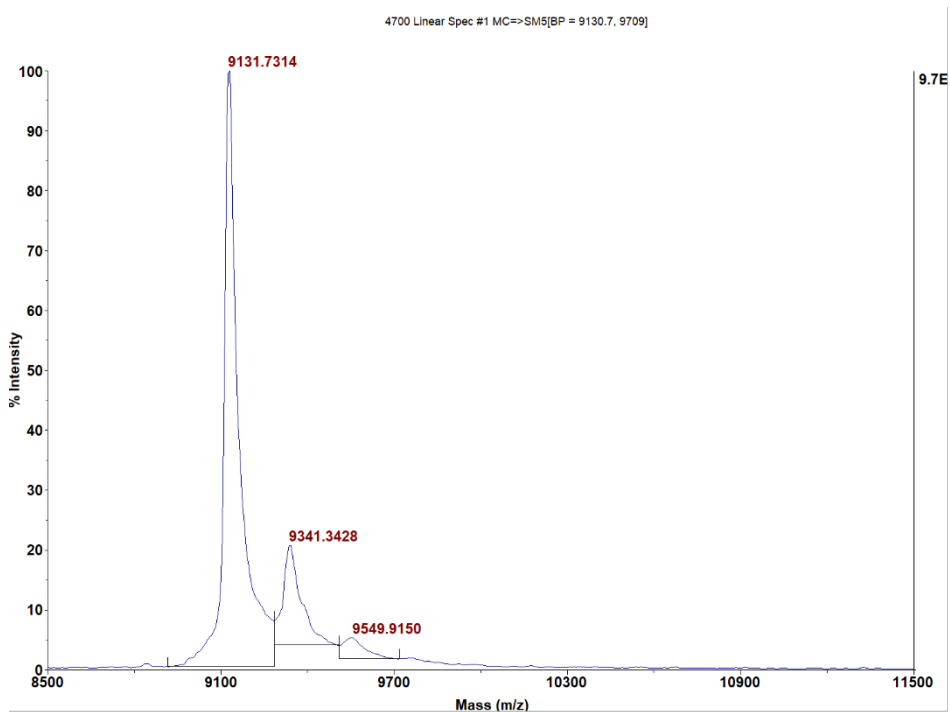
and purified by ultrafiltration (PBS-DMSO buffer - PBS pH 7.4 + 10% DMSO, 5 x 150 mL; MWCO 3000 Da, YM3 membrane). SDS-PAGE (15%; coomassie staining, quantification by ImageLab software) showed a 25% of non-reduced C5-S dimer accompanying a 75% of monomers (C5-BCN and C5-SH). Analysis by MALDI-TOF MS revealed 95% conversion of C5-SH monomer to C5-BCN, which accounts for a total 71% C5-BCN conversion (complete protein recovery was confirmed by UV-Vis). C5-BCN was not further purified and directly used for SPAAC conjugation with the dendrimers. UV-Vis (BBS-DMSO - 100 mM borate buffer, 500 mM NaCl, 10% DMSO, pH 10.5) λ_{\max} : 280 nm.

MALDI-TOF MS (SA, linear mode, m/z) C5-SH: 9131.7. Calcd. for [C5-SH+H]⁺: 9136.7.

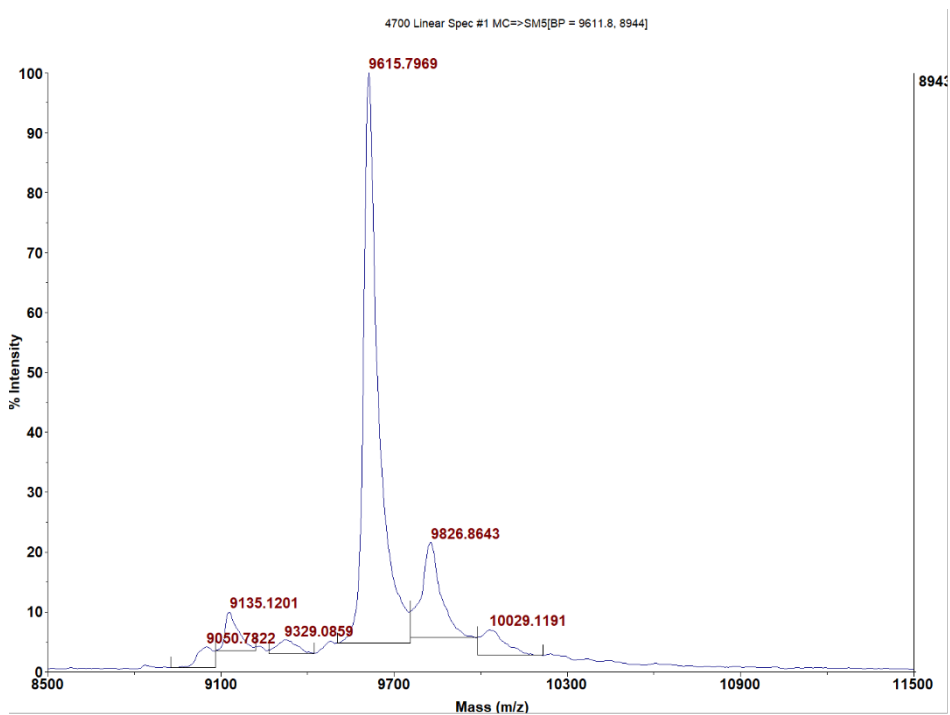
MALDI-TOF MS (SA, linear mode, m/z) C5-BCN: 9615.8 (peak area: 95%), 9135.1 (peak area: 5%, starting C5-SH). Calcd. for [C5-BCN+H]⁺: 9626.2.



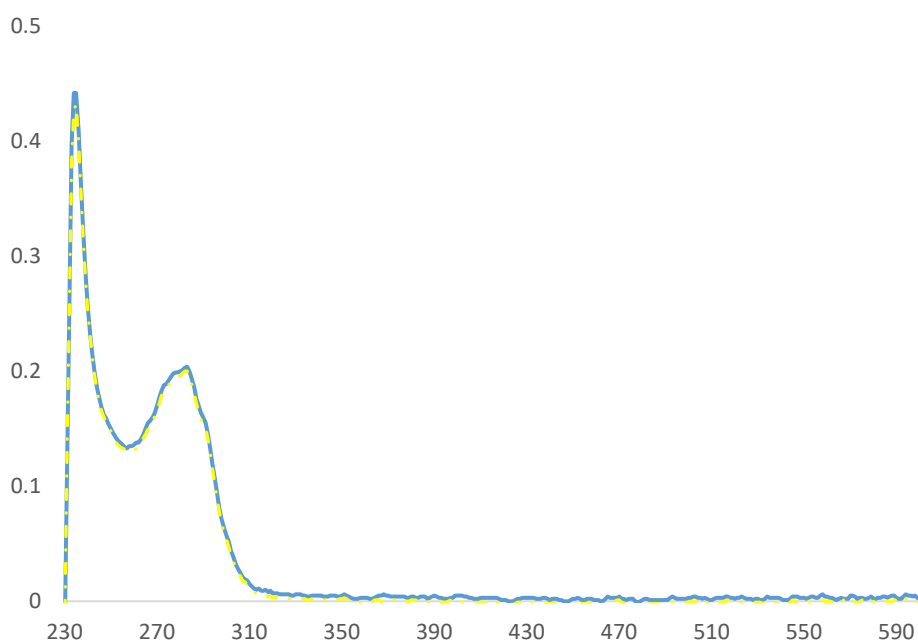
SDS-PAGE (15%) of C5-BCN reaction. (L) Ladder, (1) C5-BCN reaction



MALDI-TOF MS spectrum of C5-SH.



MALDI-TOF MS spectrum of C5-BCN.



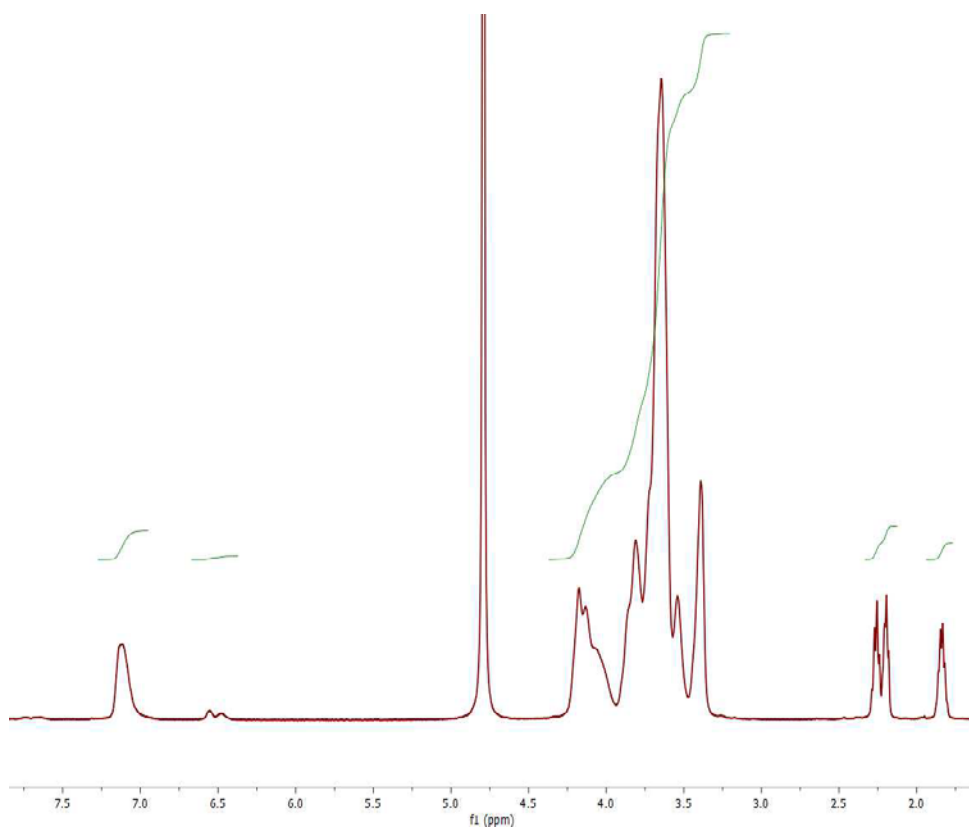
UV-Vis spectrum of C5-BCN (in BBS-DMSO buffer).

II.5.2 2[Gn]-FITC synthesis

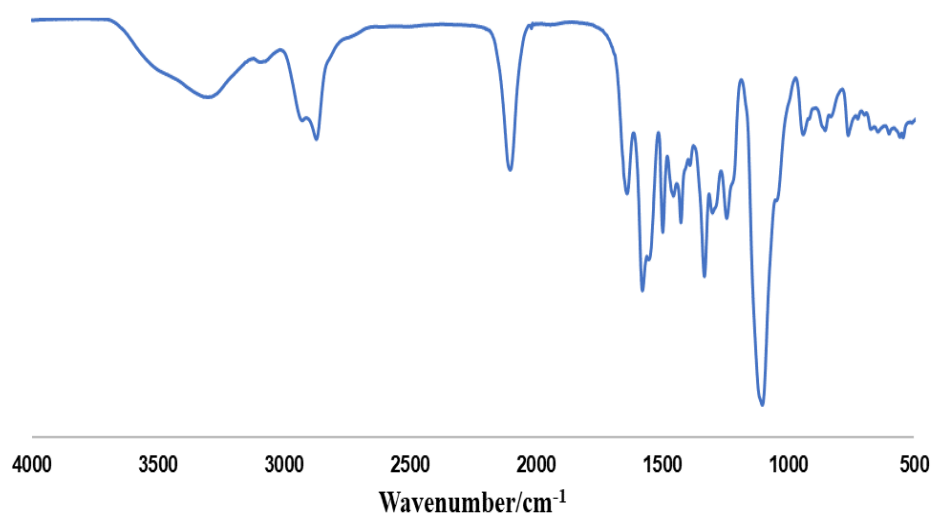
General procedure. 2[Gn]-N₃, synthesized as described previously,²⁶ was added to a 33 mM solution of Ph₃P in H₂O-CHCl₃-MeOH (1:5:5) to give a 0.1 M final concentration of azides. The mixture was stirred at rt under Ar for 16 h till 33% of the terminal azides were reduced to primary amines. Then, the solvent was evaporated. A freshly prepared solution of FITC in DMSO (3.7 mol % of FITC per terminal group) and Et₃N (600 mol % per terminal NH₂) were added and the reaction was stirred at rt under Ar for 8 h, protected from light. Finally, glutaric anhydride was added (600 mol % per terminal NH₂) and stirring continued at rt for 12 h, protected from light. The reaction mixture was filtered through a cotton plug and purified by

ultrafiltration (2% NaHCO₃:acetone (1:1), 5 x 200 mL; then H₂O, 3 x 200 mL; MWCO 10000Da, YM10 membrane) to afford 2[Gn]-FITC/CO₂H/N₃ (abb. 2[Gn]-FITC).

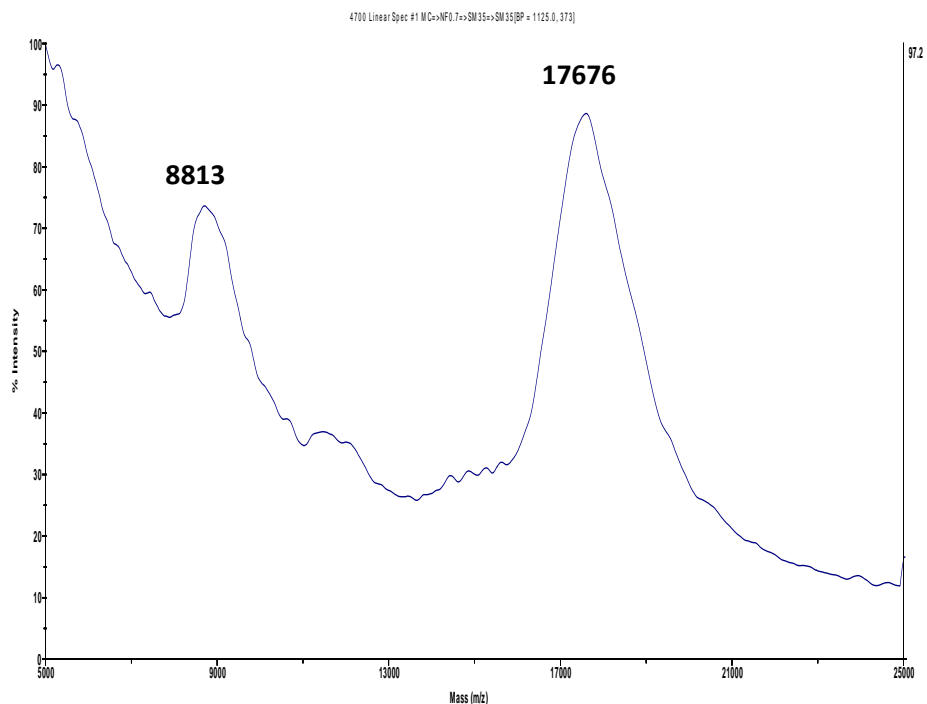
2[G3]-FITC. Following the general procedure described above from 2[G3]-N₃ (75 mg, 4.8 μmol) and Ph₃P (22.5 mg, 0.086 mmol) dissolved in H₂O (0.235 mL) - CHCl₃ (1.17 mL) - MeOH (1.17 mL), and using FITC (3.71 mg, 0.01 mmol) in DMSO (2.57 mL), Et₃N (0.073 mL, 0.524 mmol) and glutaric anhydride (60 mg, 0.524 mmol), the dendrimer 2[G3]-(FITC)₂/(CO₂H)₁₅/(N₃)₃₇ (2[G3]-FITC hereafter) was obtained as a yellow oil (78 mg, 92%). ¹H NMR (500 MHz, D₂O) δ: 7.14-7.09 (m, 52H), 6.55-6.49 (m, 8H), 4.37–3.20 (m, 948H), 2.26 (t, *J*=7.7 Hz, 30H), 2.19 (t, *J*=6.6 Hz, 30H), 1.91–1.77 (m, 30H). IR (ATR, cm⁻¹): 3298, 2928, 2873, 2102, 1640, 1579, 1497, 1426, 1330, 1100. UV-Vis (DMSO) λ_{max}: 519 nm. UV-Vis (BBS-DMSO) λ_{max}: 260, 500 nm. MALDI-TOF MS (DHB, linear mode, *m/z*) 2[G3]-FITC: 17676, 8813. Calcd. for [M+H]⁺: 17777, [M+2H]²⁺: 8888. An average of 1.5 fluorescein and 15 glutaric acid groups were determined by integration of the multiplets at 6.55-6.49 ppm (fluorescein) and 1.91–1.77 ppm (glutaric acid) in the ¹H NMR (D₂O) spectrum. Same degree of fluorescein functionalization was obtained by absorbance at 519 nm in DMSO, applying an extinction coefficient of 60800 M⁻¹ cm⁻¹.



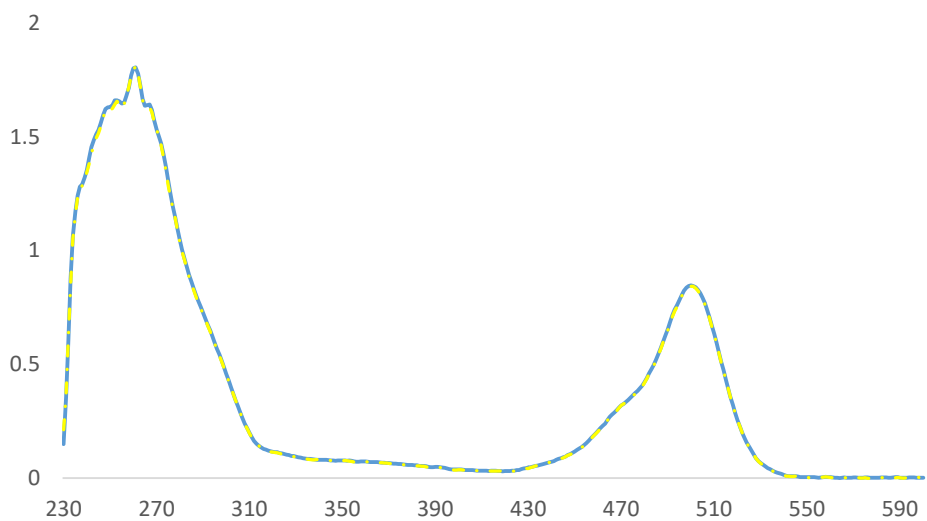
^1H NMR spectrum (D_2O) of 2[G3]-FITC.



IR spectrum of 2[G3]-FITC.



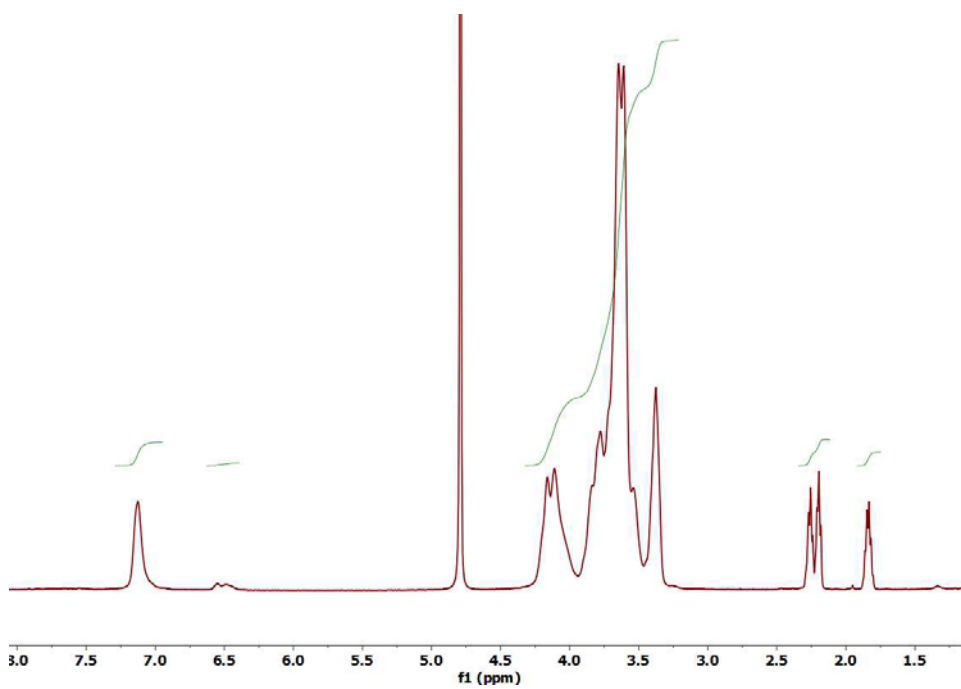
MALDI-TOF MS spectrum of 2[G3]-FITC.



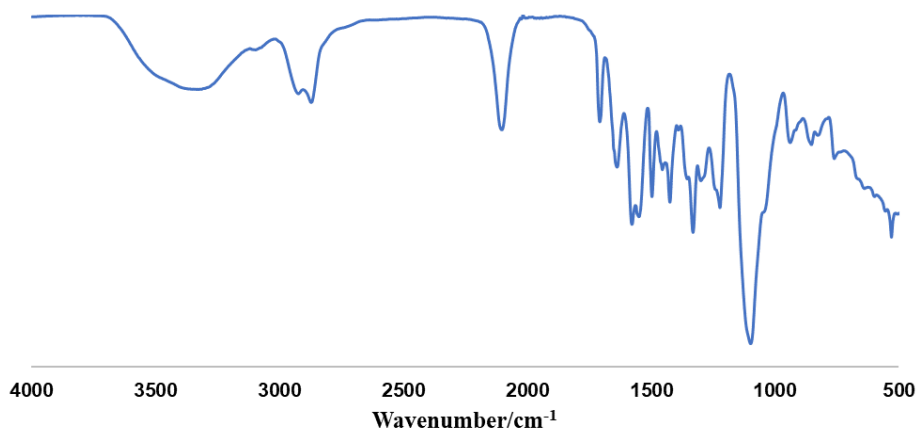
UV-Vis spectrum of 2[G3]-FITC (in BBS-DMSO buffer).

2[G4]-FITC. Following the general procedure described above from 2[G4]-N₃ (75 mg, 1.6 μmol) and Ph₃P (22.1 mg, 0.084 mmol) dissolved in H₂O (0.230 mL) - CHCl₃ (1.15 mL) - MeOH (1.15 mL), and using FITC (3.65 mg, 9.4

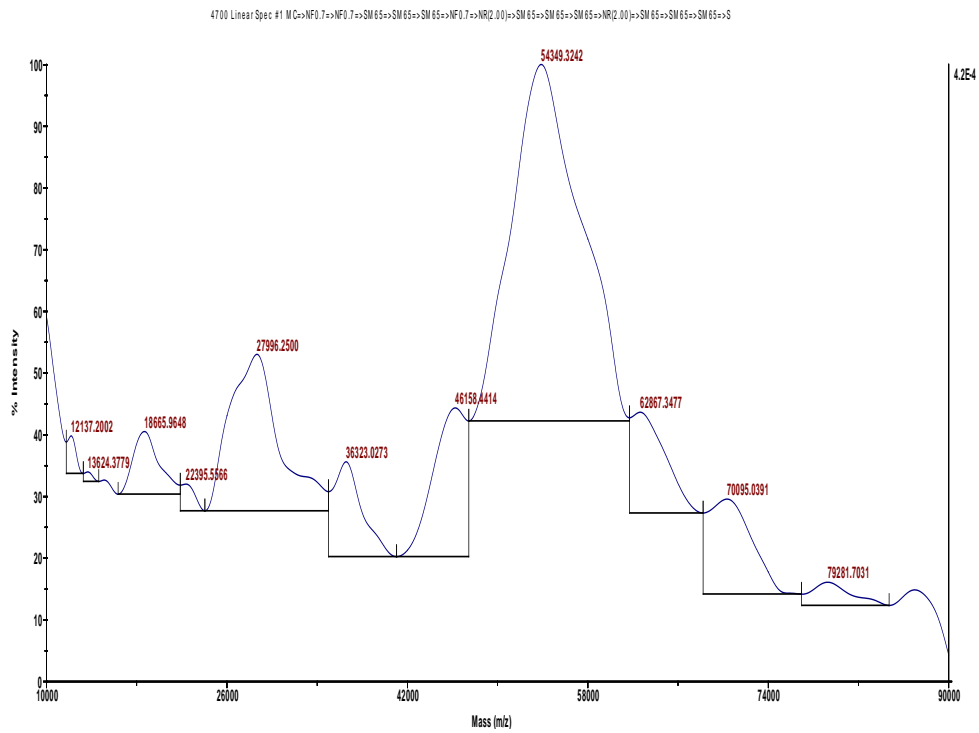
μmol) in DMSO (2.53 mL), Et_3N (0.071 mL, 0.508 mmol) and glutaric anhydride (58 mg, 0.508 mmol), the dendrimer $2[\text{G4}]-(\text{FITC})_5/(\text{CO}_2\text{H})_{44}/(\text{N}_3)_{113}$ ($2[\text{G4}]$ -FITC hereafter) was obtained as a yellow oil (77 mg, 92%). ^1H NMR (500 MHz, D_2O) δ : 7.15-7.08 (m, 160H), 6.54-6.49 (m, 20H), 4.48-3.13 (m, 2892H), 2.26 (t, $J=7.7$ Hz, 88H), 2.19 (t, $J=6.6$ Hz, 88H), 1.90-1.77 (m, 88H). IR (ATR, cm^{-1}): 3357, 2926, 2872, 2103, 1708, 1637, 1576, 1552, 1497, 1425, 1332, 1097. UV-Vis (DMSO) λ_{max} : 519 nm. UV-Vis (BBS-DMSO) λ_{max} : 260, 500 nm. MALDI-TOF MS (DHB, linear mode, m/z) $2[\text{G4}]$ -FITC: 54349, 27996 . Calcd. for $[\text{M}+\text{H}]^+$: 53672, $[\text{M}+2\text{H}]^{2+}$: 26836. An average of 5.5 fluorescein and 44 glutaric acid groups were determined by integration of the multiplets at 6.54-6.49 ppm (fluorescein) and 1.90-1.77 ppm (glutaric acid) in the ^1H NMR (D_2O) spectrum. A similar degree of fluorescein functionalization (5.2) was obtained by absorbance at 519 nm in DMSO, applying an extinction coefficient of $60800 \text{ M}^{-1} \text{ cm}^{-1}$.



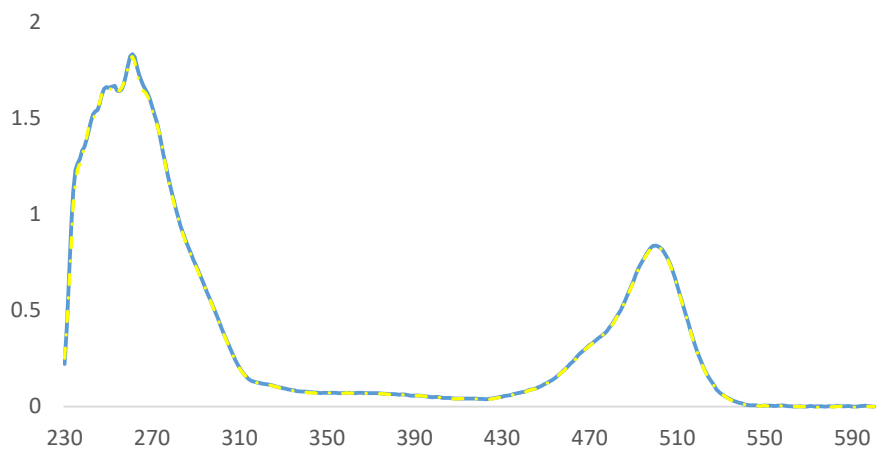
^1H NMR spectrum (D_2O) of 2[G4]-FITC.



IR spectrum of 2[G4]-FITC.



MALDI-TOF MS spectrum of 2[G4]-FITC.



UV-Vis spectrum of 2[G4]-FITC (in BBS-DMSO buffer).

II.5.3 2[Gn]-[C5] synthesis

General procedure. 2[Gn]-FITC was dissolved in BBS-DMSO to give a 0.3 mM concentration of terminal azides. An equal volume of either 0.05 mM C5-BCN (16.6 mol % per terminal N₃, low loading) or 0.1 mM C5-BCN (33.3 mol % per terminal N₃, high loading) in BBS-DMSO was added dropwise (buffer exchanged from PBS-DMSO to BBS-DMSO using Vivaspin 20, MWCO 3000). The resulting solution was stirred at rt under Ar, protected from light. Analysis of the reaction mixture after 24 h by SDS-PAGE revealed the presence of high molecular weight 2[Gn]-[C5] conjugates that were separated from unreacted Affitin by SEC (Superdex 75 gel filtration column, GE Healthcare) using BBS-DMSO as running buffer. The purity and monodispersity of the conjugates were verified by SEC (Superdex 200 gel filtration column, GE Healthcare; BBS-DMSO) and DLS (BBS-DMSO buffer), which showed the expected increase in size with G and degree of C5 functionalization.

Determination of the degree of functionalization of the conjugates with C5 Affitin (N, average valency). 2[G3]-[C5]_{low} was analysed by MALDI-TOF and the average number of conjugated C5 Affitins per dendrimer (N) was determined by integration of the peaks corresponding to the conjugates containing 2-10 Affitins per dendrimer. Since MALDI spectra of adequate quality could not be obtained for the remaining conjugates, probably due to their much larger MW and higher powers required, a UV-Vis quantification

method (described below) was validated by comparison with the N value determined via integration of the MALDI MS of 2[G3]-[C5]_{low}.

UV-Vis method. The average number of conjugated C5 Affitins per dendrimer (N) was determined by UV-Vis comparing the relative absorbances at 280 nm (dendrimer and Affitin; λ_{\max} for the Affitin) and 500 nm (FITC at dendrimer, λ_{\max} for the dendrimer) in BBS-DMSO, using the equation:

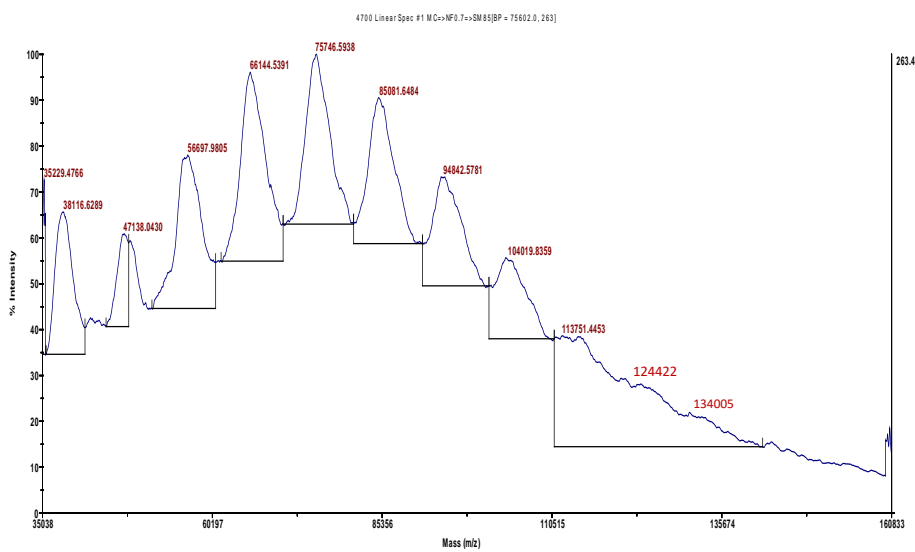
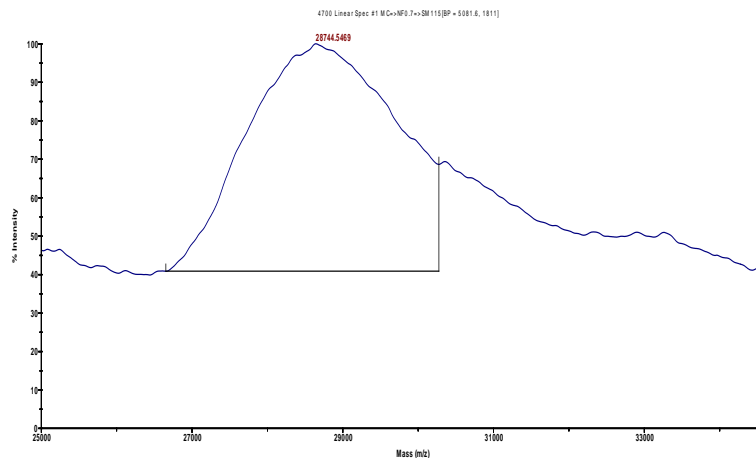
$$N = \frac{\left(A_{280} - \frac{A_{500} * \epsilon_{280}^{\text{dend}}}{\epsilon_{500}^{\text{dend}}} \right) * \epsilon_{500}^{\text{dend}}}{\epsilon_{280}^{\text{Aff}} * A_{500}}$$

where A_{280} and A_{500} are the absorbances of the conjugates at 280 nm and 500 nm in BBS-DMSO, and $\epsilon_{280}^{\text{dend}}$, $\epsilon_{500}^{\text{dend}}$ and $\epsilon_{280}^{\text{Aff}}$ the extinction coefficients of 2[Gn]-FITC dendrimers and C5-BCN in BBS-DMSO at given wavelengths (table below). All the spectra used for quantification were recorded in duplicate. Similar results were obtained by the analysis of 260/280 nm signal ratios (data not shown).

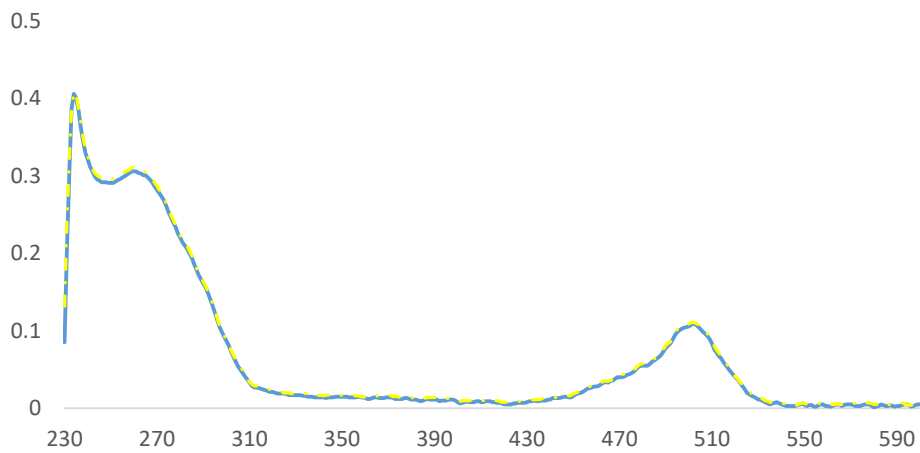
Extinction coefficients ϵ ($M^{-1} \text{ cm}^{-1}$) of dendrimers and C5-BCN.

| | 2[G3]-FITC | 2[G4]-FITC | C5-BCN |
|------------------|-------------------|-------------------|---------------|
| ϵ_{280} | 131300 | 414710 | 13710 |
| ϵ_{500} | 106050 | 326680 | 0 |

2[G3]-[C5]_{low}. From 2[G3]-FITC (1.6 mg, 90 nmol) and C5-BCN (5.3 mg, 540 nmol), following the general procedure described above, 2[G3]-[C5]_{low} was obtained with an average (N) of 6 Affitins per dendrimer (N=5.69 determined by UV-Vis, 5.83 by MALDI-TOF (peaks 2[G3]-[C5]₂₋₁₀); 95% C5-BCN conversion). MALDI-TOF MS (SA, linear mode, m/z) 2[G3]-[C5]₁₋₁₂: 28745, 38117, 47138, 56698, 66145, 75747, 85082, 94843, 104020, 113751, 124422, 134005. Calculated for [M+H]⁺: 27398, 37019, 46639, 56260, 65881, 75502, 85123, 94744, 104365, 113985, 123606, 133227. UV-Vis (BBS-DMSO) λ_{max} : 260, 500 nm.

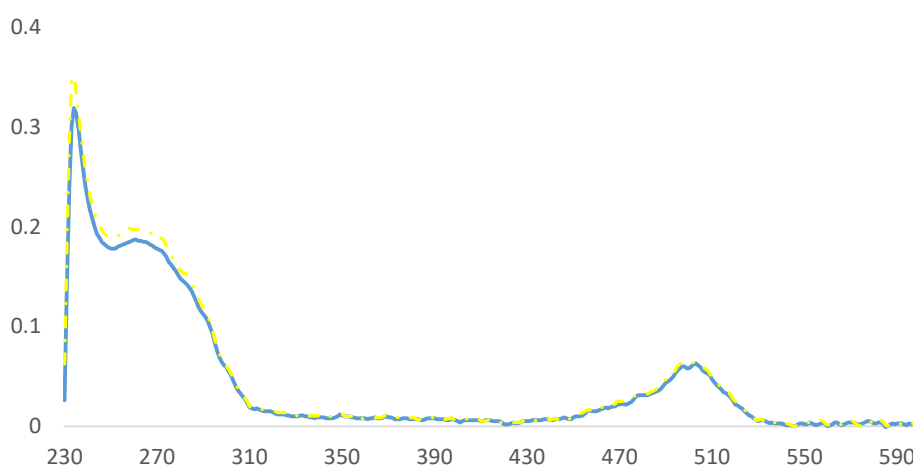


MALDI-TOF MS spectrum of 2[G3]-[C5]_{low}.



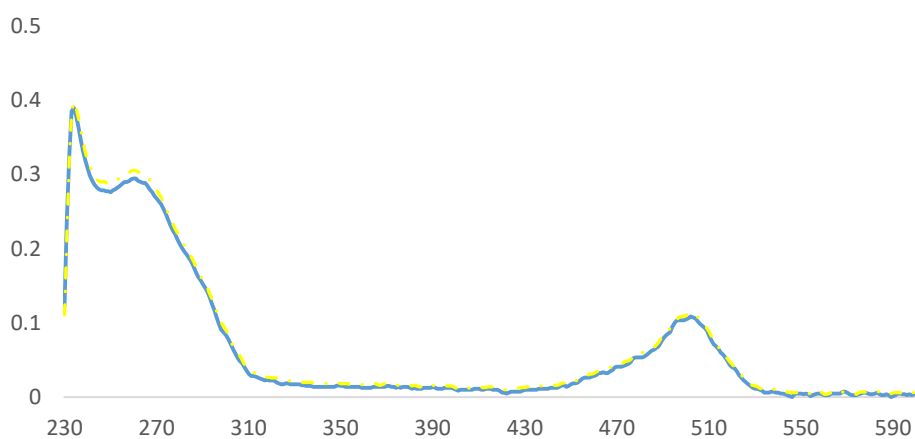
UV-Vis spectrum of 2[G3]-[C5]_{low} (in BBS-DMSO buffer).

2[G3]-[C5]_{high}. From 2[G3]-FITC (1.6 mg, 90 nmol) and C5-BCN (10.6 mg, 1080 nmol), following the general procedure described above, 2[G3]-[C5]_{high} was obtained with an average (N) of 10 Affitins per dendrimer as determined by UV-Vis (88% C5-BCN conversion). UV-Vis (BBS-DMSO) λ_{max} : 260, 500 nm.



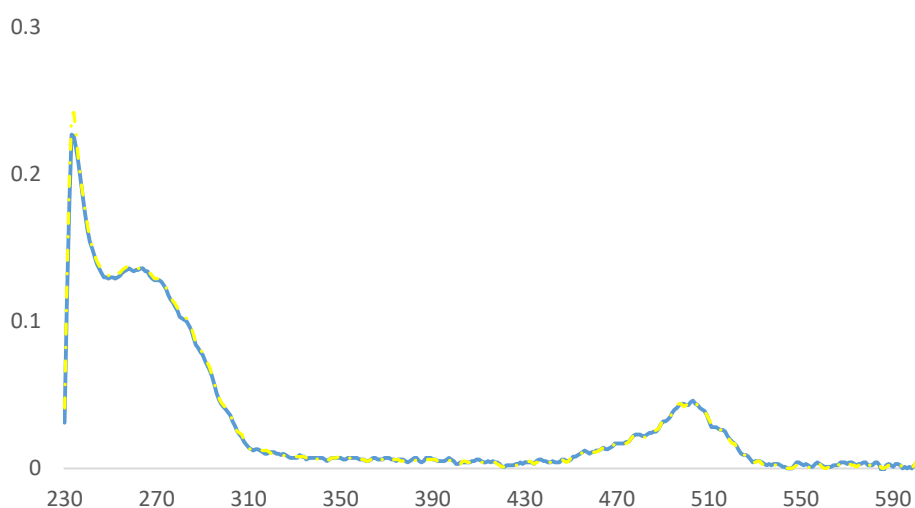
UV-Vis spectrum of 2[G3]-[C5]_{high} (in BBS-DMSO buffer).

2[G4]-[C5]_{low}. From 2[G4]-FITC (1.6 mg, 30 nmol) and C5-BCN (5.3 mg, 540 nmol), following the general procedure described above, 2[G4]-[C5]_{low} was obtained with an average (N) of 12 Affitins per dendrimer as determined by UV-Vis (67% C5-BCN conversion). UV-Vis (BBS-DMSO) λ_{max} : 260, 500 nm.



UV-Vis spectrum of 2[G4]-[C5]_{low} (in BBS-DMSO buffer).

2[G4]-[C5]_{high}. From 2[G4]-FITC (1.6 mg, 30 nmol) and C5-BCN (10.6 mg, 1080 nmol), following the general procedure described above, 2[G4]-[C5]_{high} was obtained with an average (N) of 27 Affitins per dendrimer as determined by UV-Vis (74% C5-BCN conversion). UV-Vis (BBS-DMSO) λ_{max} : 260, 500 nm.



UV-Vis spectrum of 2[G4]-[C5]_{high} (in BBS-DMSO buffer).

II.6 Surface plasmon resonance

SPR binding assays. Biotinylated SpA domain A was immobilized on a streptavidin-chip to a low density of 25 resonance units (RU) for the analysis of 2[G3]-[C5]_{low}, 2[G3]-[C5]_{high}, 2[G4]-[C5]_{low} and 2[G4]-[C5]_{high}. A higher density immobilization was necessary to obtain kinetic data for C5 and C5-S dimer (400 RU). All the tested samples were diluted in the running buffer HBSEP pH 7.4 (20 mM HEPES, 150 mM NaCl, and 0.005% Surfactant P20) in a range of concentrations (15.6-250 nM for C5 and C5-S dimer, 6.25-100 nM for 2[G3]-[C5]_{low} and 2[G3]-[C5]_{high}, 1.56-12.5 nM for 2[G4]-[C5]_{low} and 2[G4]-[C5]_{high}). Association times were 3 min for C5, 6 min for C5-S dimer and 8 min for 2[G3]-[C5]_{low}, 2[G3]-[C5]_{high}, 2[G4]-[C5]_{low} and 2[G4]-[C5]_{high}. Dissociation times were 3 min for C5, 5 min for C5-S dimer and 12 min for 2[G3]-[C5]_{low}, 2[G3]-[C5]_{high}, 2[G4]-[C5]_{low} and 2[G4]-[C5]_{high}. Regeneration between cycles was performed with 10 mM glycine, pH 1.5.

SPR data analysis. All the experimental data were corrected for instrumental and bulk artefacts using reference curves obtained from the buffer injections in the pre-processing step in the BIAevaluation software version 3.1. C5 binding curves were analysed using a 1:1 Langmuir binding model incorporated in the BIAevaluation software and kinetic constants k_{on} , k_{off} and K_D were obtained. All other binding curves were exported to R Studio software and analysed as follows.

SPR analysis of multivalent binding modes. Multivalency of the conjugates causes heterogeneous binding profiles representative of both low and high affinity binding modes. To perform the SPR analysis of the conjugates, we applied our previously described method³⁹ that focuses on analysing early association and late dissociation phases of sensograms, where high affinity multivalent binding modes prevail, providing kinetic constants $k_{on-high}$, $k_{off-high}$ and K_D . This way, meaningful kinetic and thermodynamic data was obtained for 2[G3]-[C5]_{low}. The remaining conjugates with larger valency (N) showed no observable dissociation from the target, which hampered quantitative analysis. For 2[G3]-[C5]_{low} the analysis was performed in three steps:

Step one: Analysis of the late dissociation phase. $k_{off-high}$ was obtained by global fitting of the late dissociation phase data to the classical equation for pseudo first order kinetics:

$$R_t = R_0 \exp(-k_{off-high} (t-t_0)) \quad [1]$$

Where R_t is the SPR response at time “t”, R_0 is the response at the beginning of late dissociation ($t_0=780$ s).

Step two: Linear analysis of the early association phase. Observable rate constants, k_{obs} were calculated for each analyte concentration by locally fitting early association phase ($t<30$ s) of the sensograms to the equation:

$$R_t = R_{eq} (1-\exp(-k_{obs} t)) \quad [2]$$

Then, plots of k_{obs} against C_d (concentration of the analyte) were represented, where deviations from the standard linear behaviour were indicative of binding heterogeneity, and used to select the conditions representative of either higher or lower affinity binding modes for step three of the analysis.

Step three: Non-linear analysis of the early association phase. $k_{on-high}$ and k_{on-low} values were calculated by global fitting of the early association phase of the sensograms selected in step two to the equation:

$$R_t = R_{eq} (1 - \exp(-(k_{on} C_d + k_{off-high}) t)) \quad [3]$$

III. Results and discussion

III.1 Making Affitin C5 “clickable”

Using site-directed mutagenesis we were able to replace LN residues at the C-terminal of C5 Affitin sequence with GC, introducing a unique cysteine residue that will allow a site-specific thiol coupling far away from the Affitin binding site (Figure 9).

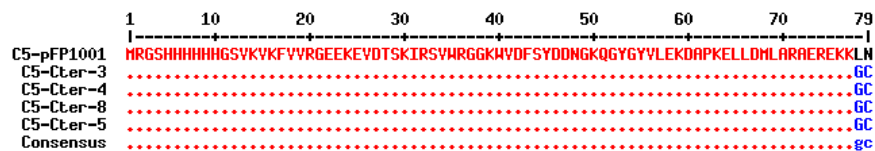


Figure 9. C5 sequence as expressed in pFP1001 vector aligned against a consensus from the four sequencing results of the modified C5-SH. At N-terminal, there is a His₆ tag to facilitate purification of the Affitin, while C-terminal modification provided a unique thiol group for chemical functionalization.

C5-SH Affitin sequence ligated in the pFP1001 vector was then used to transfect *E. coli DH5α lq* and produce the protein with yields up to 40 mg per liter of culture. SEC and SDS-PAGE analysis of the purified protein revealed that it spontaneously forms C5-S dimers in the absence of a reducing agent (Figure 10), while adding tris(2-carboxyethyl)phosphine (TCEP) reduces most of the dimers. Even though dimerization is not

complete, in all further experiments where no reducing agent is added, C5-SH is considered as C5-S dimer and the concentration is given according to the dimeric form.

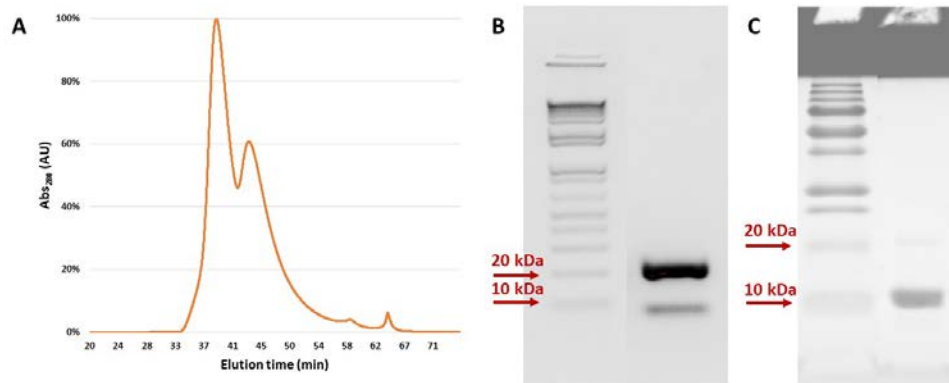


Figure 10. C5-SH on (a) SEC in PBS, (b) 15% SDS-PAGE and (c) 15% SDS-PAGE after 1h stirring in PBS in the presence of TCEP (TCEP:C5-SH = 30:1)

The ELISA test of C5-S dimer shows a significant, concentration-dependent inhibition of the signal originating from biotinylated C5. This confirms binding of C5-S dimer to SpA, which leaves fewer binding sites available for C5 binding, and suggests a low dissociation constant (Figure 11).

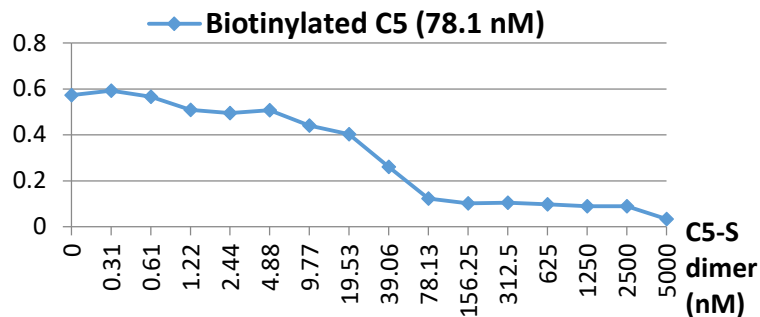


Figure 11. ELISA test of C5-S dimer against biotinylated C5

Obtained Affitin C5-SH was then reacted with a maleimide-BCN construct with an overall yield of 71%, effectively making it azide-reactive and so, “clickable” to the dendrimer surface (Figure 12)

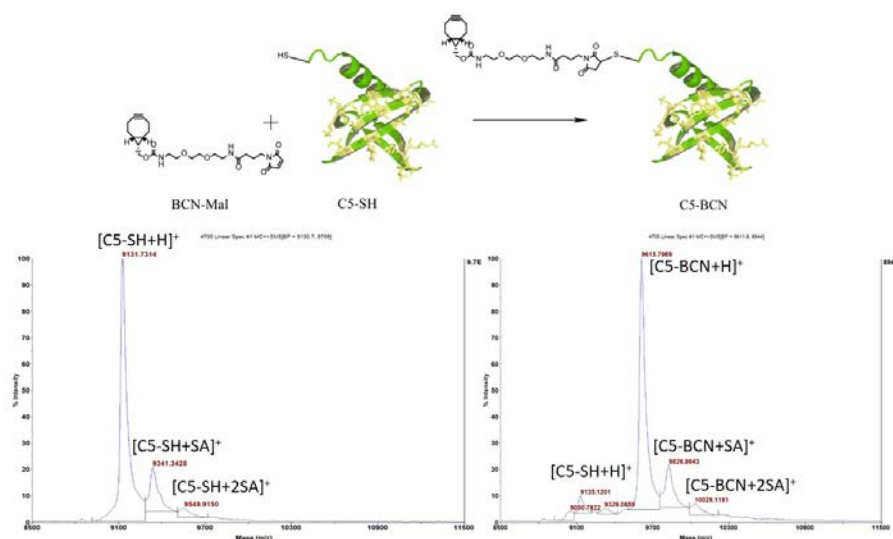


Figure 12. C5-SH functionalization with BCN and MALDI-TOF of C5-SH (left) and C5-BCN reaction (right).

III.2 Surface engineering of 2[Gn]-FITC

Starting from 2[G3]-N₃ and 2[G4]-N₃ (containing 54 and 162 terminal azides), synthesized as described before,⁸ we exploited the versatility of the terminal azide groups to introduce carboxylates on the dendrimer surface to improve the water solubility, as well as to achieve fluorescein labelling in order to facilitate downstream quantification and detection. We devised a simple, one-pot three-step protocol that allows complete control over the surface functionality of the dendrimer. To this end, an initial reduction of a

third of the terminal azides to primary amines via Staudinger reaction was followed by fluorescent labeling with fluorescein isothiocyanate (FITC). Finally, since cationic dendrimers have been shown to cause unspecific bacterial clustering^{52,53} and cyto-toxicity,^{54,55} we used glutaric anhydride to replace positively charged amines with negatively charged carboxylates. Resulting water-soluble, fluorescent 2[G3]-FITC and 2[G4]-FITC were obtained in very good yield. NMR analysis confirmed that around 30% of the terminal azides present in dendrimers were converted into carboxylates, while an average of 1.5 and 5.5 fluorescein molecules was determined for 2[G3]-FITC and 2[G4]-FITC, respectively (NMR and UV analysis). An abundance of azide groups remained available on the modified dendrimer surface for SPAAC conjugation of Affitin or other desired agents (Table 1).

Table 1. Surface functionalization of 2[G3]-FITC / 2[G4]-FITC.

| | Average number of peripheral functions | | | |
|------------|--|--------------------|-------------|-------|
| | N ₃ | CO ₂ Na | Fluorescein | Total |
| 2[G3]-FITC | 37 | 15 | 2 | 54 |
| 2[G4]-FITC | 113 | 44 | 5 | 162 |

III.3 Affitin-dendrimer conjugates

Using the devised SPAAC conjugation strategy, four distinct Affitin-dendrimer conjugates were devised. The Mansfield-Tomalia-Rakesh equation⁵⁶ predicted a maximum of 25 and 50 Affitins (N_{max}) to be accommodated on the dendritic surface of 2[G3]-FITC and 2[G4]-FITC based on their relative radii (ca 4.5 nm for 2[G3]-FITC, 7.5 nm for 2[G4]-FITC,²⁶ and

1.4 nm for C5-SH⁵⁷). Accordingly, two degrees of labeling were pursued for each dendrimer G accounting for half, and a quarter of the N_{max}. As a result, four Affitin-dendrimer conjugates, labeled as 2[G_n]-[C5]_x [where n signifies dendrimer generation (3 or 4), and x is Affitin valency (low or high)], were obtained with a 70-95% conjugation efficiency. The obtained conjugates were purified from any unreacted Affitin molecules and characterized in terms of their multivalency, size, monodispersity and affinity for the target.

MALDI-TOF analysis of 2[G3]-[C5]_{low} provided detailed insight into the structure and size distribution of the conjugates. The distribution of MWs followed a theoretical Poisson distribution predicted for such a conjugation (Figure 13).

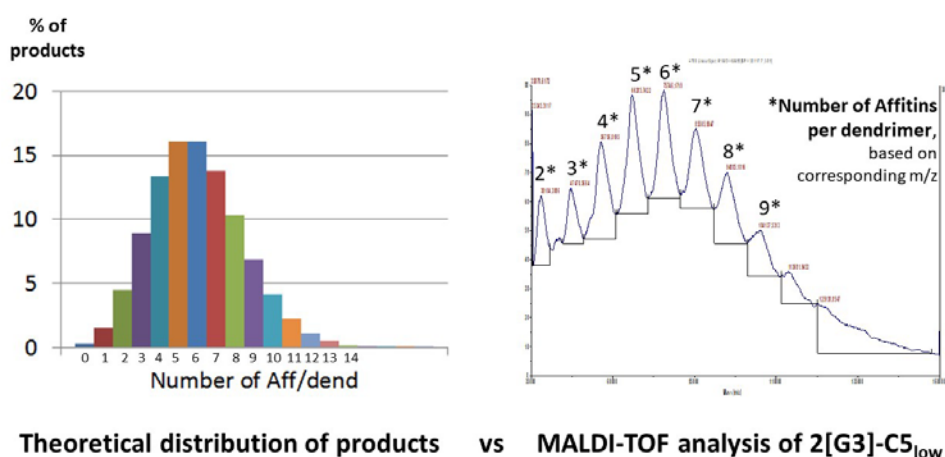


Figure 13. Poisson distribution predicts sizes of obtained products with high correlation.

Since MALDI spectra of adequate quality could not be obtained for the remaining conjugates because of their high molecular weight, a UV-Vis method that allows facile concentration measurement and determination of average Affitin valency (N) was successfully validated by comparison with the results obtained by MALDI for $2[G3]-[C5]_{low}$. As expected, the size of conjugates, analyzed by DLS, was found to be increasing with G and N of conjugates: $2[G3]-[C5]_{low}$ ($N=6$, 13 nm), $2[G3]-[C5]_{high}$ ($N=10$, 15 nm), $2[G4]-[C5]_{low}$ ($N=12$, 17 nm), and $2[G4]-[C5]_{high}$ ($N=27$, 22 nm). Their purity and monodispersity were confirmed by SEC and DLS (Figure 14).

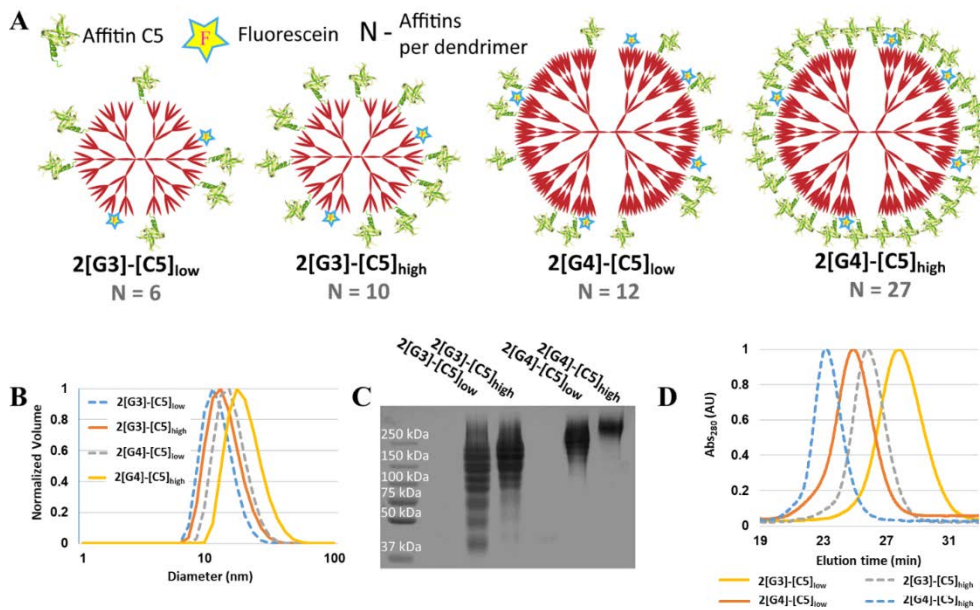


Figure 14. A) Schematic representation of Affitin-dendrimer conjugates $2[Gn]-[C5]_x$ (n : dendrimer generation, x : Affitin valency, low or high) reflecting the average number of Affitins per dendrimer (N). B) DLS size distribution, C) 10% SDS-PAGE, and D) SEC analysis of the conjugates.

III.4 Surface plasmon resonance

Affinity of the monovalent interaction of Affitin C5 with SpA domain A, immobilized on the chip as a target, was found to be 103 nM, using a one-site-binding model from the instrument software - which is very similar to the 107 nM value previously obtained by bio-layer interferometry.⁹

Visual inspection of sensograms (Figure 15) obtained by the analysis of spontaneously formed C5-S dimer on the same high-ligand-density chip (400 RU) used for the monomer reveals much slower dissociation rates, indicating stabilization by either rebinding or chelating effect, due to the bivalency of this product. However, a heterogeneous binding profile, reflecting both monomer and dimer forms present in the sample, doesn't fit any of the available kinetic models, rendering it impossible to reliably obtain kinetic constants.

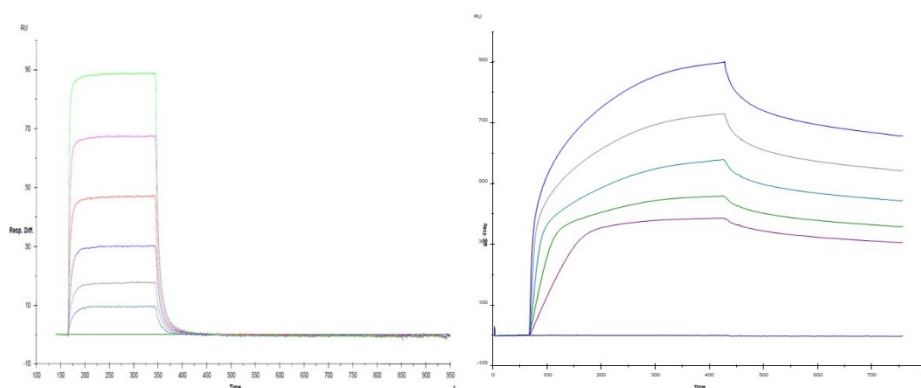


Figure 15. SPR sensograms of Affitin C5 (left) and C5-S dimer (right) analyzed with a 400 RU SpA domain A chip loading

Affitin-dendrimer conjugates were analyzed on a chip loaded with ligand at lower density (25 RU) (Figure 16 shows full sensograms of all conjugates).

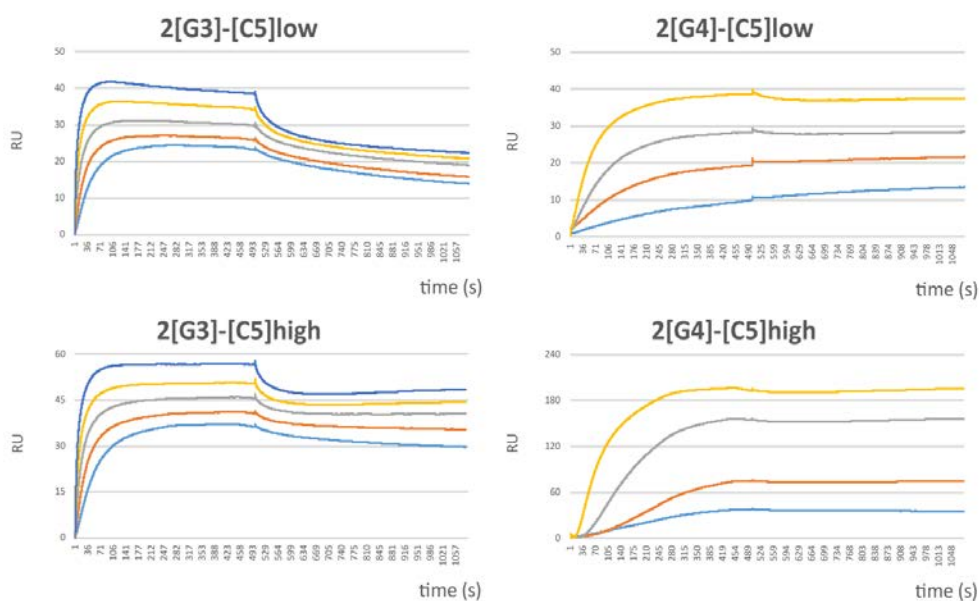


Figure 16. SPR sensograms of the Affitin-dendrimer conjugates analyzed at 25 RU initial response chip loading (Concentrations: 6.25-100 nM for 2[G3]-[C5]_{low} and 2[G3]-[C5]_{high}; 1.56-12.5 nM for 2[G4]-[C5]_{low} and 2[G4]-[C5]_{high})

Using our previously described kinetic analysis method,³⁹ which allows insight into multivalent, high affinity binding modes by studying the early association and late dissociation phases of the sensorgrams, we were able to determine meaningful thermodynamic and kinetic constants for 2[G3]-[C5]_{low}, which showed around three orders of magnitude

improvement of K_D over the monovalent interaction, mostly due to improved dissociation rate. Furthermore, larger k_{on} values compared to the monomer Affitin were also observed at the early association phase (Figure 17, Table 2). While decreased dissociation of the complexes can be due to rebinding and chelation effects, increased association rates unambiguously point to the conjugate's ability to bind two target molecules on chip simultaneously,^{41,58-60} confirming the efficient chelating character of the design.

Remaining conjugates showed no observable dissociation at given conditions, in agreement with an almost irreversible binding. Therefore, the conjugates were compared by the percentage of SPR signal decay during early dissociation rate, which reflects the portion of each conjugate population that is capable of multivalency-stabilized complexes with the target (Table 3). For G3 conjugates, there is an improvement from 24% signal decay for the lower valency to 10% for the higher valency, indicating that extra Affitin loading translates into higher affinity interactions with the target. Remarkably, both conjugates of G4 dendrimers show almost no signal decay, clearly indicating that their larger size has a great impact on the stabilization of the complexes, while higher Affitin loading doesn't seem to provide additional advantage at this dendrimer generation.

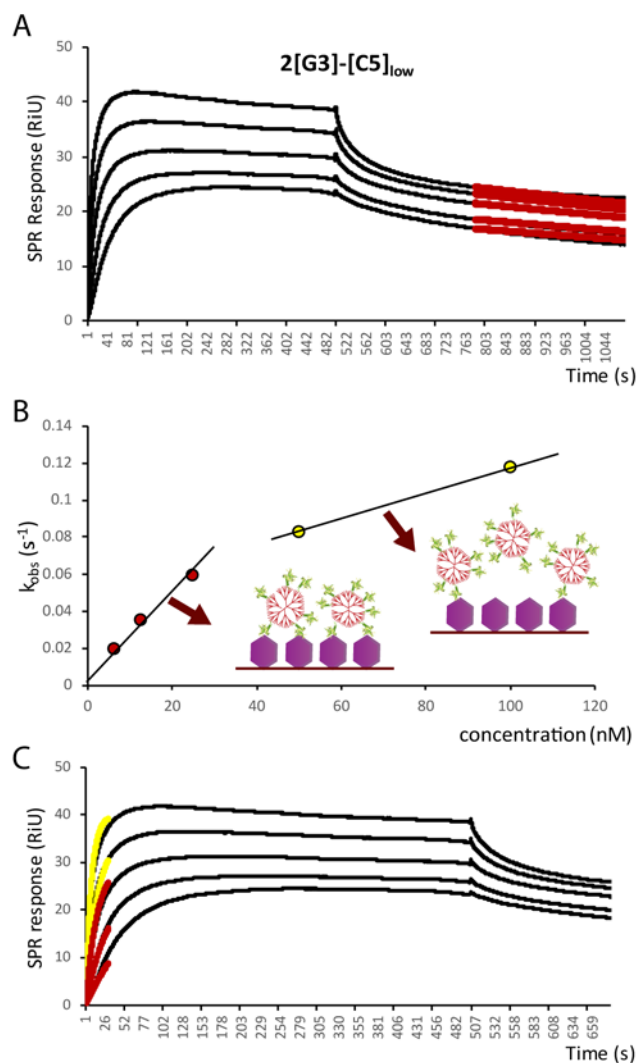


Figure 17. SPR kinetic analysis (ref. 37) of the multivalent interaction of 2[G3]-[C5]_{low} (6.25-100 nM) with SpA domain A. Step I (late dissociation phase kinetic analysis): (a) sensograms (black) and global fitting (red) to equation [1]. Step II and III (early association phase kinetic analysis): B. plots of observed rates k_{obs} determined by local fitting to equation [2] against the concentrations for which they are determined (red points for higher affinity modes observed, yellow for lower) and C. sensograms (black) and their global fitting (red for higher affinity modes observed, yellow for lower) to equation [3] (see equations and analysis description in materials and methods).

Table 2. Binding data from separate SPR kinetic analysis of C5 and 2[G3]-

[C5]_{low}: k_{on} ($\times 10^6 M^{-1} s^{-1}$), k_{off} ($\times 10^{-4} s^{-1}$) and K_D (nM).

| | k_{on} | k_{off} | K_D |
|-----------------------------|----------|-----------|-------|
| C5 | 0.95 | 979 | 103 |
| 2[G3]-[C5] _{low} * | 2.50 | 4.30 | 0.17 |

* $k_{on-high}$, $k_{off-high}$, and K_{D-high} for 2[G3]-[C5]_{low} based on the early association and late dissociation phase analysis.

Table 3. Percentage of SPR signal decay at early dissociation times calculated

as $(1 - R_{t=780}/R_{t=480})\times 100$, where $R_{t=480}$ is the SPR response at the end of analyte injection.

| Analyte (conc=12.5 nM) | % SPR signal decay |
|----------------------------|--------------------|
| 2[G3]-[C5] _{low} | 24 |
| 2[G3]-[C5] _{high} | 10 |
| 2[G4]-[C5] _{low} | 2 |
| 2[G4]-[C5] _{high} | 2 |

IV. Acknowledgements

This work was financially supported by the Spanish Ministry of Economy, Industry, and Competitiveness (MINECO) (CTQ2015-69021-R), the Xunta de Galicia (GRC2014/040 and Centro Singular de Investigación de Galicia Accreditation 2016–2019, ED431G/09), and the European Union (European Regional Development Fund, ERDF). SPR spectra were acquired at Plateforme IMPACT Biogenouest (Nantes, France) by Mike Maillason, whom we thank dearly. For MALDI-TOF spectra that were acquired at Laboratorio de Proteómica, Complejo Hospitalario Universitario (Santiago de Compostela, Spain), we owe gratitude to Susana Bravo López. P.V. thanks the European Commission and the Education, Audiovisual and Cultural Executive Agency (EACEA) for an Erasmus Mundus grant under the Nanomedicine and Pharmaceutical Innovation (NanoFar) Joint Doctoral Program.

V. References

1. Mouratou B, Schaeffer F, Guilvout I, Tello-Manigne D, Pugsley AP, Alzari PM, Pecorari F. Remodeling a DNA-binding protein as a specific in vivo inhibitor of bacterial secretin PulD. *Proceedings of the National Academy of Sciences*. 2007 Nov 13;104(46):17983-8.
2. Pecorari, F. & Alzari, P. M. OB-fold used as scaffold for engineering new specific binders. *Pat. Publ. Nos. PCT/IB2007/004388* (2008).
3. McAfee JG, Edmondson SP, Datta PK, Shriver JW, Gupta R. Gene cloning, expression, and characterization of the Sac7 proteins from the hyperthermophile *Sulfolobus acidocaldarius*. *Biochemistry*. 1995 Aug 1;34(31):10063-77.
4. Baumann H, Knapp S, Karshikoff A, Ladenstein R, Härd T. DNA-binding surface of the Sso7d protein from *Sulfolobus solfataricus*.
5. McCrary BS, Edmondson SP, Shriver JW. Hyperthermophile protein folding thermodynamics: differential scanning calorimetry and chemical denaturation of Sac7d. *Journal of molecular biology*. 1996 Dec 13;264(4):784-805.
6. Catanzano F, Graziano G, Fusi P, Tortora P, Barone G. Differential scanning calorimetry study of the thermodynamic stability of some mutants of Sso7d from *Sulfolobus solfataricus*. *Biochemistry*. 1998 Jul 21;37(29):10493-8.

7. Béhar G, Bellinzoni M, Maillasson M, Paillard-Laurance L, Alzari PM, He X, Mouratou B, Pecorari F. Tolerance of the archaeal Sac7d scaffold protein to alternative library designs: characterization of anti-immunoglobulin G Affitins. *Protein Engineering, Design & Selection*. 2013 Jan 11;26(4):267-75.
8. Béhar G, Pacheco S, Maillasson M, Mouratou B, Pecorari F. Switching an anti-IgG binding site between archaeal extremophilic proteins results in Affitins with enhanced pH stability. *Journal of biotechnology*. 2014 Dec 20;192:123-9.
9. Kalichuk V, Renodon-Cornière A, Béhar G, Carrión F, Obal G, Maillasson M, Mouratou B, Préat V, Pecorari F. A novel, smaller scaffold for Affitins: Showcase with binders specific for EpCAM. *Biotechnology and bioengineering*. 2018 Feb;115(2):290-9.
10. Krehenbrink M, Chami M, Guilvout I, Alzari PM, Pécóari F, Pugsley AP. Artificial binding proteins (Affitins) as probes for conformational changes in secretin PulD. *Journal of molecular biology*. 2008 Nov 28;383(5):1058-68.
11. Buddelmeijer N, Krehenbrink M, Pecorari F, Pugsley AP. Type II secretion system secretin PulD localizes in clusters in the Escherichia coli outer membrane. *Journal of bacteriology*. 2009 Jan 1;191(1):161-8.
12. Correa A, Pacheco S, Mechaly AE, Obal G, Béhar G, Mouratou B, Oppezzo P, Alzari PM, Pecorari F. Potent and specific inhibition of

- glycosidases by small artificial binding proteins (Affitins). PLoS One. 2014 May 13;9(5):e97438.
13. Cinier M, Petit M, Williams MN, Fabre RM, Pecorari F, Talham DR, Bujoli B, Tellier C. Bisphosphonate adaptors for specific protein binding on zirconium phosphonate-based microarrays. *Bioconjugate chemistry*. 2009 Nov 23;20(12):2270-7.
 14. Mouratou B, Béhar G, Pecorari F. Artificial affinity proteins as ligands of immunoglobulins. *Biomolecules*. 2015 Jan 30;5(1):60-75.
 15. Matous E. *Développement d'une Affitin anti-CD138 comme nouvel outil pour l'imagerie phénotypique* (Doctoral dissertation, Nantes).
 16. Béhar G, Renodon-Cornière A, Kambarev S, Vukojicic P, Caroff N, Corvec S, Mouratou B, Pecorari F. Whole-bacterium ribosome display selection for isolation of highly specific anti-Staphylococcus aureus Affitins for detection- and capture-based biomedical applications. **Submitted to** *Biotechnology and Bioengineering*.
 17. Miranda FF, Brient-Litzler E, Zidane N, Pecorari F, Bedouelle H. Reagentless fluorescent biosensors from artificial families of antigen binding proteins. *Biosensors and Bioelectronics*. 2011 Jun 15;26(10):4184-90.
 18. Béhar G, Renodon-Cornière A, Mouratou B, Pecorari F. Affitins as robust tailored reagents for affinity chromatography purification of antibodies and non-immunoglobulin proteins. *Journal of Chromatography A*. 2016 Apr 8;1441:44-51.

19. Fernandes CS, Dos Santos R, Ottengy S, Viecinski AC, Béhar G, Mouratou B, Pecorari F, Roque AC. Affitins for protein purification by affinity magnetic fishing. *Journal of Chromatography A*. 2016 Jul 29;1457:50-8.
20. Kalichuk V. A novel generation of Affitins for targeting cancer cells with drug-loaded nanocapsules (Doctoral dissertation, UCL-Université Catholique de Louvain).
21. Sashiwa H, Shigemasa Y, Roy R. Chemical modification of chitosan. 10. Synthesis of dendronized chitosan– sialic acid hybrid using convergent grafting of preassembled dendrons built on gallic acid and Tri (ethylene glycol) backbone. *Macromolecules*. 2001 Jun 5;34(12):3905-9.
22. Roy R, Park WK, Wu Q, Wang SN. Synthesis of hyper-branched dendritic lactosides. *Tetrahedron letters*. 1995 Jun 19;36(25):4377-80.
23. Sousa-Herves A, Novoa-Carballal R, Riguera R, Fernandez-Megia E. GATG dendrimers and PEGylated block copolymers: from synthesis to bioapplications. *The AAPS journal*. 2014 Sep 1;16(5):948-61.
24. Fernandez-Megia E, Correa J, Rodríguez-Meizoso I, Riguera R. A click approach to unprotected glycodendrimers. *Macromolecules*. 2006 Mar 21;39(6):2113-20.
25. Amaral SP, Fernandez-Villamarin M, Correa J, Riguera R, Fernandez-Megia E. Efficient multigram synthesis of the repeating unit of gallic acid-triethylene glycol dendrimers. *Organic letters*. 2011 Aug 5;13(17):4522-5.

26. Amaral SP, Tawara MH, Fernandez-Villamarin M, Borrajo E, Martínez-Costas J, Vidal A, Riguera R, Fernandez-Megia E. Tuning the Size of Nanoassemblies: A Hierarchical Transfer of Information from Dendrimers to Polyion Complexes. *Angewandte Chemie International Edition*. 2018 May 4;57(19):5273-7.
27. Albertazzi L, Fernandez-Villamarin M, Riguera R, Fernandez-Megia E. Peripheral functionalization of dendrimers regulates internalization and intracellular trafficking in living cells. *Bioconjugate chemistry*. 2012 Apr 16;23(5):1059-68.
28. Sousa-Herves A, Espinel CS, Fahmi A, González-Fernández Á, Fernandez-Megia E. In situ nanofabrication of hybrid PEG-dendritic-inorganic nanoparticles and preliminary evaluation of their biocompatibility. *Nanoscale*. 2015;7(9):3933-40.
29. Fernandez-Villamarin M, Sousa-Herves A, Porto S, Guldris N, Martínez-Costas J, Riguera R, Fernandez-Megia E. A dendrimer-hydrophobic interaction synergy improves the stability of polyion complex micelles. *Polymer Chemistry*. 2017;8(16):2528-37.
30. Sousa-Herves A, Fernandez-Megia E, Riguera R. Synthesis and supramolecular assembly of clicked anionic dendritic polymers into polyion complex micelles. *Chemical Communications*. 2008(27):3136-8.
31. Sousa-Herves A, Fernandez-Megia E, Riguera-Vega R, inventors; Universidade de Santiago de Compostela, assignee. Ph-sensitive

- dendritic polymeric micelles. United States patent application US 13/056,823. 2012 Jan 5.
32. Ravina M, de La Fuente M, Correa J, Sousa-Herves A, Pinto J, Fernandez-Megia E, Riguera R, Sanchez A, Alonso MJ. Core– shell dendriplexes with sterically induced stoichiometry for gene delivery. *Macromolecules*. 2010 Aug 6;43(17):6953-61.
33. De La Fuente M, Raviña M, Sousa-Herves A, Correa J, Riguera R, Fernandez-Megia E, Sánchez A, Alonso MJ. Exploring the efficiency of gallic acid-based dendrimers and their block copolymers with PEG as gene carriers. *Nanomedicine*. 2012 Nov;7(11):1667-81.
34. Leiro V, Garcia JP, Moreno PM, Spencer AP, Fernandez-Villamarin M, Riguera R, Fernandez-Megia E, Pêgo AP. Biodegradable PEG–dendritic block copolymers: synthesis and biofunctionality assessment as vectors of siRNA. *Journal of Materials Chemistry B*. 2017;5(25):4901-17.
35. Doménech R, Abian O, Bocanegra R, Correa J, Sousa-Herves A, Riguera R, Mateu MG, Fernandez-Megia E, Velázquez-Campoy A, Neira JL. Dendrimers as potential inhibitors of the dimerization of the capsid protein of HIV-1. *Biomacromolecules*. 2010 Jul 13;11(8):2069-78.
36. Klajnert B, Wasiak T, Ionov M, Fernandez-Villamarin M, Sousa-Herves A, Correa J, Riguera R, Fernandez-Megia E. Dendrimers reduce toxicity of A β 1-28 peptide during aggregation and accelerate fibril formation. *Nanomedicine: Nanotechnology, Biology and Medicine*. 2012 Nov 1;8(8):1372-8.

37. Fernández-Trillo F, Pacheco-Torres J, Correa J, Ballesteros P, Lopez-Larrubia P, Cerdán S, Riguera R, Fernandez-Megia E. Dendritic MRI contrast agents: an efficient prelabeling approach based on CuAAC. *Biomacromolecules*. 2011 Jul 15;12(8):2902-7.
38. Munoz EM, Correa J, Fernandez-Megia E, Riguera R. Probing the relevance of lectin clustering for the reliable evaluation of multivalent carbohydrate recognition. *Journal of the American Chemical Society*. 2009 Nov 17;131(49):17765-7.
39. Fernandez-Villamarin M, Sousa-Herves A, Correa J, Munoz EM, Taboada P, Riguera R, Fernandez-Megia E. The Effect of PEGylation on Multivalent Binding: A Surface Plasmon Resonance and Isothermal Titration Calorimetry Study with Structurally Diverse PEG-Dendritic GATG Copolymers. *ChemNanoMat*. 2016 May;2(5):437-46.
40. Stenberg E, Persson B, Roos H, Urbaniczky C. Quantitative determination of surface concentration of protein with surface plasmon resonance using radiolabeled proteins. *Journal of colloid and interface science*. 1991 May 1;143(2):513-26.
41. Munoz EM, Correa J, Riguera R, Fernandez-Megia E. Real-time evaluation of binding mechanisms in multivalent interactions: a surface plasmon resonance kinetic approach. *Journal of the American Chemical Society*. 2013 Apr 12;135(16):5966-9.
42. Leire E, Amaral SP, Louzao I, Winzer K, Alexander C, Fernandez-Megia E, Fernandez-Trillo F. Dendrimer mediated clustering of bacteria:

- Improved aggregation and evaluation of bacterial response and viability. *Biomaterials science*. 2016;4(6):998-1006.
43. Aubin-Tam ME. Conjugation of nanoparticles to proteins. In *Nanomaterial Interfaces in Biology 2013* (pp. 19-27). Humana Press, Totowa, NJ.
44. Maza JC, McKenna JR, Raliski BK, Freedman MT, Young DD. Synthesis and incorporation of unnatural amino acids to probe and optimize protein bioconjugations. *Bioconjugate chemistry*. 2015 Aug 21;26(9):1884-9.
45. Schmohl L, Schwarzer D. Sortase-mediated ligations for the site-specific modification of proteins. *Current opinion in chemical biology*. 2014 Oct 1;22:122-8.
46. Chen X, Muthoosamy K, Pfisterer A, Neumann B, Weil T. Site-selective lysine modification of native proteins and peptides via kinetically controlled labeling. *Bioconjugate chemistry*. 2012 Feb 29;23(3):500-8.
47. Kratz H, Haeckel A, Michel R, Schönzart L, Hanisch U, Hamm B, Schellenberger E. Straightforward thiol-mediated protein labelling with DTPA: Synthesis of a highly active ¹¹¹In-annexin A5-DTPA tracer. *EJNMMI research*. 2012 Dec 1;2(1):17.
48. Kolb HC, Finn MG, Sharpless KB. Click chemistry: diverse chemical function from a few good reactions. *Angewandte Chemie International Edition*. 2001 Jun 1;40(11):2004-21.

49. Huisgen R. 1, 3-dipolar cycloadditions. Past and future. *Angewandte Chemie International Edition in English*. 1963 Oct;2(10):565-98.
50. Lallana E, Riguera R, Fernandez-Megia E. Reliable and efficient procedures for the conjugation of biomolecules through Huisgen azide-alkyne cycloadditions. *Angewandte Chemie International Edition*. 2011 Sep 12;50(38):8794-804.
51. Agard NJ, Prescher JA, Bertozzi CR. A strain-promoted [3+ 2] azide-alkyne cycloaddition for covalent modification of biomolecules in living systems. *Journal of the American Chemical Society*. 2004 Nov 24;126(46):15046-7.
52. Louzao I, Sui C, Winzer K, Fernandez-Trillo F, Alexander C. Cationic polymer mediated bacterial clustering: Cell-adhesive properties of homo-and copolymers. *European Journal of Pharmaceutics and Biopharmaceutics*. 2015 Sep 1;95:47-62.
53. Perez-Soto N, Creese O, Fernandez-Trillo F, Krachler AM. Aggregation of *Vibrio cholerae* by cationic polymers enhances quorum sensing but over-rides biofilm dissipation in response to autoinduction. *bioRxiv*. 2018 Jan 1:333823.
54. Jain K, Kesharwani P, Gupta U, Jain NK. Dendrimer toxicity: Let's meet the challenge. *International journal of pharmaceutics*. 2010 Jul 15;394(1-2):122-42.
55. Bodewein L, Schmelter F, Di Fiore S, Hollert H, Fischer R, Fenske M. Differences in toxicity of anionic and cationic PAMAM and PPI

- dendrimers in zebrafish embryos and cancer cell lines. *Toxicology and applied pharmacology*. 2016 Aug 15;305:83-92.
56. Mansfield ML, Rakesh L, Tomalia DA. The random parking of spheres on spheres. *The Journal of chemical physics*. 1996 Aug 22;105(8):3245-9.
57. Erickson HP. Size and shape of protein molecules at the nanometer level determined by sedimentation, gel filtration, and electron microscopy. *Biological procedures online*. 2009 Dec;11(1):32.
58. Mulder A, Auletta T, Sartori A, Del Ciotto S, Casnati A, Ungaro R, Huskens J, Reinhoudt DN. Divalent binding of a bis (adamantyl)-functionalized calix [4] arene to β -cyclodextrin-based hosts: an experimental and theoretical study on multivalent binding in solution and at self-assembled monolayers. *Journal of the American Chemical Society*. 2004 Jun 2;126(21):6627-36.
59. Ercolani G, Piguet C, Borkovec M, Hamacek J. Symmetry numbers and statistical factors in self-assembly and multivalency. *The Journal of Physical Chemistry B*. 2007 Oct 25;111(42):12195-203.
60. Reynolds M, Perez S. Thermodynamics and chemical characterization of protein–carbohydrate interactions: The multivalency issue. *Comptes Rendus Chimie*. 2011 Jan 1;14(1):74-95.

Chapter IV:

Interaction of Affitin-dendrimer conjugates with

Staphylococcus aureus

Table of Contents

| | |
|--|------------|
| I. Introduction | 172 |
| II. Materials and methods | 176 |
| II.1 Materials | 176 |
| II.2 Bacterial strains..... | 176 |
| II.3 Fluorescence microscopy..... | 177 |
| II.4 Agglutination assay | 178 |
| II.5 Precipitation assay | 179 |
| II.6 Biofilm assay | 179 |
| III. Results and discussion | 181 |
| III.1 Fluorescent labelling of <i>S. aureus Newman</i> | 181 |
| III.2 SpA-specific agglutination of bacteria | 185 |
| III.3 Modulating biofilm formation of <i>S. aureus</i> | 191 |
| IV. Acknowledgements | 196 |
| V. References | 197 |

I. Introduction

Multivalency is often seen as a way to enhance affinities via simultaneous interaction of multiple copies of ligands and targets located onto biological surfaces. This effect usually results in the crosslinking of particles,¹ a mechanism observed in many naturally occurring phenomena, such as transcription regulation,² cell adhesion,³ coagulation,⁴ biofilm formation,⁵ etc.

Crosslinking between bacterial cells (bacterial clustering) is of special relevance as an underlying principle of many complex multicellular behaviours that activate different kinds of quorum sensing responses.⁶ For example, the mechanism of biofilm formation in *S. aureus* has been shown to be controlled by a quorum sensing system.⁷ Furthermore, beside naturally occurring bacterial clustering, multivalency is exploited for agglutination of bacteria by external agents, which is the most widely used principle for quick identification of different bacterial strains for over 100 years.⁸

Significance of *S. aureus* as a human pathogen⁹ and food contaminant¹⁰ cannot be overstated, especially due to its notorious ability to become resistant to antibiotics.¹¹ Staphylococcal biofilms are the most frequent cause of biofilm-associated infections, including those related to wounds, valve endocarditis and devices.¹² Furthermore, the ability to form biofilms has been demonstrated as a critical factor for pathogenicity and outcomes of *S. aureus* infections,¹³ as well as for antibiotic resistance.¹⁴ SpA,

which is the most common protein found on the surface of *S. aureus* cells and which plays many important roles in bacterial virulence and immune evasion mechanisms, has also been shown to be involved in the bacterial self-aggregation and biofilm formation.¹⁵

Due to the multiple roles played in pathogenicity and the fact that it is the most common protein expressed at the surface of *S. aureus*, SpA represents a molecular target of great interest. Traditionally, it is targeted using IgGs, since it binds with great affinity to their Fc fragment. However, this interaction lacks specificity since there are many other proteins that bind IgGs, particularly expressed in different bacteria – IgG Binding Proteins (IBPs). Examples include a second IBP of *S. aureus*, named Sbi, as well as IBPs present in other gram-positive bacteria such as streptococci and peptostreptococci.¹⁶ Therefore, since no human IgG can be developed to specifically targets SpA and no other IBPs, alternative binder scaffolds are extremely useful for such purposes. Examples of non-IgG binders include an Affibody molecule that binds SpA with high affinity¹⁷ and Affitin C5, whose demonstrated specificity for SpA over Sbi and other IBPs is, to the best of our knowledge, unprecedented.¹⁸ An aptamer specific to *S. aureus* has also been developed, but no molecular target of this binder has been identified.¹⁹

Rapid and facile identification of *S. aureus* often relies on longstanding agglutination assays, that consist of particles usually displaying clumping factor A (ClfA) and/or SpA binding molecules on their surface. Since

not all *S. aureus* strains are ClfA-positive, while an SpA binding ligand used in all available agglutination reagents is IgG-based, none of them are 100% specific to *S. aureus*. Cross reactivity with other IBPs is often observed giving false-positives, while ClfA-based tests are ineffective for ClfA-negative strains.²⁰ Thus, an SpA-specific agglutination provided by multivalent presentation of a highly specific Affitin C5 could be useful for designing a fully specific and accurate agglutination assay for identifying SpA-presenting *S. aureus* without any cross reactivity with other IBPs potentially present on other bacteria.

SpA plays a role in the process of bacterial self-aggregation, as well as in the second phase of biofilm maturation, both of which include multivalent cell-to-cell adhesion.^{15,21} Blocking SpA has been shown to prevent biofilm formation in a microtiter dish assay.¹⁵ However, since the role of SpA in biofilm formation is related to bacterial clumping and the resulting quorum-sensing-controlled phenotype changes, multivalent SpA-blocking agents that cause agglutination of bacteria could replace or even outperform this role of SpA. Supporting that hypothesis is the fact that dendrimer-mediated agglutination of *Vibrio harveyi* has been shown to switch to a quorum-sensing phenotype,²² while cationic polymers promote biofilm induction via transcriptional changes in *Vibrio cholerae*.²³

Here, we set out to explore the usefulness of Affitin-dendrimer conjugates as SpA-specific agglutination agents of *S. aureus* and the effect of agglutination on the formation and inhibition of biofilm.

II. Materials and methods

II.1 Materials

UV-Vis spectra were recorded on a NanoDrop 2000c device (Thermo Scientific), using either the drop method or the cuvettes. Absorbance from 96-well microplates was measured using an Infinite M200 PRO plate reader (Tecan). Micrographs for the agglutination assay were obtained on an Olympus CKX41 inverted microscope. Nikon A1 RSi fluorescence microscope (Nikon Instruments) was used for fluorescence microscopy. Images were captured with a 60x/1.4 oil immersion objective and analysed with Fiji software.

II.2 Bacterial strains

The five different strains used in this study were: a *Staphylococcus aureus* strain available in the laboratory (termed *ST25* hereafter), *Staphylococcus aureus Newman*, *Staphylococcus aureus Newman ΔSpA*, *Staphylococcus epidermidis* and *Escherichia coli DH5α lq*.

The draft genome sequence of the *ST25* strain is deposited at DDBJ/EMBL/GenBank under the accession number NZ_LXFD000000000.1. The *S. aureus Newman* strain and its protein A (ΔSpA) deficient mutant were kindly provided by Prof. Timothy Foster (Dublin, Ireland).²⁴ The *Staphylococcus epidermidis* bacterial strain was available from the

Bacteriology and Infection control unit at Nantes University Hospital. Non-ATCC strain identification was confirmed by MALDI-TOF spectrometry.

Broth cultures were grown overnight at 37 °C with shaking in LB (Luria Bertani) medium.

II.3 Fluorescence microscopy

Affitin C5 and human IgGs (Sigma) were labelled with Alexa Fluor 647 (ThermoFisher Scientific) using the protocol provided by the manufacturer. Labelled Affitin was obtained and determined to have 0.4 Alexa Fluor 647 dyes per molecule, while labelled IgG had 7.8. *Newman* culture was grown in LB to mid-log phase ($OD_{600} \sim 0.8$) and 30 mL of culture was centrifuged for 15 min at 8000 g. The bacterial pellets were washed three times with 25 mL of PBS and resuspended in 10 mL of PBS. Wells of μ -Slide 18 Well - Flat ibiTreat (Clinisciences) were coated with 30 μ L of poly L-Lysine for 30 min at rt and washed three times with 30 μ L PBS before adding 35 μ L of bacteria suspensions. After incubation for 30 min at rt, wells were washed three times with PBS and saturated with 35 μ L PBS-BSA 3% O/N at 4 °C. After removal of the blocking solution, 30 μ L of a solution containing IgGs-Alexa Fluor 647 (5 μ g/L), C5-Alexa Fluor 647 (5 μ M) and/or either 2[G3]-[C5]_{high} (500 nM) or 2[G4]-[C5]_{high} (50nM) in PBS₅₀₀ buffer (PBS pH 7.4 + 500 mM NaCl) supplemented with BSA (0.15%) were added to the wells for an

incubation of 1 h in the dark. Wells were then washed 15 times with 30 μ l of PBS₅₀₀ and observed under the microscope.

II.4 Agglutination assay

Agglutination assay was performed by adapting the method previously described by Xiao et al.²⁵ Aliquots from separate cultures of five different strains grown overnight were centrifuged at 5000 x g for 10 min. Pellets were then washed with and resuspended in PBS₅₀₀ buffer (PBS pH 7.4 + 500 mM NaCl) and OD₆₀₀ was set to 0.5. 60 μ l aliquots of each of these bacterial dispersions were then incubated in separate wells of a 96 flat-bottom polystyrene well plate (Thermo Scientific™ Nunc™) with either PBS₅₀₀ (negative control), C5-S dimer (500 nM, 50 nM), 2[G3]-[C5]_{high} (500 nM, 50 nM, and 5 nM), 2[G4]-[C5]_{high} (50 nM and 5 nM) or C5 (1 μ M) for 30 min at ambient temperature with mild shaking. Wells were then observed under the microscope (Olympus CKX41) with 40x magnification and multiple brightfield image fields of each sample were acquired. Using ImageJ software, those samples where agglutination was observed were analysed by digitally encircling 50 bacterial clusters per sample as regions of interest and calculating the average area of these clusters. The average cluster size induced by different agents was normalized by setting the sample with the largest average cluster size to a relative value of 1.0.

II.5 Precipitation assay

Precipitation assay was performed by adapting the method previously described by Merino et al.¹⁵ Aliquots from separate cultures of five different strains grown overnight were diluted, using LB₅₀₀ (LB medium containing 500 mM NaCl) and LB₁₀₀₀ (LB medium containing 1000 mM NaCl), to obtain final 1 mL suspensions of bacteria with 500 mM NaCl and OD₆₀₀=1. These were mildly shaken in glass cuvettes at room temperature with either C5 (1 μ M), C5-S dimer (500 nM), 2[G3]-[C5]_{high} (500 nM), 2[G4]-[C5]_{high} (50 nM), or with LB₅₀₀ as negative control. OD₆₀₀ of the upper part of the cuvettes was measured periodically throughout a 4 h period. Assays were performed in triplicate.

II.6 Biofilm assay

Biofilm assay was performed by adapting the protocol published by O'Toole et al.²⁶ Overnight cultures of *S. aureus* ST25, *S. aureus* Newman, *S. aureus* Newman Δ SpA and *Staphylococcus epidermidis* (positive control) were diluted 1:100 in LB, LB₅₀₀ or LB₅₀₀-Glc (LB₅₀₀ medium containing 0.2% glucose) fresh medium. One hundred microliters of these dilutions per well were added to a 96 well round-bottom polystyrene plate (Thermo Scientific™ Nunc™) and incubated at 37 °C for 48 h without shaking with different concentrations of either C5, C5-S dimer, 2[G3]-[C5]_{high}, 2[G4]-[C5]_{high} or with the corresponding volume of medium added (positive control). Sterile medium was used as a negative control and all the samples

were tested in triplicate. After incubation, biofilms were washed twice with water and heat-fixed at 60 °C for 30 min. Fixed biofilms were stained with 1% solution of crystal violet for 15 min and then washed 3 times with water and dried overnight. Crystal violet was then solubilized by adding 125 µL of 30% aqueous acetic acid to each well and incubating for 15 min. Finally, the absorbance was quantified in a plate reader at 600 nm.

III. Results and discussion

III.1 Fluorescent labelling of *S. aureus Newman*

Having demonstrated enhanced binding of Affitin-dendrimer conjugates compared to monomeric C5 to the molecular target by SPR, we used fluorescence microscopy to verify the ability of the conjugates to also outcompete the monomer in binding to the native target on the cell surface.

Figure 1 shows the result of a competitive experiment between the conjugates and monomeric Affitin towards a *Newman* strain. Both Affitin-dendrimer conjugates were able to outcompete C5 for binding on the surface of the cell with the concentrations 10-fold lower for 2[G3]-[C5]_{high} and 100-fold lower for 2[G4]-[C5]_{high}. Good colocalization is observed between the fluorescein channel, where signal coming from the conjugates is observed, and the bright-field showing the position of the cells. Very faint signal coming from the Alexa 647 channel, originating from C5, is observed as opposed to strong colocalization when only C5 is used.

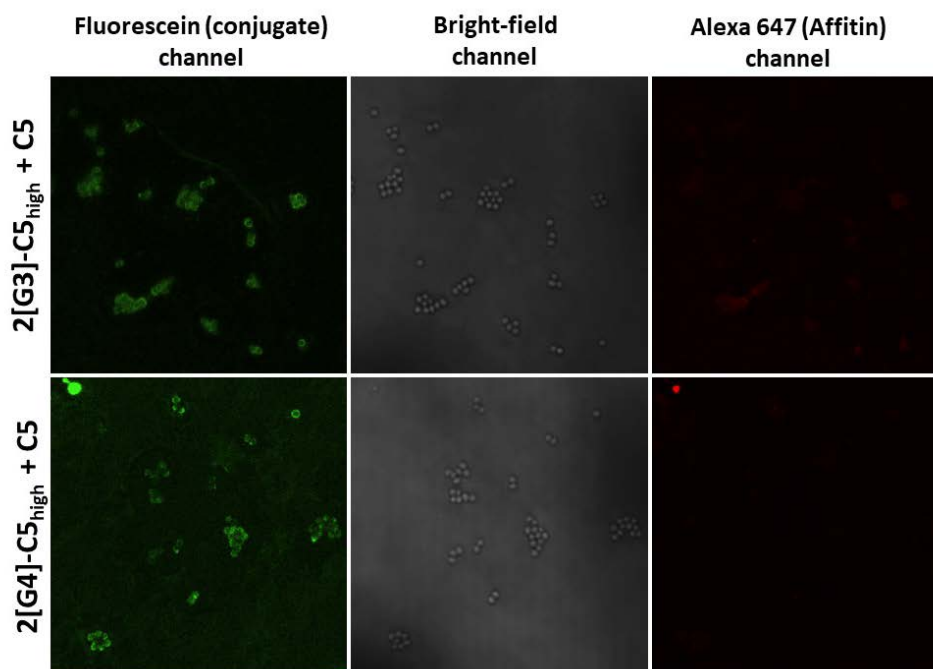


Figure 1. *Newman* strain. Competition between 500 nM 2[G3]-[C5]_{high} and 5 μM C5-Alexa 47 (upper row); 50 nM 2[G4]-[C5]_{high} and 5 μM C5-Alexa 647 (lower row).

To demonstrate that Affitin-dendrimer conjugates were binding SpA on the surface of the *Newman* strain in a highly specific manner, we used an SpA deficient *Newman* Δ SpA strain and performed fluorescent labelling with the conjugates (Figure 2). We also tested for presence of Sbi or other IgG-binding proteins of *S. aureus*, in order to verify that Affitin-dendrimer conjugates retain their specificity for SpA even in the presence of other IBPs. To this end, we performed another competition experiment, this time between Affitin-dendrimer conjugates and human IgGs on *Newman* Δ SpA (Figure 3).

Remarkably, no colocalization between *Newman* Δ SpA and either of the Affitin-dendrimer conjugates was observed in the two experiments. On the other side, strong colocalization between IgG and *Newman* Δ SpA (Figure 3) proves that other IBPs such as Sbi, are present on the surface of this SpA deficient strain. This suggests narrow specificity of the Affitin-dendrimer conjugates for SpA. In order to avoid the background noise in the fluorescein channel observed in both experiments with *Newman* Δ SpA, a new round of experiments is needed where further washing optimization should resolve this problem and confirm given observations.

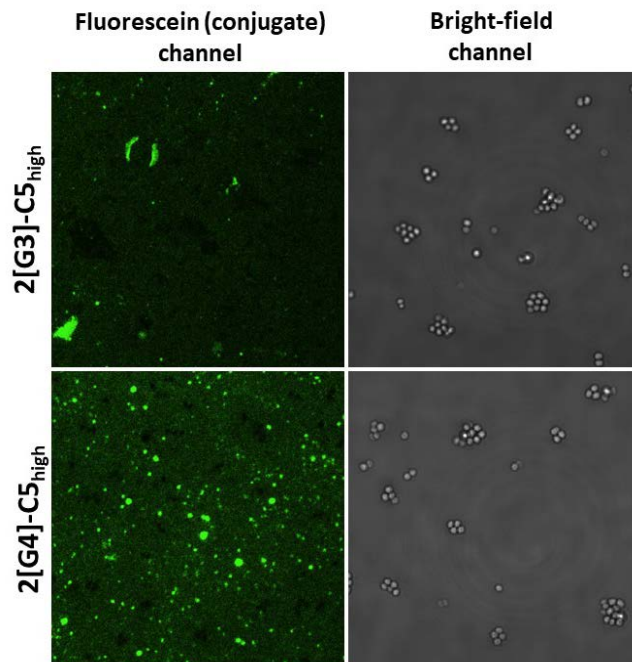


Figure 2. *Newman* Δ SpA strain. 500 nM 2[G3]-[C5]_{high} (upper row) and 50 nM 2[G4]-[C5]_{high} (lower row).

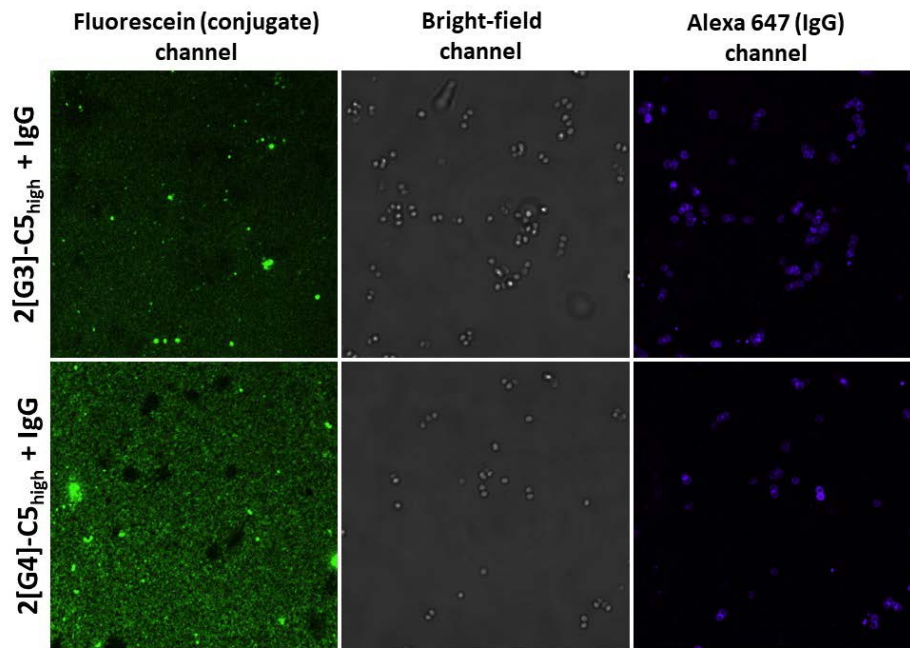


Figure 3. Newman Δ SpA strain. Competition between 500 nM 2[G3]-[C5]_{high} and 5 μ g/L IgG-Alexa 647 (upper row); 50 nM 2[G4]-[C5]_{high} and 5 μ g/L IgG-Alexa 647 (lower row).

III.2 SpA-specific agglutination of bacteria

Affitin-dendrimer conjugates, C5-S dimer and monomeric C5 (as a control), were used for agglutination of *ST25*, *Newman* and *Newman* Δ SpA strains of *S. aureus*, as well as *S. epidermidis* and gram-negative *E. coli* DH5 α *lq* strains. The resulting bacterial clusters were observed under microscope (see representative micrographs in Figure 4) and their average relative sizes were quantified and compared (Table 1, largest observed clusters normalized to the value of 1.0).

Agglutination was only triggered in SpA-expressing strains by multivalent binders, while monomeric C5 showed no ability to agglutinate any of the tested strains, in accordance with the fact that this is a multivalency-related phenomenon. The absence of agglutination in *E. coli*, *S. epidermidis* and an SpA-deficient mutant of *Newman* confirms that agglutination occurs via highly specific binding to the SpA molecule. Clusters formed by the C5-S dimer were smaller than those formed by the conjugates, while their shapes tended to be more string-like or “*strepto*” compared to fuller, grape-like or “*staphylo*” clusters observed for the conjugates (Figure 5). These observations are in line with the possibility of the dimer to bind only two target molecules at once, which have to be on two different cells for crosslinking to occur; while conjugates can bind many more target molecules simultaneously, thus exhibiting multivalency-enhanced interaction with each cell.

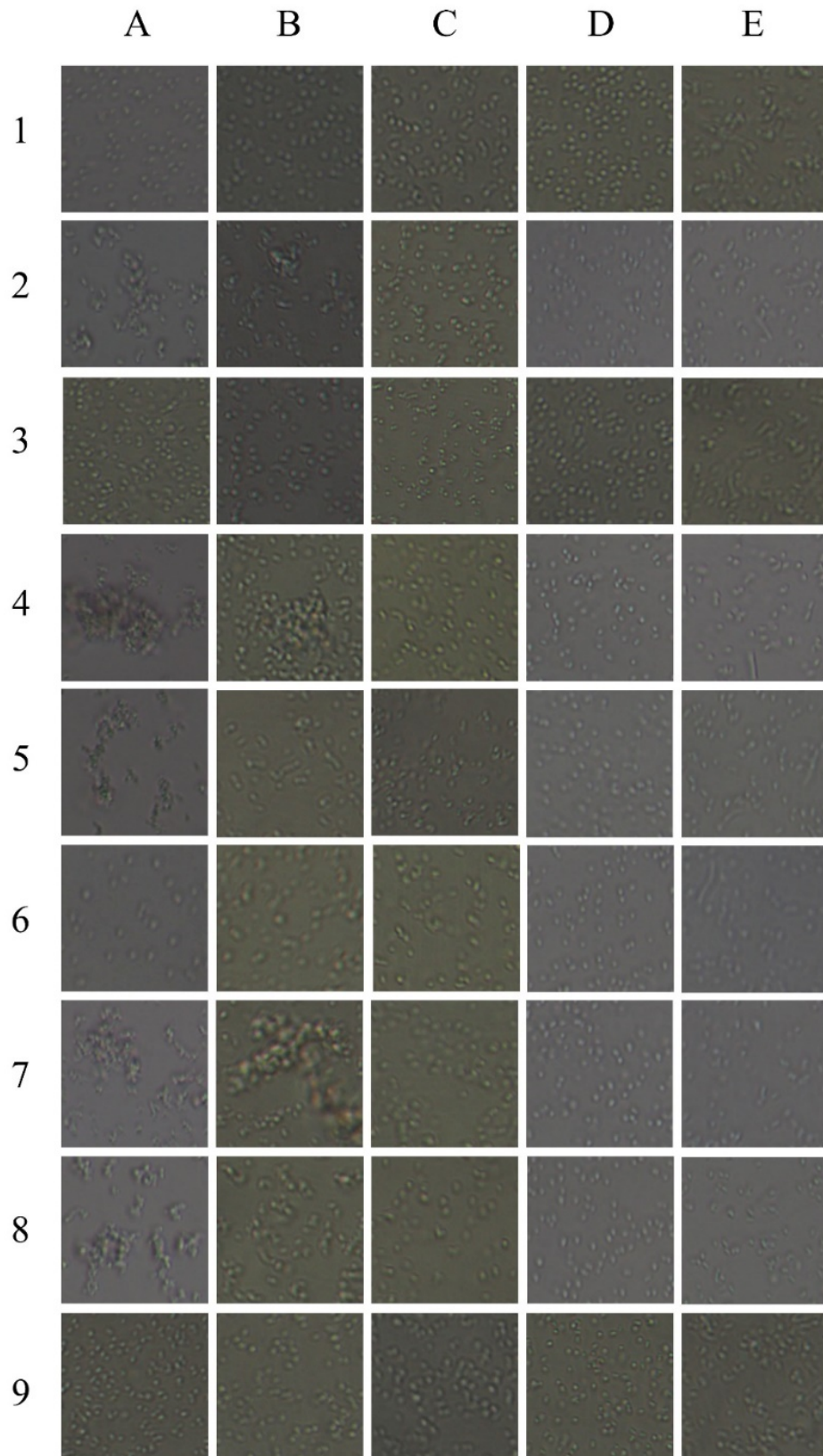


Figure 4. Typical bright-field images of agglutinated bacterial clusters (A2, A4, A5, A7, A8, B2, B4, and B7) or bacterial dispersions where no agglutination was observed. ST25 (column A), Newman (column B), Newman Δspa (column C), *S. epidermidis* (column D), and *E. coli* DH5 α Iq (column E) strains treated with PBS₅₀₀ (top, row 1), C5-S dimer (rows 2: 500 nM; 3: 50 nM), 2[G3]-[C5]_{high} (rows 4: 500 nM; 5: 50 nM; 6: 5 nM), 2[G4]-[C5]_{high} (rows 7: 50 nM; 8: 5 nM), and C5 (row 9: 1 μ M).

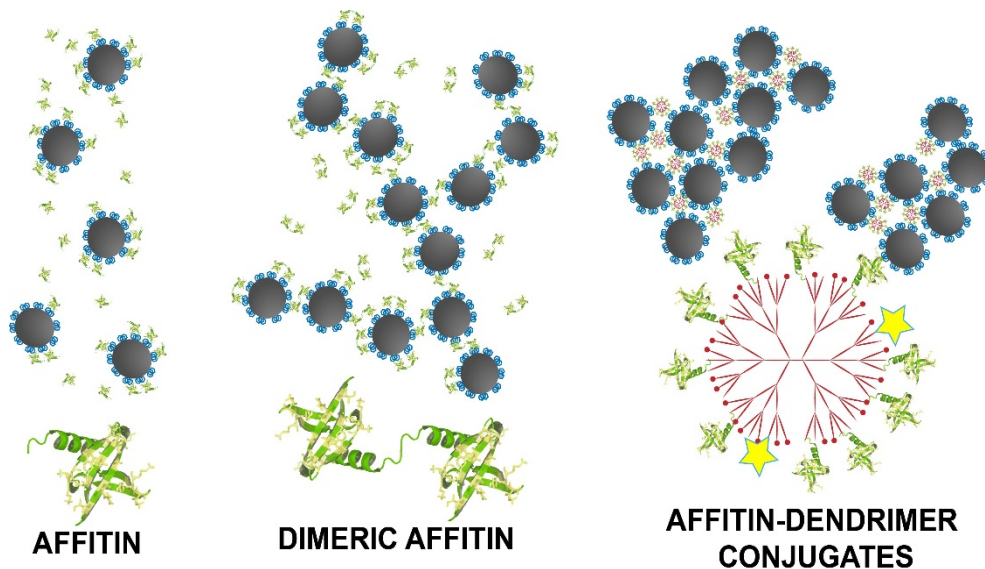


Figure 5. Illustration of chain-like (“strepto”) and grape-like (“staphylo”) clusters of bacteria formed by the C5-S dimer and Affitin-dendrimer conjugates, respectively.

Minimum Agglutination Concentrations (MAC) of the conjugates varied between the strains. In ST25 they were 50 nM and 5 nM for 2[G3]-

[C5]_{high} and 2[G4]-[C5]_{high}, respectively, while they were higher in *Newman* strain: 500 nM and 50 nM for 2[G3]-[C5]_{high} and 2[G4]-[C5]_{high}, respectively. This variation is absent in the case of C5-S dimer, which has a MAC of 500 nM for both strains. Stronger agglutination, manifested as larger clusters (Table 1), higher extent of agglutination (Table 2) and lower MAC values, is observed with the increasing valency of the agent (2[G4]-[C5]_{high} ≥ 2[G3]-[C5]_{high} > C5-S dimer). Similarly stronger effects are observed for *ST25* compared to *Newman*, which points to possible different SpA local densities on the surface of both strains.

Table 1. Average relative cluster sizes as determined by agglutination assay, normalized relative to the sample of largest clusters observed which is given value of 1.0 (500 nM 2[G3]-[C5]_{high} + *ST25*).

| Bacterial strain | Agglutination agent | | | | | | | |
|------------------------|---------------------|------------|-------|----------------------------|-------|------|----------------------------|------|
| | C5 | C5-S dimer | | 2[G3]-[C5] _{high} | | | 2[G4]-[C5] _{high} | |
| | 1 μM | 500 nM | 50 nM | 500 nM | 50 nM | 5 nM | 50 nM | 5 nM |
| <i>ST25</i> | - | 0.2 | - | 1.0 | 0.8 | - | 0.5 | 0.2 |
| <i>Newman</i> | - | 0.2 | - | 0.4 | - | - | 0.5 | - |
| <i>Newman ΔSpA</i> | - | - | - | - | - | - | - | - |
| <i>S. epidermidis</i> | - | - | - | - | - | - | - | - |
| <i>E. coli DH5α Iq</i> | - | - | - | - | - | - | - | - |

(-) no agglutination observed

To examine the scope of agglutination (percentage of cells agglutinated) with time, we analyzed the process macroscopically by measuring the OD₆₀₀ of the upper part of samples where agglutination of cell clusters was occurring throughout time. The drop of OD₆₀₀ relative to a negative control (cells in suspension with no agglutination agent) is directly proportional to the extent of agglutination. Figure 6 shows the dynamics of cell precipitation, while Table 2 sums up percentages of OD₆₀₀ signal decay for each sample tested.

All of the samples tested achieved maximum precipitation at 90-120 minutes, after which their OD₆₀₀ remained at those levels or slightly rose during the following 2 hours. The extent of precipitation induced by the C5-S dimer was lower in both strains (55% in *ST25* and 33% in *Newman*) compared to the conjugates. Both conjugates behaved almost identically, although the concentration used for 2[G4]-[C5]_{high} was 10-fold smaller. They precipitated around 85% of *ST25* cells and 60% of *Newman*, confirming the overall higher capacity of all tested agents to agglutinate *ST25* compared to *Newman*.

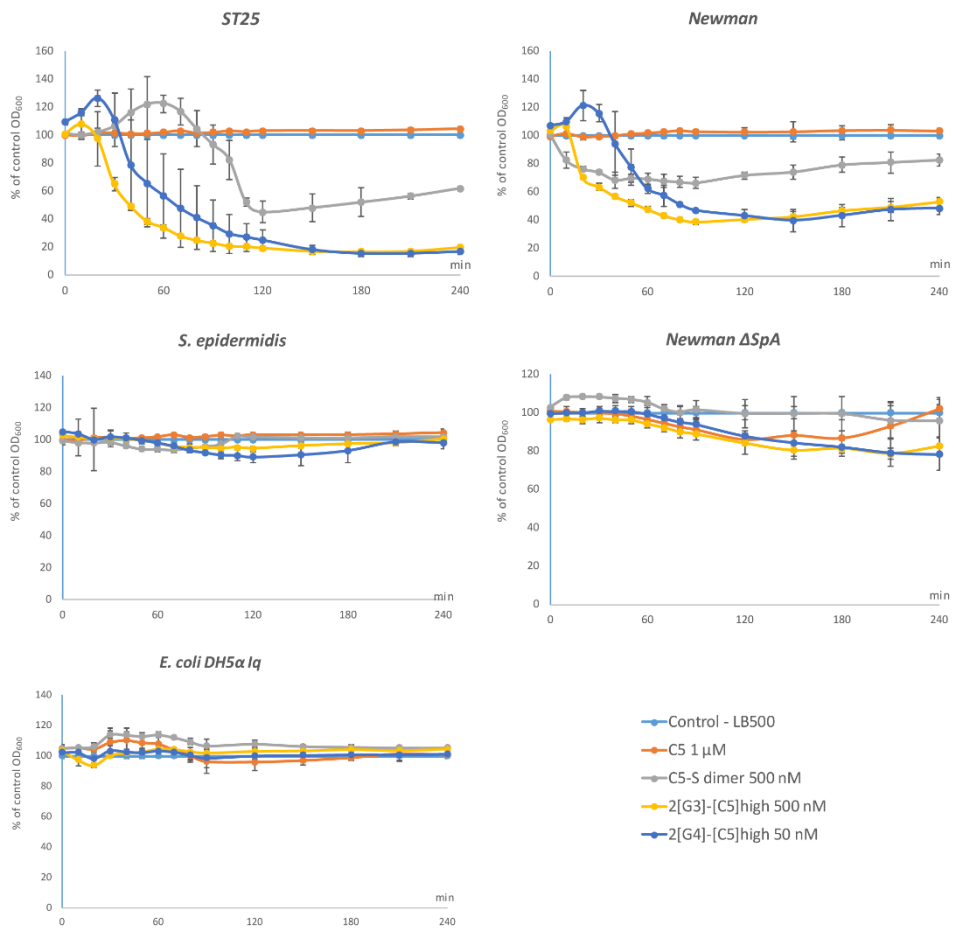


Figure 6. Precipitation assay with C5 (1 μM), C5-S dimer (500 nM), 2[G3]-[C5]_{high} (500 nM), and 2[G4]-[C5]_{high} (50 nM) on 5 different bacterial strains expressed as a change of OD₆₀₀ throughout time. Error bars – SD from 3 replicates.

Table 2. Percentage of maximum OD₆₀₀ signal decay in the precipitation assay illustrative of the extent of agglutination.

| Analyte | % OD ₆₀₀ signal decay | |
|----------------------------|----------------------------------|---------------|
| | <i>ST25</i> | <i>Newman</i> |
| C5 | 0 | 0 |
| C5-S dimer | 55 | 33 |
| 2[G3]-[C5] _{high} | 84 | 62 |
| 2[G4]-[C5] _{high} | 85 | 61 |

III.3 Modulating biofilm formation of *S. aureus*

Beside *ST25* and *Newman*, *Staphylococcus epidermidis*, a strain that forms robust biofilms, was used in all biofilm assays as a positive control. *Newman* ΔSpA couldn't be used as a control since no significant biofilm formation was observed under any of the tested conditions. Many different protocols were tested and optimized in order to achieve robust biofilm formation for all three tested strains. Finally, three different growth media were tested under optimized conditions (Figure 7). Glucose and NaCl were added as supplements since they have been shown to stimulate biofilm formation.^{27,28} LB₅₀₀ medium supplemented with 0.2% glucose was chosen, considering that no biofilm was observed in LB medium, while LB supplemented with glucose provided signals with less than 10:1 signal-to-noise ratios. Furthermore, 500 mM NaCl enables comparison with the agglutination experiments, performed with the same salt concentration.

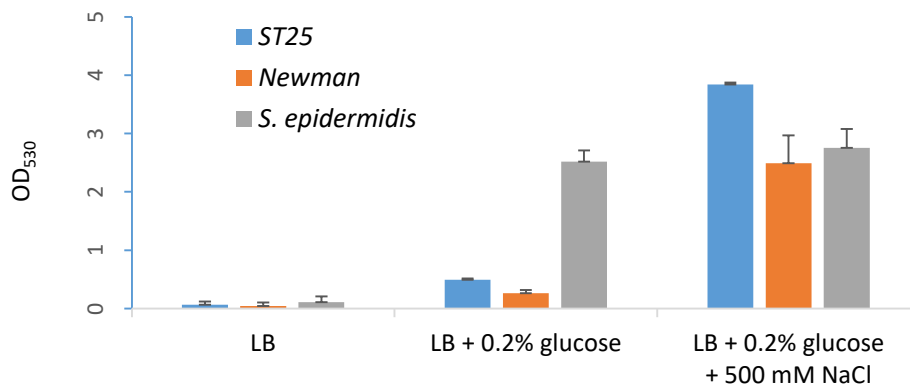


Figure 7. Intensity of biofilms formed by the three tested strains in different media. Error bars – SD from three replicates.

Since blocking SpA via IgG inhibits biofilm formation,¹⁵ we speculated that a similar inhibition could be achieved using C5, C5-S dimer and Affitin-dendrimer conjugates as SpA blocking agents. However, considering that agglutination of bacteria has been shown to trigger quorum-sensing phenotypes^{22,23} and that the role of SpA in biofilm formation is related to bacterial aggregation, we hypothesised that the agglutination caused by the multivalent agents might substitute this blocked function, therefore hampering efficient biofilm inhibition. To test these hypotheses, we performed the biofilm assay under previously optimized conditions (Figure 8)

First observation is that *S. aureus* ST25 biofilms are more intense and robust than *Newman* biofilms under the tested conditions. Their initial intensity is higher, while only slight inhibition is observed with 5 μ M C5 and

500 nM – 8 μ M C5-S dimer, compared to almost complete inhibition of *Newman* biofilms with the same agents (Figure 8-A).

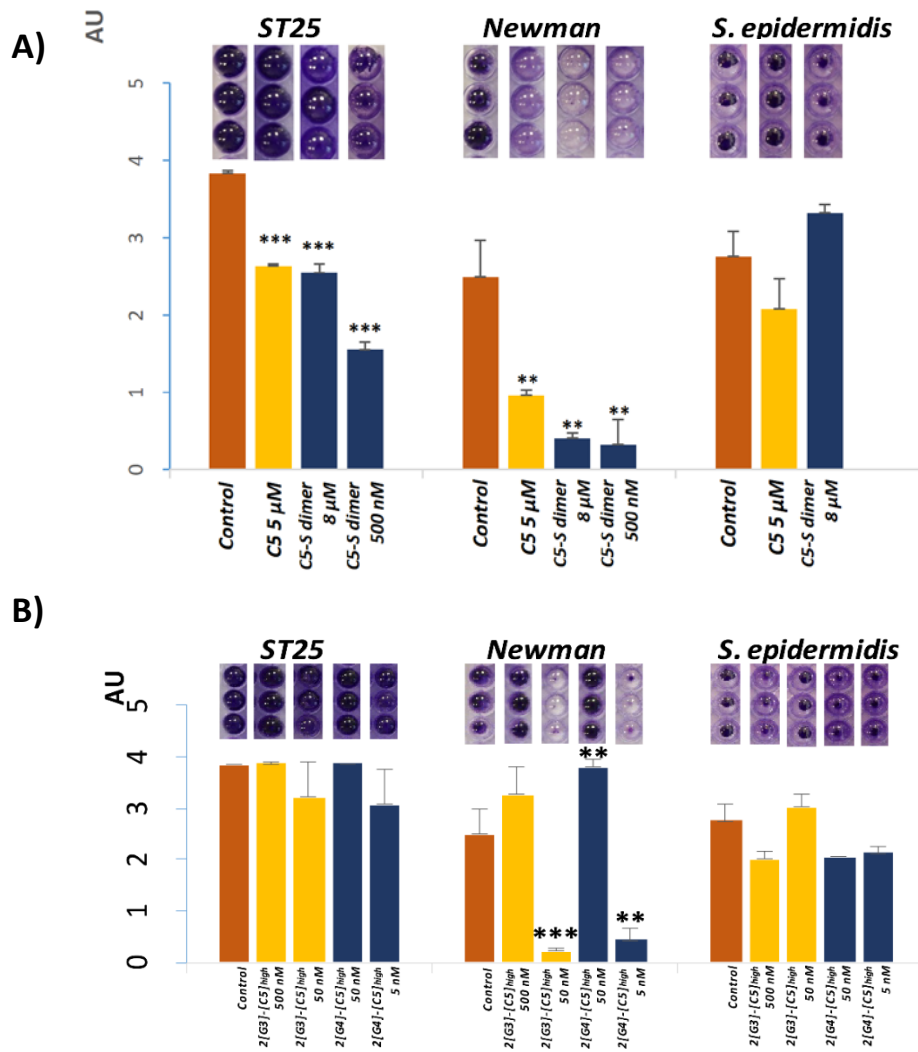


Figure 8. (a) Biofilm inhibition by monomeric C5 and C5-S dimer **(b)** Biofilm modulation by Affitin-dendrimer conjugates. Error bars – SD from three replicates. *** $p < 0.001$; ** $p < 0.01$.

Second, the ability of Affitin-dendrimer conjugates to inhibit biofilms seems to be in negative correlation with their agglutination power. Namely, biofilm inhibition is observed for the *Newman* strain in the non-agglutinating concentrations (50 nM for 2[G3]-[C5]_{high} and 5 nM for 2[G4]-[C5]_{high}) of the conjugates. On the other hand, higher concentrations previously shown to efficiently agglutinate *Newman* strain (500 nM for 2[G3]-[C5]_{high} and especially 50 nM for 2[G4]-[C5]_{high}), induce even stronger biofilms compared to the control (Figure 8-B). This suggests that Affitin-dendrimer conjugates are able to modulate biofilm formation in a concentration-dependent manner, with concentrations higher than those shown to efficiently agglutinate bacteria reinforcing biofilms, while lower concentrations inhibit it by blocking SpA function.

It is evident, both visually and by OD measurement, that no significant biofilm inhibition is observed for any of the *ST25* samples. Since the concentrations tested have all shown the ability to efficiently agglutinate *ST25* (500 and 50 nM for 2[G3]-[C5]_{high}; 50 nM and 5 nM for 2[G4]-[C5]_{high}), this lack of biofilm inhibition is in line with the assertion that the agglutination effect substitutes the role of SpA and promotes biofilm formation. However, it is impossible to say if any enhancement in biofilms is present, especially for samples with higher conjugate concentrations, due to signal overflow.

Third, even though 500 nM C5-S dimer causes slight agglutination of both *ST25* and *Newman*, it maintains the ability to inhibit biofilm formation of both of these strains in the same concentration. This indicates that weaker agglutination caused by the dimer isn't capable of achieving the same biofilm modulation effect that is observed with the conjugates.

Traditionally, biofilm formation is divided into three main phases: attachment, maturation and detachment.⁵ The attachment phase is characterized by cell-to-surface interactions, where only single cells attach to the surface, while the maturation phase is characterized by complex cell-to-cell interactions, starting with the cell clustering that triggers further responses. However, recent observations confirm that initial seeding can happen either by single cells or by preformed multicellular aggregates, suggesting an update of the existing model to include for the possibility of cell clustering happening before the attachment.²⁹ Our results further these observations, indicating that beside self-aggregated cells, externally-agglutinated cell clusters can also seed biofilms and apparently outperform the single-cell derived biofilm formation.

IV. Acknowledgements

This work was financially supported by the Spanish Ministry of Economy, Industry, and Competitiveness (MINECO) (CTQ2015-69021-R), the Xunta de Galicia (GRC2014/040 and Centro Singular de Investigación de Galicia Accreditation 2016–2019, ED431G/09), and the European Union (European Regional Development Fund, ERDF). Fluorescence microscopy images were acquired in the Plate-Forme MicroPICell of SFR-Santé François Bonamy by Steven Nedellec. We are grateful to Prof. Tim Foster (Dublin, Ireland) for kindly providing *Newman* strain and its SpA deficient mutant, as well as Dr. Stephane Corvec (Bacteriology and Infection control unit, Nantes University Hospital) for kindly providing *S. epidermidis* strain. P.V. thanks the European Commission and the Education, Audiovisual and Cultural Executive Agency (EACEA) for an Erasmus Mundus grant under the Nanomedicine and Pharmaceutical Innovation (NanoFar) Joint Doctoral Program.

V. References

1. Mammen M, Choi SK, Whitesides GM. Polyvalent interactions in biological systems: implications for design and use of multivalent ligands and inhibitors. *Angewandte Chemie International Edition*. 1998 Nov 2;37(20):2754-94.
2. Chen H, Privalsky ML. Cooperative formation of high-order oligomers by retinoid X receptors: an unexpected mode of DNA recognition. *Proceedings of the National Academy of Sciences*. 1995 Jan 17;92(2):422-6.
3. Fasting C, Schalley CA, Weber M, Seitz O, Hecht S, Kokschi B, Dornedde J, Graf C, Knapp EW, Haag R. Multivalency as a chemical organization and action principle. *Angewandte Chemie International Edition*. 2012 Oct 15;51(42):10472-98.
4. Spronk HM, Govers-Riemslog JW, ten Cate H. The blood coagulation system as a molecular machine. *Bioessays*. 2003 Dec;25(12):1220-8.
5. O'Toole G, Kaplan HB, Kolter R. Biofilm formation as microbial development. *Annual Reviews in Microbiology*. 2000 Oct;54(1):49-79.
6. Li YH, Tian X. Quorum sensing and bacterial social interactions in biofilms. *Sensors*. 2012 Feb 23;12(3):2519-38.
7. Yarwood JM, Bartels DJ, Volper EM, Greenberg EP. Quorum sensing in *Staphylococcus aureus* biofilms. *Journal of bacteriology*. 2004 Mar 15;186(6):1838-50.

8. Olopoenia LA, King AL. Widal agglutination test– 100 years later: still plagued by controversy. *Postgraduate medical journal*. 2000 Feb 1;76(892):80-4.
9. Tong SY, Davis JS, Eichenberger E, Holland TL, Fowler VG. *Staphylococcus aureus* infections: epidemiology, pathophysiology, clinical manifestations, and management. *Clinical microbiology reviews*. 2015 Jul 1;28(3):603-61.
10. Le Loir Y, Baron F, Gautier M. *Staphylococcus aureus* and food poisoning. *Genet Mol Res*. 2003 Mar 31;2(1):63-76.
11. Chambers HF, DeLeo FR. Waves of resistance: *Staphylococcus aureus* in the antibiotic era. *Nature Reviews Microbiology*. 2009 Sep;7(9):629.
12. Otto M. Staphylococcal infections: mechanisms of biofilm maturation and detachment as critical determinants of pathogenicity. *Annual review of medicine*. 2013 Jan 14;64:175-88.
13. Schierle CF, De la Garza M, Mustoe TA, Galiano RD. Staphylococcal biofilms impair wound healing by delaying reepithelialization in a murine cutaneous wound model. *Wound Repair and Regeneration*. 2009 May;17(3):354-9.
14. McCarthy H, Rudkin JK, Black NS, Gallagher L, O'Neill E, O'Gara JP. Methicillin resistance and the biofilm phenotype in *Staphylococcus aureus*. *Frontiers in cellular and infection microbiology*. 2015 Jan 28;5:1.
15. Merino N, Toledo-Arana A, Vergara-Irigaray M, Valle J, Solano C, Calvo E, Lopez JA, Foster TJ, Penadés JR, Lasa I. Protein A-mediated

- multicellular behavior in *Staphylococcus aureus*. *Journal of bacteriology*. 2009 Feb 1;191(3):832-43.
16. Sidorin EV, Solov'eva TF. IgG-binding proteins of bacteria. *Biochemistry (Moscow)*. 2011 Mar 1;76(3):295.
 17. Lindborg M, Dubnovitsky A, Olesen K, Björkman T, Abrahmsén L, Feldwisch J, Härd T. High-affinity binding to staphylococcal protein A by an engineered dimeric Affibody molecule. *Protein Engineering, Design & Selection*. 2013 Aug 7;26(10):635-44.
 18. Béhar G, Renodon-Cornière A, Kambarev S, Vukojicic P, Caroff N, Corvec S, Mouratou B, Pecorari F. Whole-bacterium ribosome display selection for isolation of highly specific anti-*Staphylococcus aureus* Affitins for detection- and capture-based biomedical applications. **Submitted to** *Biotechnology and Bioengineering*.
 19. Moon J, Kim G, Park SB, Lim J, Mo C. Comparison of whole-cell SELEX methods for the identification of *Staphylococcus aureus*-specific DNA aptamers. *Sensors*. 2015 Apr 15;15(4):8884-97.
 20. Weist K, Cimal AK, Lecke C, Kampf G, Rüden H, Vonberg RP. Evaluation of six agglutination tests for *Staphylococcus aureus* identification depending upon local prevalence of methicillin-resistant *S. aureus* (MRSA). *Journal of medical microbiology*. 2006 Mar 1;55(3):283-90.
 21. Speziale P, Pietrocola G, Foster TJ, Geoghegan JA. Protein-based biofilm matrices in *Staphylococci*. *Frontiers in cellular and infection microbiology*. 2014 Dec 10;4:171.

22. Leire E, Amaral SP, Louzao I, Winzer K, Alexander C, Fernandez-Megia E, Fernandez-Trillo F. Dendrimer mediated clustering of bacteria: Improved aggregation and evaluation of bacterial response and viability. *Biomaterials science*. 2016;4(6):998-1006.
23. Perez-Soto N, Creese O, Fernandez-Trillo F, Krachler AM. Aggregation of *Vibrio cholerae* by cationic polymers enhances quorum sensing but over-rides biofilm dissipation in response to autoinduction. *bioRxiv*. 2018 Jan 1:333823.
24. Patel AH, Nowlan P, Weavers ED, Foster T. Virulence of protein A-deficient and alpha-toxin-deficient mutants of *Staphylococcus aureus* isolated by allele replacement. *Infection and Immunity*. 1987 Dec 1;55(12):3103-10.
25. Xiao S, Abu-Esba L, Turkyilmaz S, White AG, Smith BD. Multivalent dendritic molecules as broad spectrum bacteria agglutination agents. *Theranostics*. 2013;3(9):658.
26. O'Toole GA. Microtiter dish biofilm formation assay. *Journal of visualized experiments: JoVE*. 2011(47).
27. Lim Y, Jana M, Luong TT, Lee CY. Control of glucose-and NaCl-induced biofilm formation by *rbf* in *Staphylococcus aureus*. *Journal of bacteriology*. 2004 Feb 1;186(3):722-9.
28. Waldrop R, McLaren A, Calara F, McLemore R. Biofilm growth has a threshold response to glucose in vitro. *Clinical Orthopaedics and Related Research*[®]. 2014 Nov 1;472(11):3305-10.

29. Kragh KN, Hutchison JB, Melaugh G, Rodesney C, Roberts AE, Irie Y, Jensen PØ, Diggle SP, Allen RJ, Gordon V, Bjarnsholt T. Role of multicellular aggregates in biofilm formation. MBio. 2016 May 4;7(2):e00237-16.

Chapter V:

Conclusion and perspectives

Conclusion and perspectives

The specific recognition of molecular targets characteristic of infectious agents broadens the range of strategies currently available for fighting pathogens, decreasing their chances of developing resistance. Although the concept of “molecular targeting” has been most extensively used for innovative strategies in the field of cancer, reducing antibiotic resistance and a deeper understanding of the molecular mechanisms of different pathogens could also benefit from its application to the infectious diseases arena. For instance, radioimmunotherapy has been adapted for antimicrobial therapy by using antibodies for targeted delivery of radiation to pathogens.¹

Even though antibodies are the most commonly used targeting agents today, alternative scaffolds are emerging that overcome certain limitations of antibodies, most importantly their large sizes and intricate structure, often incompatible with chemical synthesis. One such scaffold are Affitins, whose narrow specificity and high affinity for many different targets has been demonstrated, along with a small size and high thermal and chemical stability. Affitin C5, whose molecular target is *S. aureus* protein A, allows highly specific targeting of this bacterial species with nanomolar affinity (107 nM), opening many potential avenues for diagnostic, therapeutic and imaging applications. Furthermore, it can be a useful tool for molecular and cellular studies of the microbe itself.

Targeted nanoparticles are a promising tool for biomedical applications that combines multivalent molecular targeting and large capacity to carry therapeutic, diagnostic and/or imaging agents. Rational design is an important feature of targeted nanoparticles, which is enabled by extraordinary versatility of certain nanoparticle classes, such as GATG dendrimers. Facile control over the dendrimer generation and surface functionalization allows for customizable physicochemical and pharmacokinetic properties.

We hypothesised that combining advantages of Affitins as targeting agents and GATG dendrimers as versatile, multivalent carriers, could provide powerful nanoscale devices with application in many different fields, including infectious diseases. Thus, we set two main goals for this thesis. First, to develop and validate a robust conjugation method that will allow customization of size, physicochemical and recognition properties, maximising their potential for different purposes (Chapter III). Then, to exploit the obtained Affitin-dendrimer conjugates for specific targeting of *S. aureus* and assess their potential for modulating multicellular behaviours, such as agglutination and biofilm formation (Chapter IV).

Main contributions

In order to achieve a fully rational design of targeted nanoparticles, their preparation has to allow a versatile control over some critical design parameters. In theory, such a process would take any molecular target of choice and any desired biological effect as input, and provide a straightforward preparation of custom targeted nanoparticles as output. The versatile properties of GATG dendrimers as carriers and Affitins as targeting agents already meet most of rational design criteria, such as customizable specificity for any molecular target of interest and control over size and other important physicochemical properties. In chapter III, we report a robust conjugation method that combines these strengths with a versatile surface functionalization to provide control over the nature and strength of interactions with the target via multivalency.

We take advantage of the abundance of “clickable” azides on the dendrimer surface and lack of cysteine residues in the Affitin sequence, to achieve site-specific conjugation via SPAAC and insure proper orientation of the Affitin. In a simple sequence of reactions, performed in one pot with no purification required, we first convert some of the azide functions into amines; then we use some of those amines for fluorescent labelling with FITC; finally, we convert all the remaining amines into carboxylates. This demonstrates full flexibility over surface charge, as well as the capacity to

use two different chemistries for surface functionalization, providing additional versatility in design.

We have validated the conjugation method by preparing four distinct populations of conjugates, combining two generations of dendrimers with two different loadings of Affitins. Obtained conjugates were of good purity and monodispersity, with the expected differences in size, valency and affinity. They all combine multivalency-enhanced specific recognition and binding, an incorporated fluorescent dye, and the ability to carry additional loads after a simple SPAAC functionalization via the abundance of remaining azides on their surface.

In chapter IV, we explored the interactions of the conjugates with their target cells (*S. aureus*). We have demonstrated that they possess enhanced affinity not only to the molecular target, as previously shown by SPR, but also to *S. aureus* cells. We have unambiguously shown that this binding is specific to SpA as the molecular target with no cross-reactivity with any other molecules present on the surface of cells, including other IgG-binding proteins. Considering the lack of specificity displayed by most agents used to agglutinate bacteria, particularly those used in agglutination slide assays for identification of *S. aureus*,² we decided to test our conjugates as agglutination agents. Massive, highly specific agglutination, makes them ideal candidates for creating a fully specific agglutination test that could outcompete all currently available ones in terms of specificity and reliability.

Having in mind that biofilm formation is proving to be one of the most significant factors in pathogenicity and antibiotic resistance of *S. aureus*,³⁻⁵ we have explored how Affitin-dendrimer conjugates affect biofilm formation. In accordance with recent observations of similar phenomena by some of us and others^{6,7}, we found that inducing agglutination with conjugates might be promoting biofilm growth, even though blocking SpA with lower, non-agglutinating concentrations of the conjugates, inhibits biofilm formation. To the best of our knowledge, this is the first report of such concentration-dependent modulation of biofilm formation that could have implications in novel approaches to manipulating biofilm phenotypes of bacteria.

Perspectives and potential pitfalls

There are two distinct perspectives arising from the results obtained here: (i) to extend the work done with *S. aureus* in chapter IV using the described conjugates and (ii) to apply the method described in chapter III to obtain conjugates targeting either cancer cells or some other pathologies, taking advantage of the versatility of the platform for enhanced imaging, diagnostic and therapy purposes.

One way to continue the research done with *S. aureus* is by expanding on the hypothesis already set here. For example, while we did demonstrate negative correlation between the ability of conjugates to agglutinate bacteria and the ability to inhibit biofilm formation, experiments that would include more elaborate controls, wider range of concentrations and statistical significance based on independent experiments instead of replicates in a single experiment, would allow much deeper insight into this phenomenon. Furthermore, analysing the signalling pathways that become active during these processes could further elucidate the mechanisms involved and reveal useful applications of the observed behaviour. Nevertheless, importance of the observation that agglutination can hamper biofilm inhibition caused by multivalent agents is that it reveals an important potential pitfall to be considered in design of biofilm-targeting agents.

Massive, SpA-specific agglutination that has been demonstrated can be exploited to develop a slide agglutination assay for rapid identification of *S. aureus*. Furthermore, a trend in bacterial detection is using specific nanoparticles combined with sensitive techniques, such as flow cytometry.⁸ Affitin-dendrimer conjugates, combining virtually irreversible binding to *S. aureus* and a fluorescence label, could allow for very sensitive, flow-cytometry-based, detection method.

Another way to continue on the *S. aureus* studies is by introducing new functionalities via the clickable surface of the conjugates and exploring diverse downstream applications. An interesting example of this could involve simple SPAAC functionalization with a radionuclide, which would provide a theranostic tool for real-time imaging of *S. aureus* infections, as well as a potentially powerful antimicrobial agent against resistant strains. This strategy could also prove useful for reducing toxicity and increasing the effectiveness of different antimicrobial agents, allowing for lower doses and higher selectivity.

Beside the further studies of the existing conjugates, synthesizing new conjugates with different targets and fine-tuning their properties in agreement with the intended application, opens up a wide range of potential applications. In this case, it is important to consider a potential pitfall in design of new Affitin-dendrimer conjugates using the method described here, which is the opposite charge of dendrimer surface and Affitins at

physiological pH. Carboxylates were chosen as terminal functions on the dendrimer surface mainly for the purpose of making the dendrimer water-soluble. As a result, conjugates tend to form irreversible aggregates when centrifuged at high speeds or when concentrated to high concentrations at physiological pH. Here, we avoid this problem by using high pH values for the synthesis and purification - exploiting once again high chemical stability of Affitins, but this puts a limit to the concentration range that can be obtained for downstream applications at more neutral pH values. In hindsight, alternative solubilisation with hydrophilic non-charged molecules such as sugars or short-chain PEG, even though possessing limitations of their own, might be a superior choice.

Affitins specific to cancer markers, such as CD138 and EpCAM are already available, while any other molecular target of choice could be used for selection of new Affitins. Conjugating them to GATG dendrimers, while optimizing the properties of the products to the intended purpose, constitutes a wide-reaching, robust methodology for biomedical applications.

References

1. Dadachova E, Casadevall A. Radioimmunotherapy of infectious diseases. In Seminars in nuclear medicine 2009 Mar 1 (Vol. 39, No. 2, pp. 146-153). WB Saunders.
2. Weist K, Cimbal AK, Lecke C, Kampf G, Rüden H, Vonberg RP. Evaluation of six agglutination tests for *Staphylococcus aureus* identification depending upon local prevalence of methicillin-resistant *S. aureus* (MRSA). *Journal of medical microbiology*. 2006 Mar 1;55(3):283-90.
3. Otto M. Staphylococcal infections: mechanisms of biofilm maturation and detachment as critical determinants of pathogenicity. *Annual review of medicine*. 2013 Jan 14;64:175-88.
4. Schierle CF, De la Garza M, Mustoe TA, Galiano RD. Staphylococcal biofilms impair wound healing by delaying reepithelialization in a murine cutaneous wound model. *Wound Repair and Regeneration*. 2009 May;17(3):354-9.
5. McCarthy H, Rudkin JK, Black NS, Gallagher L, O'Neill E, O'Gara JP. Methicillin resistance and the biofilm phenotype in *Staphylococcus aureus*. *Frontiers in cellular and infection microbiology*. 2015 Jan 28;5:1.
6. Leire E, Amaral SP, Louzao I, Winzer K, Alexander C, Fernandez-Megia E, Fernandez-Trillo F. Dendrimer mediated clustering of bacteria: Improved aggregation and evaluation of bacterial response and viability. *Biomaterials science*. 2016;4(6):998-1006.

7. Perez-Soto N, Creese O, Fernandez-Trillo F, Krachler AM. Aggregation of *Vibrio cholerae* by cationic polymers enhances quorum sensing but over-rides biofilm dissipation in response to autoinduction. *bioRxiv*. 2018 Jan 1:333823.
8. Colino C, Millán C, Lanao J. Nanoparticles for Signaling in Biodiagnosis and Treatment of Infectious Diseases. *International journal of molecular sciences*. 2018 Jun;19(6):1627.

Titre : Conjugués Affitines-dendrimères pour un ciblage amélioré par multivalence

Mots clés : Affitine, dendrimères GATG, *Staphylococcus aureus*, multivalence, biofilm

Résumé : Les nanoparticules décorées de ligands de ciblage sont des dispositifs puissants développés pour servir d'outils thérapeutiques efficaces contre des maladies graves comme le cancer ou les maladies infectieuses. En raison des limitations importantes des anticorps en tant que ligands de ciblage, comme une grande taille et une faible stabilité, les protéines d'affinité modifiées à façon offrent une alternative intéressante pour la fonctionnalisation des nanoparticules. Les Affitines sont de petites protéines thermiquement et chimiquement stables, dérivées d'une famille de protéines d'archées de 7 kDa liant l'ADN, dont la spécificité et l'affinité pour leurs cibles sont comparables à celles des anticorps. Les dendrimères de l'acide gallique-triéthylène glycol (GATG) sont des macromolécules monodispersées, synthétiques, globulaires, en forme d'arbre,

préparées de façon itérative (générations) permettant une présentation multivalente des ligands de ciblage. L'objectif de ce travail de thèse est de combiner les propriétés de ciblage des Affitines et la polyvalence des dendrimères pour obtenir des conjugués Affitines-dendrimères pour des applications biomédicales. Le premier objectif était de mettre au point une méthode de conjugaison orientée pour incorporer des Affitines ciblant *Staphylococcus aureus* (*S. aureus*) et un traceur fluorescent pour la détection et l'imagerie, puis de les caractériser en termes de taille, d'hétérogénéité, de composition et d'affinité. Le deuxième objectif était d'évaluer leur potentiel à moduler des comportements multicellulaires complexes, comme l'agglutination et la formation de biofilms de *S. aureus* grâce aux interactions multivalentes implémentées.

Title : Affitin-dendrimer conjugates for multivalency-enhanced targeting

Keywords : Affitin, GATG dendrimer, *Staphylococcus aureus*, multivalency, biofilm

Abstract : Smart targeted nanoparticles are powerful devices developed to serve as efficient theranostic tools against severe disorders such as cancer or infectious diseases. Due to important limitations of antibodies as targeting ligands, such as large size and low stability, engineered affinity binding proteins offer an attractive alternative for nanoparticle functionalization. Affitins are small, thermally and chemically stable proteins derived from an archaeal 7 kDa DNA-binding family, with specificity and affinity for their targets comparable to that of antibodies. Gallic acid-triethylene glycol (GATG) dendrimers are monodisperse, synthetic globular tree-like macromolecules prepared in a stepwise fashion (generations) allowing multivalent presentation of targeting

ligands. The aim of this project is to combine the targeting properties of Affitins and the versatility and multivalency of dendrimers to obtain Affitin-dendrimer conjugates for biomedical applications. The first goal of this work was to develop a site-specific conjugation method to incorporate Affitins targeting *Staphylococcus aureus* (*S. aureus*) and a fluorescent dye for detection and imaging, and then to thoroughly characterize them in terms of size, heterogeneity, composition and affinity. The second goal was to assess the potential of these conjugates to modulate complex multicellular behaviors, such as agglutination and biofilm formation of *S. aureus* due to enhanced multivalent interactions.